Commissural white matter disconnectivity in normal ageing and Alzheimer's disease

Brian Scally

Submitted in conformity with the requirements for the degree of

Doctor of Philosophy

University of Leeds

School of Psychology

September 2018

Intellectual Property and Publication Statements

The candidate confirms that the work submitted is his/her/their own, except where work which has formed part of jointly authored publications has been included. The contribution of the candidate and the other authors to this work has been explicitly indicated below. The candidate confirms that appropriate credit has been given within the thesis where reference has been made to the work of others.

The study described in Chapter 4 is published in *Neurobiology of Aging*[1]. The candidate is responsible for the study design, participant recruitment and testing, data analysis, and writing of the manuscript. J. F. Delvenne made theoretical and editorial contributions to the manuscript. M. R. Burke and D. Bunce made editorial contributions to the manuscript.

The study described in Chapter 5 is published in *Neurobiology of Aging*[2]. The candidate is responsible for the study design, participant recruitment and testing, data analysis, and writing of the manuscript. J. F. Delvenne, M. R. Burke and D. Bunce made editorial contributions to the manuscript.

[1]Scally, B., Burke, M. R., Bunce, D., & Delvenne, J. F. (2018). Visual and visuomotor interhemispheric transfer time in older adults. *Neurobiology of Aging*, *65*, 69-76.

[2]Scally, B., Burke, M. R., Bunce, D., & Delvenne, J. F. (2018). Resting state EEG power and connectivity are associated with alpha peak frequency slowing in healthy ageing. *Neurobiology of Aging, 71*, 149-155.

Acknowledgements

I am greatly indebted to Jean-Francois Delvenne for taking me on as his Research Assistant, and subsequently, PhD student. From the collection of success and horror stories I've collected from other PhD students, it's clear that a PhD is really only as good as the relationship between the candidate and supervisor. I assume that it's rare for your supervisor to be excited for you to go on tour with your band. I'd like to thank Jeff for his incredible flexibility and support during the PhD, permitting me to study methods and techniques in cognitive neuroscience that were novel to us both. It probably would have made more sense to study working memory binding, but I think he agrees that the studies in this thesis are just as "sexy".

I extend massive thanks to Mel Burke, for inviting me to work with eye-tracking, MRI, TMS and other neuroscience methods during the course of the PhD. Thanks to Mel, my skillset has expanded considerably, which I'm sure will be indispensable in the future. Work aside, thanks for being a good friend over the years! Many thanks to David Bunce for imparting his wisdom and guidance over the years. Above all he has helped me become a better writer and scholar.

Finally, massive thanks to Meg, my housemates, bandmates, friends, family and anybody else that helped keep me sane since 2015. The last few years would have been terrible without you all to blow off steam with. I appreciate you all very much, and now you have that in writing.

Abstract

The network of commissural white matter fibres responsible for connecting the hemispheres of the brain is known as the corpus callosum (CC). Atrophy to the CC is evident in studies of aging and Alzheimer's disease (AD), but patterns and functional implications of neurodegeneration are still somewhat unclear. In this thesis, neuroimaging methods were used to further examine how structural and functional CC properties are affected by normal ageing and AD. In Study 1, diffusion tensor imaging (DTI) was used to examine the posterior CC tract bundles in young and older adults. Parietal and temporal midsagittal CC segments were particularly impaired in older adults, while occipital tracts were relatively preserved. Study 2 applied this methodology to study Mild Cognitive Impairment (MCI) and AD. MCI patients exhibited reduced integrity in midsagittal parietal segments compared to controls. AD patients exhibited reductions in parietal and temporal segments, yielding high classification accuracy (95-98%) against controls. Study 3 assessed visual interhemispheric transfer in aging using electroencephalography (EEG). Transfer speed was elongated in older adults, but was driven by earlier activation of the input hemisphere rather than delayed activation of the receiving hemisphere. This was not interpreted as impairment in older age, in line with findings of preserved occipital tracts in Study 1. Study 5 examined EEG functional connectivity methodology. We showed that connectivity was strongest at the dominant EEG frequency, which experiences slowing in older age. Previous studies using conventional frequency bands may therefore be biased against older adults. Study 6 applied these findings to study interhemispheric functional connectivity in older adults, while controlling for age-related frequency slowing. Age-related disconnectivity between frontal sites was evident, reflecting typical anterior-posterior neurodegeneration in older

adults (Bennett, Madden, Vaidya, Howard, & Howard, 2010). These studies provide novel spatial and methodological insight into the CC during ageing and AD.

Table of Contents

List of Tables

List of Figures

Abbreviations

CC Corpus callosum

DWI Diffusion-weighted imaging

DTI Diffusion tensor imaging

fMRI Functional magnetic resonance imaging

EEG Electroencephalography

ERP Event-related potential

MEG Magnetoencephalography

FA Fractional anisotropy

MD Mean diffusivity

RD Radial diffusivity

DA Axial Diffusivity

PLI Phase-lag index

WPLI Weighted phase-lag index

AD Alzheimer's disease

MCI Mild cognitive impairment

CSF Cerebrospinal fluid

PET Positron emission tomography

IHTT Interhemispheric transfer time

CUD Crossed-uncrossed difference

IFC Interhemispheric functional connectivity

ROI Region of interest

RT Reaction time

Chapter 1

1. Background

1.1 White matter

The functional distinction between the grey and white matter of the brain can be traced back to the 1800s, when Francis Gall reported that white matter had conductive properties (Gall & Spurzheim, 1809). White matter consists of nerve fibres (axons) that pass signals between neurons of the grey matter. Axons are coated in myelin, a fatty white substance that facilitates conductivity between axon terminals. In the late 1800's, German-Austrian born psychiatrist Theodor Hermann Meynert, the pioneer of histological mapping of the brain (or cerebral cytoarchitecture), classified the white matter pathways of the brain into three distinct categories: (i) *Association fibres* linking intrahemispheric regions, (ii) *projection fibres* connecting cortical to subcortical regions and (iii) *commissural fibres* bridging the left and right cerebral hemispheres of the brain (Catani & Ffytche, 2005; Seitelberger, 1997). Concurrent investigations of language pathology by Wernicke (1874) hypothesised that conduction aphasia (preserved aural comprehension with poor phonological repetition) arose from damage to the white matter fibres linking Broca's area of language production to the superior temporal gyrus (the location of *Wernicke's area* of language comprehension). This, and other hypotheses regarding the origins of visual agnosia, apraxia and pure alexia led to the emergence of the classical associationist theory of cognition (Catani & Ffytche, 2005), which posited that higher cognition was dependent on links between independent brain regions. Despite these seminal ideas, associationism was overtaken by the locationist model of the brain for the following half century, which conceptualised the brain as strictly modular.

A revival of interest in white matter architecture in the early 1960s was generated from a series of experiments conducted by Roger Sperry (1961) on split-brain animals and humans. Sperry surgically dissected the corpus callosum (CC; the network of commissural fibres described by Meynert) in cats and monkeys. While the animals that had undergone callosotomy (surgical sectioning of the CC) expressed no immediately discernible differences to their colossally-intact counterparts, they exhibited significant impairments in tasks designed to probe the transfer of sensory information from one cerebral hemisphere to the other. For example, Sperry severed the optical chiasm in cats, thus wiring the right eye to the ipsilateral right hemisphere and vice versa. These cats learned to navigate a maze with an eye patch blocking the vision of one eye. With the CC intact, cats sufficiently transferred visual information about the maze to the hemisphere contralateral to the unblocked eye, and were still able to navigate the maze when the eye patch was swapped to the alternate eye. In contrast, callosotomised cats were unable to navigate the maze using the alternate eye. Among Sperry's conclusions from such experiments was that the CC fibres were vital for the transfer of information between hemispheres.

The revival of interest in white matter connectivity was somewhat hindered by the lack of *in vivo* neuroimaging methods with which to study it. In the 1980s, the development of diffusion-weighted imaging (DWI) enabled scientists to non-invasively investigate the microstructure of white matter from outside the human brain for the first time (Le Bihan et al., 1986). DWI is a magnetic resonance imaging (MRI) protocol that yields images with contrasts that are sensitive to the mobility of water molecules (diffusion) in the brain (O'Donnell & Westin, 2011; Soares, Marques, Alves, & Sousa, 2013). By nature, white matter is more anisotropic than grey matter, meaning it is

characterised by a directional dominance of water diffusion. DWI is therefore a powerful tool for imaging the white matter of the brain, due to the high image contrast between white and grey matter. The contrast at each voxel (unit of 3D space in MRI scans) reflects the apparent diffusion coefficient, a measure of diffusion magnitude. Diffusion tensor imaging (DTI), on the other hand, is a method of modelling DWI data to generate 3D information about the direction of anisotropy within a given voxel. Various parameters can be extracted from the diffusion tensor model. *Mean diffusivity* (MD), akin to the apparent diffusion coefficient, describes the average magnitude of diffusivity within a voxel (Soares et al., 2013). Correlations between diffusion metrics and *in vitro* histological properties have suggested that high MD reflects atrophy of axons, dendrites and myelin density (Bronge, Bogdanovic, & Wahlund, 2002; Seehaus et al., 2015; Van Camp et al., 2012). *Radial diffusivity* (RD) measures diffusion along the axis perpendicular to the direction of general diffusivity. RD has been significantly correlated with myelination and fibre density as measured by histological staining (Song et al., 2002; Wei et al., 2013). *Axial diffusivity* (DA) quantifies diffusion along the axis parallel to the direction of general diffusivity. Disruption to DA likely infers atrophy of the axon (also known as Wallerian degeneration; Song et al., 2002; Xie et al., 2009). *Fractional anisotropy* (FA) is probably the most commonly employed diffusion metric in neuroscience, and describes the general degree of anisotropy, or directionality dependence, within a voxel. Because FA is a summary index of microstructural integrity, it is correlated with both RD and DA. It has been suggested that FA is more sensitive to RD than DA, and that it correlates with similar histological indices of myelination and fibre density (Wei et al., 2013). Notably, MD and RD are inverse measures, with increasing values reflecting reduced integrity. In contrast, higher values of FA and DA indicate increased white matter integrity.

DTI has been heavily applied to the study of white matter degeneration in many clinical and non-clinical settings. Alterations in white matter microstructure have been observed across the typically healthy lifespan and during the onset and progression of neurodegenerative diseases (O'Donnell & Westin, 2011). The following paragraphs describe the application of DTI to the study of white matter degeneration due to ageing and Alzheimer's disease.

1.2 Normal ageing and Alzheimer's Disease

According to the National Institutes of Health, 8.5% of the world's population is over 65 years of age, a figure which is expected to rise to 12% by the year 2030 (He, Goodkind, & Kowal, 2016). In the UK, 18% of the population were over 65 in 2016, projected to increase to 25% by 2036 (Randall, 2017). While some cognitive facets, such as declarative knowledge, improve with age, many abilities exhibit a degree of decline in older age, for example processing speed (Rabbitt & Goward, 1994), memory (De Jager, Milwain, & Budge, 2002) and executive functions (Wasylyshyn, Verhaeghen, & Sliwinski, 2011). Changes to brain structure (Allen, Bruss, Brown, & Damasio, 2005; Lu et al., 2013) and functional organisation (Daselaar & Cabeza, 2005; Dolcos, Rice, & Cabeza, 2002; Reuter-Lorenz & Cappell, 2008) are expected to account for this age-related deterioration. The predicted surge in numbers of older adults across the globe makes it imperative that scientists understand these brain-behaviour relationships, which may alleviate the medical and economic burden associated with cognitive deterioration in the elderly, by making recommendations for care and intervention.

As a consequence of population ageing, the numbers of individuals suffering from Alzheimer's disease (AD) are predicted to rise. AD is an age-related neurological disease. There are currently 850,000 older adults living with AD in the UK, with a projected increase to 1 million by the year 2025 (Alzheimer's Association, 2017). Clinically, full-onset AD is characterized by a severe episodic memory deficit far beyond the level of impairment expressed by unaffected older adults (Jack et al., 2011), with auxiliary impairments in language functions, visuospatial processing and constructional apraxia evident at later stages of the disease (Crawford, 2013; Ishizaki, Meguro, Nara, Kasai, & Yamadori, 2013; Serra et al., 2014; Snowden et al., 2007). AD neuropathology is characterised by the presence of beta amyloid and tau protein abnormalities in the brain, as measured by cerebrospinal fluid (CSF) analysis or positron emission tomography (PET) imaging (Dubois et al., 2016). AD is thought to progress along a continuum ranging from healthy ageing, through preclinical and prodromal stages, to full-onset AD. *Preclinical* AD refers to asymptomatic individuals who either have a genetic susceptibility to developing AD, or present with the two molecular biomarkers (Dubois et al., 2016; Sperling et al., 2011). *Prodromal* AD encompasses the stages of AD where individuals are both clinically and biologically symptomatic and are likely to progress to full-onset AD (Albert et al., 2011).

The diagnosis of preclinical and prodromal AD is constrained by several economic factors: CSF and PET measurements are expensive, require specialist training and equipment, and CSF lumbar punctures are highly invasive and associated with unpleasant side effects. Consequently, such "gold standard" biomarkers are rarely available in the identification and monitoring of AD at early stages. Instead, clinicians and researchers have relied on classifications defined by neuropsychological profiling, such as Mild

Cognitive Impairment due to AD (MCI), to measure progression along the AD trajectory (Albert et al., 2011; Petersen, 2004). MCI is characterised by a subjective report of cognitive decline by the person or an informant (i.e. relative/spouse), a marked deficit in episodic memory performance compared to age and education-matched control subjects, preserved ability to perform routine activities (i.e. washing/eating/clothing) and an absence of dementia (Albert et al., 2011). In a 2013 review, conversion rates from MCI to AD ranged from 10-33% over the course of one year (Ward, Tardiff, Dye, & Arrighi, 2013).

To place AD within the historical context of white matter connectivity, neuropathology caused by AD was initially perceived to be modular, whereby the medial temporal lobes were thought to be solely targeted by the disease, leading to the prominent episodic memory deficits characteristic of AD (Ball et al., 1985). In fact, individuals at earlier preclinical and prodromal stages of the AD continuum have demonstrated marked reductions in other memory functions, such as visual short-term memory binding (Ibanez & Parra, 2014; Parra et al., 2010), preceding the onset of the classic hippocampal symptoms. Binding functions cannot be localised to a specific grey matter structure (Parra, Della Sala, Logie, & Morcom, 2014) and have instead been linked to a distributed network of frontal and parietal regions (Birba et al., 2017; Parra et al., 2015). This contributes to the mounting evidence that AD symptomology may be better explained by disruption to connections within the brain, which are materialised in the brain's white matter (Brier, Thomas, & Ances, 2014; Delbeuck, Van der Linden, Collette, & Linden, 2003). Therefore, investigations of white matter integrity and its associated functions in the context of AD are warranted. While a considerable amount of empirical research has focused on this topic, the present thesis will attempt to build on that

research while addressing methodological and theoretical considerations of investigations into white matter connectivity in ageing and AD.

One such theoretical consideration is the need to distinguish between disease-sensitive and disease-specific features of AD. Disease-sensitive features are not independent of ageing, meaning they relate to phenomena that occur in healthy older adults that are exacerbated or accelerated by AD pathology. A classic example from cognitive neuropsychology is that of paired-associate learning functions, which rely on the hippocampus and consequentially are significantly compromised in individuals with AD (Fowler, Saling, Conway, Semple, & Louis, 2002; Storandt, Cheney, Ferraro, & Duchek, 1991). However, healthy older adults also express deficits in paired-associate learning compared to younger adults (de Jager et al., 2002, 2005; Parra et al., 2010). Therefore, it is not possible to disentangle the functional deficit of AD pathology from that of healthy ageing, deeming paired-associate learning a sensitive but unspecific feature of AD (Logie, Parra, & Della Sala, 2015). Disease-specific features, on the other hand, characterise AD pathology independently of normal ageing. For example, visual short-term memory binding has been demonstrated to be exclusively affected by AD but relatively preserved in older adulthood compared to young controls (Della Sala, Parra, Fabi, Luzzi, & Abrahams, 2012; Parra et al., 2010; Parra, Abrahams, Logie, & Sala, 2009). Features of AD which specifically inform about AD pathology over age-related pathology are especially sought after, as they have the greatest potential to inform about the onset and progression of AD at its earliest stages (Dubois et al., 2016; Logie et al., 2015). Thus, it is necessary to systematically investigate the effects of normal ageing on a given feature, to determine if it is sensitive or specific to AD.

1.3 White matter in normal ageing and Alzheimer's dementia

Many studies have investigated the developmental trajectory of white matter structures across the healthy lifespan. Early preclinical work using electron microscopy acknowledged age-related deteriorations of myelin (Nielsen & Peters, 2000; Peters, Moss, & Sethares, 2000; Peters, 2002; Peters & Sethares, 2002). In contrast, age-related axonal damage was not observed, suggesting that demyelination constitutes the primary microstructural change underlying age-related changes in DTI metrics.

In general, DTI has evidenced an anterior-posterior gradient of white matter degeneration in healthy ageing (Bennett, Madden, Vaidya, Howard, & Howard, 2010; Sullivan & Pfefferbaum, 2006), consistent with the deterioration of frontal functions in older age (Kennedy & Raz, 2009; Treitz, Heyder, & Daum, 2007). Lebel et al. (2012) used DTI tractography to cross-sectionally model the development of the major white matter tracts in 403 individuals between ages 5-83. In general, FA and MD metrics assumed a non-linear relationship with age, increasing from childhood through adolescence and young adulthood, culminating between ages 20-45, and deteriorating to some degree throughout older adulthood. Considerable variability in regional peak development and trail-off of integrity was evident across tracts: Fronto-parietal tracts such as the fornix and cingulum were associated with a later peak development and were preserved in older age. Commissural tracts traversing the midbody and posterior splenium of the CC were maintained in older age compared to the anterior commissural fibres traversing the genu of the CC. Of the association fibres, the superior frontal-occipital and inferior longitudinal tracts were more stable throughout older adulthood than the inferior frontal-occipital, superior longitudinal and the uncinate fasciculus fibres. Similar patterns have been reported in other lifespan imaging datasets using voxel-wise region of interest

methods (Hasan et al., 2010; Hasan, Iftikhar, et al., 2009; Hasan, Kamali, et al., 2008, 2009; Westlye et al., 2010).

Similar to ageing, biochemical analysis points towards axonal demyelination rather than traumatic injury as the phenomenon underlying white matter degeneration in deceased full-onset AD patients (Roher et al., 2002). Demyelination in AD is accompanied by increased levels of beta amyloid senile plaque deposits in the white matter, indicating the presence of AD pathology (Roher et al., 2002). According to a number of DTI reviews, AD is consistent with widespread alterations to diffusion values, with an emphasis on posterior rather than the anterior regions that are already disrupted by healthy ageing (Amlien & Fjell, 2014; Chua, Wen, Slavin, & Sachdev, 2008; Sexton, Kalu, Filippini, Mackay, & Ebmeier, 2011; Stebbins & Murphy, 2010). Therefore, a focus on posterior regions will likely be more fruitful in identifying disease specific white matter atrophy.

Because post-mortem histological examinations of white matter in preclinical and prodromal AD are non-existent (it is rare for patients to die at such early stages), questions concerning early onset white matter pathology can only be tackled with diffusion imaging. There is strong evidence to suggest that white matter deficits are detectable at preclinical and prodromal disease stages, before the onset of memory symptoms and classic hippocampal grey matter atrophy (Sachdev, Zhuang, Braidy, & Wen, 2013). Zhuang et al. (2012) studied a cohort of older adults, 20 of whom went on to develop MCI after a two year period. They investigated white matter differences between MCI converters and non-converters at the baseline stage, detecting significant FA reductions in the precuneus, parahippocampal regions and fornix of converters, which was independent of grey matter atrophy. Similar results were reported in studies of

individuals with high genetic risk for AD (Heise, Filippini, Ebmeier, & MacKay, 2011; Rieckmann et al., 2016).

1.4 Corpus Callosum

While global reductions in white matter are observed in both typical and abnormal ageing (Lebel, Walker, Leemans, Phillips, & Beaulieu, 2008; Liu et al., 2011), the first chapters of this thesis are primarily focused on addressing age and AD-related differences to white matter in the corpus callosum (CC). The CC encompasses the largest assembly of white matter connections in the brain (Figure 1-1A).

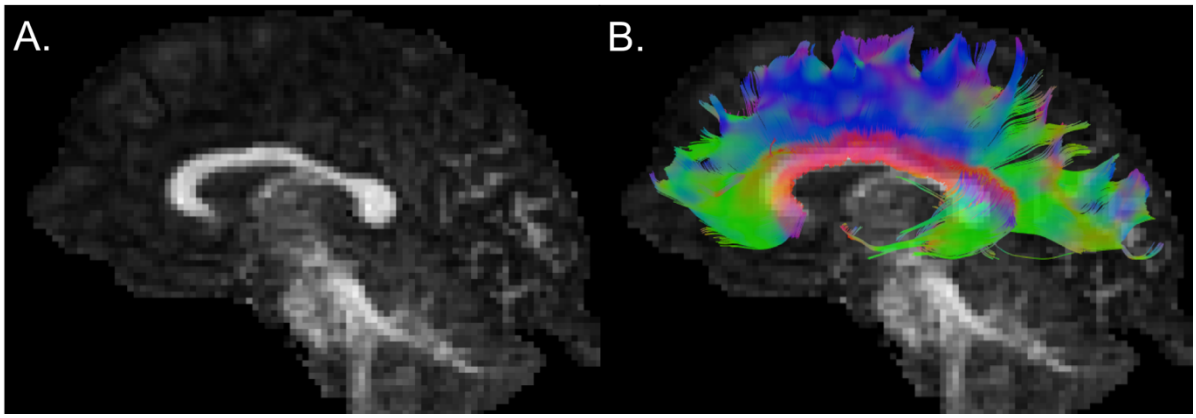

Figure 1-1: Illustration of the CC of a young healthy participant. (A) Sagittal view of the CC in a fractional anisotropy map. Light contrast indicates high FA, while dark contrast indicates low FA. (B) The same FA map with DTI tractography of the entire CC overlaid. The colouring of the tracts represents the directionality of the fibres (red = sagittal, green = coronal, blue = axial).

The primary function of the CC is thought to be the facilitation of communication between the hemispheres, be it the transfer of information between hemispheres or the inhibition of one hemisphere to utilise hemispheric dominance during a particular task (Bloom & Hynd, 2005; van der Knaap & van der Ham, 2011). Axonal fibres that traverse the CC project to many different areas of the brain, and thus it is usually appropriate to parcellate the CC in order to examine a functionally specific region of interest. Several parcellation schemes for the CC exist (Gooijers & Swinnen, 2014), which unfortunately serves as a source of great inconsistency between studies. Traditionally the CC has been roughly divided into the genu (anterior), midbody (central) and splenium (posterior) sections, which tend to have arbitrary borders (Mori et al., 2008; Wakana, Jiang, Nagae-Poetscher, Zijl, & Mori, 2004). However, using DTI tractography, the CC can be parcellated into functionally relevant bundles of commissural fibres that project to the various lobes of the bilateral cerebral cortex (see Figure 1-1B). The following paragraphs review age and AD-related differences observed in the CC using MRI and DTI methods.

1.5 Structural imaging of the CC in ageing and AD

Volumetric analysis of structural MRI scans can provide information about the size of anatomical white matter features by counting the number of voxels in the section of the image where the structure resides. Compared to young adults, reductions in total CC volume are generally not observed in typically ageing individuals (Biegon et al., 1994; Pozzilli et al., 1994; Sullivan, Rosenbloom, Desmond, & Pfefferbaum, 2001). Considering the CC subdivisions independently however, age-related differences tend to emerge, predominantly in anterior sections of the CC (Gunning-Dixon, Brickman, Cheng, &

Alexopoulos, 2009; Weis, Kimbacher, Wenger, & Neuhold, 1993). Such frontal reductions in white matter integrity are consistent with age-related reductions in frontal grey matter volume (Allen et al., 2005; Gunning-Dixon et al., 2009) and age-related deterioration of frontally localised cognitive functions such as working memory and executive functions (Heinzel, Lorenz, Duong, Rapp, & Deserno, 2017; Wasylyshyn et al., 2011). Sullivan, Pfefferbaum, Adalsteinsson, Swan and Carmelli (2002) observed that volume reductions in the genu and splenium over 4 years were uncorrelated, demonstrating that subsections may change independently of one another.

A vast amount of evidence suggests that CC volume is compromised in AD across the entire CC (Anstey et al., 2007; Biegon et al., 1994; Black et al., 2014; Chaim et al., 2007; Di Paola, Spalletta, & Caltagirone, 2010a, 2010b; Di Paola, Luders, et al., 2010; Hampel et al., 1998; Janowsky, Kaye, & Carper, 1996; Li et al., 2008; Pantel et al., 1998, 1999; Pedro et al., 2012; Pogarell et al., 2005; Teipel et al., 1999; Teipel et al., 1998; Teipel, 2003; Teipel et al., 2002; Thomann, Wustenberg, Pantel, Essig, & Schroder, 2006; Wang et al., 2006). Given that more anterior sections are targeted by ageing, central and posterior sections may be more specific to AD-related degeneration, since they project to parietal and temporal regions (Di Paola, Spalletta, et al., 2010). In earlier stages of AD, such as MCI, the results are mixed. While many studies report no difference in CC volume between MCI and healthy controls (Anstey et al., 2007; De Oliveira et al., 2011; Di Paola, Luders, et al., 2010; Pedro et al., 2012; Thomann et al., 2006), others report reductions in the posterior CC, such as the isthmus (posterior parietal projections) and splenium (Wang et al. 2006; Zhang et al. 2013). Elahi et al. (2015) showed that longitudinally, MCI-AD converters had more reductions in CC volume than non-converters, with no difference between the CC subdivisions.

Countless studies have investigated white matter diffusion in older adults and in adults with AD pathology using DTI. Cross-sectional lifespan trajectory studies with large sample sizes have demonstrated that like whole-brain white matter, tracts of the CC assume an inverted U-shaped pattern, with integrity peaking in years 20-40 before dropping off in later years of life (Hasan, Ewing-Cobbs, Kramer, Fletcher, & Narayana, 2008; Lebel, Caverhill-Godkewitsch, & Beaulieu, 2010; McLaughlin et al., 2007). A consistent finding in the ageing literature is that older age is associated with integrity reductions in the genu of the CC (Abe et al., 2002; Barrick, Charlton, Clark, & Markus, 2010; Bennett et al., 2010; Bucur et al., 2008; Davis, Kragel, Madden, & Cabeza, 2012; Ota et al., 2006; Salat et al., 2005). Ota et al. (2006) found that age was negatively correlated with FA in the rostrum (orbitofrontal projections), genu and isthmus (parietal projections) of the CC, and correlated positively with MD in the rostrum, genu, isthmus and anterior midbody of the CC. Davis et al. (2009) and Madden et al. (2009) reported increases in RD in the anterior CC and a weaker increase of splenium RD with age, suggesting a frontally weighted demyelination of fibres in older age. These results suggest that white matter in the typically ageing CC undergoes an anterior-posterior trajectory of decline. Assessing the integrity of the genu in the context of AD may therefore be redundant, as the age and disease effects will be difficult to disentangle.

DTI has been used extensively to measure CC degeneration in AD. In a comprehensive review, Di Paola et al. (2010a) found support for alterations in white matter across the CC from early stages of the disease. Alves et al. (2015) conducted a review which emphasised the mixture of findings across studies, likely due to variation between participant samples, CC parcellation schemes and DTI protocols. The majority of reviewed studies identified white matter integrity reductions in the genu, midbody and

splenium in AD patients compared to healthy controls (Agosta, Pievani, Sala, & Geroldi, 2011; Bosch et al., 2012; Di Paola et al., 2010; O'Dwyer et al., 2011; Shua, Wang, Qib, Li, & Hea, 2011). Two reviewed studies reported no group differences in the genu, but differences in the body and splenium of the CC (Acosta-Cabronero, Williams, Pengas, & Nestor, 2010; Stricker et al., 2009). This idea is supported by other studies that were omitted from the review, reporting that anterior CC integrity in AD was equivalent to that of normal controls, whereas the posterior CC was significantly compromised in AD (Di Paola, Luders, et al., 2010b; Duan et al., 2006; Head, 2004; Medina et al., 2006; Rose et al., 2000; Takahashi et al., 2002). One reviewed study (Alves et al., 2012) reported integrity differences in the genu and body but not in the splenium, which has also been sparsely supported outside the review (Bozzali, 2002; Teipel et al., 2007).

Early alterations in DTI metrics have been found in individuals with MCI (Agosta et al., 2011; Alves et al., 2012, 2015; Bosch et al., 2012; O'Dwyer et al., 2011; Shua et al., 2011; Stricker et al., 2016; Vernooij et al., 2008). Stricker et al. (2016) found that the midbody of the CC was the only section that showed reduced FA in a sample of 31 MCI patients compared to 79 matched controls. Zhang et al. (2013) observed decreased FA and increased RD in the splenium of a large sample of MCI patients, suggesting demyelination of posterior regions at early stages. Others have failed to detect any statistical differences between MCI patients and controls (Di Paola et al., 2010a; 2010c). Stricker et al. (2016) hypothesised that degeneration of white matter in the CC may adhere to a retrogenesis model. The retrogenesis model posits that the white matter connections that are formed late in development are the first to demyelinate with ageing or disease. In terms of whole brain white matter, there is little support for the retrogenesis model in healthy ageing (Brickman et al., 2012; Westlye et al., 2010;

Yeatman, Wandell, & Mezer, 2014), but no study has explicitly investigated the retrogenesis of the CC subsections. In AD, white matter degeneration seems to fit this pattern better. Initial whole-brain evidence demonstrated that early myelinating regions in development were the last to demyelinate in AD (Choi, Lim, Monteiro, & Reisberg, 2005; Stricker et al., 2009; although see Stricker et al., 2016). In terms of the CC specifically, Stricker et al. (2016) divided the CC into regions of early, middle and late myelination and found that regions of later myelination had reduced FA in MCI patients compared to controls. In particular, they reported specific reduction in FA of the CC midbody, one of the later myelinating regions. Thus, the retrogenesis model may fit the trajectory of CC degeneration in AD.

In summary, structural findings suggest that by the time patients have converted to full-onset AD, reductions in white matter integrity are present throughout the CC, with a possible focus on the central to posterior sections at earlier prodromal disease stages. Anterior commissural fibres are already sensitive to decline in healthy ageing and are unlikely to be specifically affected by AD neuropathology. Convincing, yet limited evidence, suggests that the CC may decline according to a retrogenesis model, with the inner (midbody) CC declining before the outer regions.

1.6 Functional disconnectivity in ageing and AD

While economical, portable neuroimaging techniques like electroencephalography (EEG) are available as alternatives to DTI, such methods lack the spatial resolution to make direct inferences about the integrity of specific white matter tracts in the brain. However, multimodal imaging studies have begun to show robust relationships between functional

EEG connectivity and the brain's structural integrity (Montplaisir et al., 1990; Teipel et al., 2009; Vecchio et al., 2015). In general, functional connectivity describes how two or more physiological signals are statistically dependent on one another over time. Functional connectivity may be non-directed (i.e. connectivity from signal A to signal B is the same as from signal B to A), or directed (A to B does not equal B to A), the latter implying causal links between a pair of signals. With EEG methodology, signals usually refer to neural oscillations at particular spectral frequency bands (e.g. delta: 1-3 Hz, theta: 4-7 Hz, alpha: 8-13 Hz, beta: 14-30 Hz, gamma: >30 Hz) or broadband activity across the entire spectral bandwidth. Several clinical studies, predominantly of split-brain patients and animals, have demonstrated that functional connectivity between the hemispheres relies on the structural integrity of the CC. Patients who undergo sectioning of the CC typically exhibited a reduction in interhemispheric functional connectivity (IFC; frequency-specific correlations) post-surgery (Brázdil, Brichta, Krajča, Kuba, & Daniel, 1997; Johnston et al., 2008; Montplaisir et al., 1990), providing causal evidence for the link between structure and IFC. In rats, sectioning of the CC resulted in decreased IFC in EEG and functional MRI (fMRI) signals (Magnuson, Thompson, Pan, & Keilholz, 2013). Additionally, individuals with maldevelopment of the CC express marked reductions in EEG-based IFC (Nagase, Terasaki, Okubo, Matsuura, & Toru, 1994; Nielsen, Montplaisir, & Lassonde, 1993), demonstrating that partial microstructural damage is sufficient to modulate IFC.

While the literature addressing functional decoupling in ageing and AD is extensive, there is only sparse evidence to suggest that EEG-based IFC may map onto the underlying patterns of white matter atrophy that occur in healthy and pathological ageing. Duffy, Mcanulty and Albert (1996) examined IFC in 350 individuals between age

20-79, finding a broad decrease across frontal, temporal and parietal sites, suggesting poor regional specificity of IFC with respect to the anterior-posterior gradient observed by structural imaging. However, Kikuchi et al. (2002) observed reduced IFC in older adults, predominantly between anterior channels at high alpha frequencies (11-12.5 Hz), which is consistent with expected patterns of ageing. Koyama, Hirasawa, Okubo and Karasawa (1997) examined IFC at exclusively central and occipital sites, detecting no difference between young and older adults. In AD, Pogarell et al. (2005) reported that IFC was positively correlated with total CC size in full onset AD patients. In older adults and individuals with MCI, Teipel et al. (2009) found that temporo-parietal IFC was positively correlated with integrity of a range of white matter structures including posterior callosal fibres, while frontal connectivity was associated with integrity of the anterior CC and surrounding white matter. The latter chapters of this thesis further explores whether IFC is modulated by ageing, and maps onto established patterns of CC degeneration in older age.

1.7 Overview of chapters

The first series of studies presented in this thesis address the integrity of the CC splenium in healthy ageing, MCI and AD, as measured by structural DTI. According to previous studies, the splenium seems to be relatively preserved throughout the lifespan (Abe et al., 2002; Barrick et al., 2010; Bennett et al., 2010; Bucur et al., 2008; Davis et al., 2012; Ota et al., 2006; Salat et al., 2005) and is regularly identified in studies as differentiating AD and MCI patients from healthy controls (Di Paola, Luders, et al., 2010b; Duan et al., 2006; Head, 2004; Medina et al., 2006; Rose et al., 2000; Takahashi et al., 2002). Closer

consideration of this structure is therefore warranted. The splenium has rarely been investigated in terms of its distinct interhemispheric tract bundles that project to bilateral occipital, parietal and temporal areas of the cortex. Given the knowledge that these cortices are differentially associated with independent cognitive and perceptual functions, it can be assumed that the distinct white matter pathways that connect them bilaterally also serve independent functions, and may be differentially affected by healthy and pathological ageing. This gap in the literature is addressed in Study 1 (Chapter 2) to determine whether normal ageing has differential effects on these tract bundles. In Study 2 (Chapter 3), the DTI tractography methodology utilised in Study 1 is extended to the study of MCI and AD patients, to determine if any of the sub-splenium tract bundles are specifically affected by individuals with MCI and AD compared to normal controls, and to determine the accuracy of diffusion tensor parameters for classifying individuals with AD pathology.

The latter half of this thesis is concerned with functional changes associated with structural alterations to the CC due to older age. Study 3 (Chapter 4) investigates a well-known function of the CC, interhemispheric transfer, and asks whether interhemispheric transfer time (IHTT) is elongated in older adults. Shortcomings of the traditional method for measuring IHTT using event-related potentials (ERPs) are critiqued and novel data processing techniques are proposed in an attempt to improve the method and reduce ambiguity in the literature. The following studies (Chapters 5 and 6) examine functional EEG connectivity between the hemispheres of young and older adults, and whether patterns of disconnectivity reflect age-related patterns of CC degeneration highlighted by the opening thesis chapters and by previous research. Methodological issues surrounding EEG functional connectivity are first considered in Study 4 (Chapter 5), where the

potential association between connectivity and age-related dominant EEG frequency slowing is investigated to establish whether conventional methods induce bias against older adults. In turn, Study 5 (Chapter 6) attempts to account for age-related dominant EEG frequency slowing in a comparison of IFC between groups of young and older adults.

Chapter 2

2. Study 1: The effect of ageing on the corpus callosum splenium

2.1 Introduction

It is widely accepted that the human corpus callosum (CC) experiences an anterior-posterior gradient of degeneration with advancing age (Hasan et al., 2009; Lebel et al., 2012). Specifically, normal ageing seems to target the small-diameter commissural tracts of the anterior CC genu that project to bilateral areas of the frontal cortex (Bennett & Madden, 2014; Davis, Kragel, Madden, & Cabeza, 2012; Madden et al., 2009; Pfefferbaum, Adalsteinsson, & Sullivan, 2005; Salat et al., 2005), consistent with age-related cognitive decline in frontally-localised functions such as task switching (Wasylyshyn et al., 2011), declarative memory (Rosen et al., 2002) and problem solving (Zahr, Rohlfing, Pfefferbaum, & Sullivan, 2009). In contrast, the CC splenium, which occupies the posterior quarter of the CC (Hofer & Frahm, 2006), appears to be relatively preserved in older age (Bastin et al., 2010; Hou et al., 2012; Ota et al., 2006; Salat et al., 2005; Salat, Ward, Kaye, & Janowsky, 1997). While the 'splenium' label is typically applied to the posterior quarter of the midsagittal CC, the white matter fibres that pass through this region are diverse, such that they project bilaterally to three distinct brain regions: the occipital, parietal and temporal lobes (Aboitiz & Montiel, 2003; Aboitiz, Scheibel, Fisher, & Zaidel, 1992; Knyazeva, 2013; Hofer & Frahm, 2006). Additionally, the distinct fibre bundles vary in diameter, from thin late-myelinating parietal fibres to large-diameter tracts connecting primary and extrastriate visual areas (Knyazeva, 2013). Interindividual variability in the morphology of the CC suggests that region of interest (ROI) measurements of the total splenium area are likely to be noisy, and that the splenium should be functionally parcellated according to the topography of the commissural fibres for the most accurate

measurements (Westerhausen, Grüner, Specht, & Hugdahl, 2009). These distinct fibre bundles of the splenium have rarely been investigated in the context of ageing. In this study we use diffusion tensor imaging (DTI) tractography to investigate age differences within specific tract bundles of the splenium.

Microstructural properties of the entire midsagittal splenium ROI have been associated with low-level visual processing that requires cross-hemispheric communication (as reviewed by Schulte & Müller-Oehring, 2010). For example, the transmission speed of transferring simple visual information between hemispheres has been correlated with the integrity of the CC splenium as estimated by DTI (Westerhausen et al., 2006). Similar findings have been reported for higher-order visual information. Davis and Cabeza (2015) demonstrated that fractional anisotropy (FA; a metric describing the degree of directionality of a given reconstructed white matter tract) of the splenium was positively associated with the bilateral field advantage (see e.g. Banich, 2003; Belger & Banich, 1992; Delvenne, Castronovo, Demeyere, & Humphreys, 2011; Delvenne & Holt, 2012) during a face-matching task. Interestingly, FA of the midsagittal splenium has also been correlated with a number of non-visual facets. Penke et al. (2010) reported that high splenium FA was associated with high IQ in a large cohort of 70-year-old participants. Impressively, the association was stable after controlling for childhood IQ at age 11, a strong predictor of cognitive ageing (Deary, Pattie, & Starr, 2013; Gow et al., 2011). Splenium integrity has also been linked to memory performance and executive functioning (Voineskos et al., 2012). Compromised microstructural properties of the splenium have been identified in individuals with increased hypertension (Wong, Ma, & Lee, 2017), poorer reading skills (Frye et al., 2008) and Alzheimer's dementia pathology (Fletcher et al. 2016; Genc et al. 2016; Hanyu et al. 1999; Hoy et al. 2017; Madhavan et al. 2016; Sandson et al. 1999; Tang et al. 2017).

The anatomical diversity of splenium fibre terminals suggests that distinct fibre bundles should be attributed to separate functions, and that previous studies using ROI approaches, which average over the entire splenium, may lack specificity. Additionally, the choice of parcellation scheme directly determines which tracts contribute to the splenium ROI (see Gooijers & Swinnen, 2014 for a review of parcellation schemes) ultimately adding to inconsistencies between studies. No given parcellation scheme is able to account for interindividual differences in the topography of the CC tracts, which is particularly evident in the splenium (see e.g. Hofer & Frahm, 2006). Whole-splenium approaches may therefore be unsuitable and functionally redundant. Advances in neuroimaging methods allow for the reconstruction of white matter tracts in diffusion-weighted images using DTI tractography (Behrens, Berg, Jbabdi, Rushworth, & Woolrich, 2007; Johansen-Berg & Behrens, 2006). These methods permit the identification of specific tract bundles according to the regions they project to.

A selection of studies have attempted to link the distinct splenium tract bundles with cognitive or neuropsychological variables. Sullivan, Rohlfing and Pfefferbaum (2010) observed significant correlations between processing speed and integrity of temporal and parietal splenium tracts. However, these correlations were computed across young and older age groups, and may therefore be confounded by age. They also reported no correlations between occipital tract integrity and processing speed, fine motor skill or gait abnormality. Westerhausen et al. (2009) found moderate positive correlations between the density of temporal splenium tracts and behavioural performance on a dichotic listening paradigm. Temporal tract FA has also been linked to phonological awareness and passage comprehension in children (Dougherty et al., 2007). Yin et al. (2012) reported that the timing of orienting attention during a flanker task was correlated with FA, MD and RD of interhemispheric parietal white matter that connected

the bilateral inferior parietal lobules. Occipital tracts appear to facilitate cross-hemispheric blood-oxygen-level dependent (BOLD) connectivity and support the bilateral field advantage for visual pattern stimuli (Davis & Cabeza, 2015), suggesting that splenium occipital tracts are necessary for the bihemispheric processing of visual information.

To address the limitations of previous studies, the current study used DTI tractography to reconstruct the white matter pathways that traverse the CC splenium. Splenium tracts that connected bilateral occipital, parietal and temporal areas were segregated and their diffusion metrics were compared between a group of young and older adults to determine whether specific tract bundles were affected in older age. As well as an analysis of the full unsegmented tract bundles, we conducted an analysis of the bundles segmented at +/- 6mm around the midsagittal slice, to examine group differences within the midline CC region. This was done to minimise confounding effects of tract density, and to enable comparison with previous studies that examined midsagittal sections. We analysed two independent datasets obtained from separate scanning facilities in order to validate the findings.

Previous research has suggested that age-related compensatory recruitment of brain activity in a given region is associated with reduced white matter integrity in the same region (the "less wiring more firing" hypothesis; Daselaar et al., 2015). There is evidence of age-related compensatory activity in bilateral parietal and temporal regions (Grady, McIntosh, Horwitz, & Rapoport, 2000; Maguire, 2003; Nielson, Langenecker, & Garavan, 2002), and evidence of age-related cognitive decline in parietal and temporal functions, such as visuospatial working memory (De Jager et al., 2002), spatial learning (Yamamoto & DeGirolamo, 2012) and dichotic listening (Hommet et al., 2010). We therefore hypothesised that white matter integrity would be compromised in the

splenium projections to parietal and temporal regions in older adults. We hypothesised that occipital tracts would be spared in older age, consistent with preserved interhemispheric processing of visual information in older adults (Boyson, 2013; Scally, Burke, Bunce, & Delvenne, 2018b). In the present manuscript, we use the term 'fibre' to refer anatomically to the white matter axons of the brain, and 'tract' to refer to the reconstructed tractography streamlines that attempt to model the white matter fibres in DTI tractography.

2.2 Method - Study A

2.2.1 Participants

Sixteen young adults (mean age = 22.41, *SD* = 2.42, range = 20-28, 10 females) and 10 older adults (mean age = 68.33, *SD* = 2.53, range = 65-74, 7 females) were recruited for this study. Older adults were recruited from the community, whereas young adults were recruited from the Psychology undergraduate programme at the School of Psychology, University of Leeds. No participant reported a history of neurological disease, high blood pressure, or psychiatric conditions, as validated by a medical history questionnaire. All participants were self-reported right handers with no known visual or motor impairments.

2.2.2 DTI acquisition & pre-processing

All participants were scanned for five minutes using a 3T GE MR scanner (Signa Excite HD; GE Healthcare, Milwaukee, USA) at York Neuroimaging Centre, UK. Diffusion weighted images (DWI) were acquired using an echo-planar imaging sequence (25

directions for b-values of 1000 s/mm^2, 3 scans at b = 0, TR = 15000 ms, TE = 86 ms, voxel size = 2 mm isotropic, FOV = 192 mm^2, 60 axial slices, matrix size = 96 x 96, slice gap = 0). Corrections for DWI signal drift, subject motion and eddy-current-induced distortions were made using the ExploreDTI software (Leemans, Sijbers, & Jones, 2009). Brain extraction was also implemented by ExploreDTI.

2.2.3 DTI Tractography

Whole brain probabilistic constrained spherical deconvolution tractography (Jeurissen, Leemans, Jones, Tournier, & Sijbers, 2011) was carried out using the ExploreDTI software. An angular threshold of 45°, and FA contrast threshold of 0.2 was applied to all reconstructed tracts. ROIs were drawn manually onto the DTI scans of each participant to isolate the occipital, temporal and parietal tract bundles that pass through the splenium. Firstly, the splenium was identified by drawing an 'AND' ROI on the middle slice of the sagittal plane around the posterior quarter of the entire CC (Figure 2-1A). The tracts passing through this section were drawn to visualise the different bundles (Figure 2-1B). For the occipital tracts, two 'AND' ROIs were drawn on the coronal plane to isolate the tracts projecting to the occipital lobe of each hemisphere, omitting tracts that projected to parietal areas (Figure 2-1C & 2-11D).

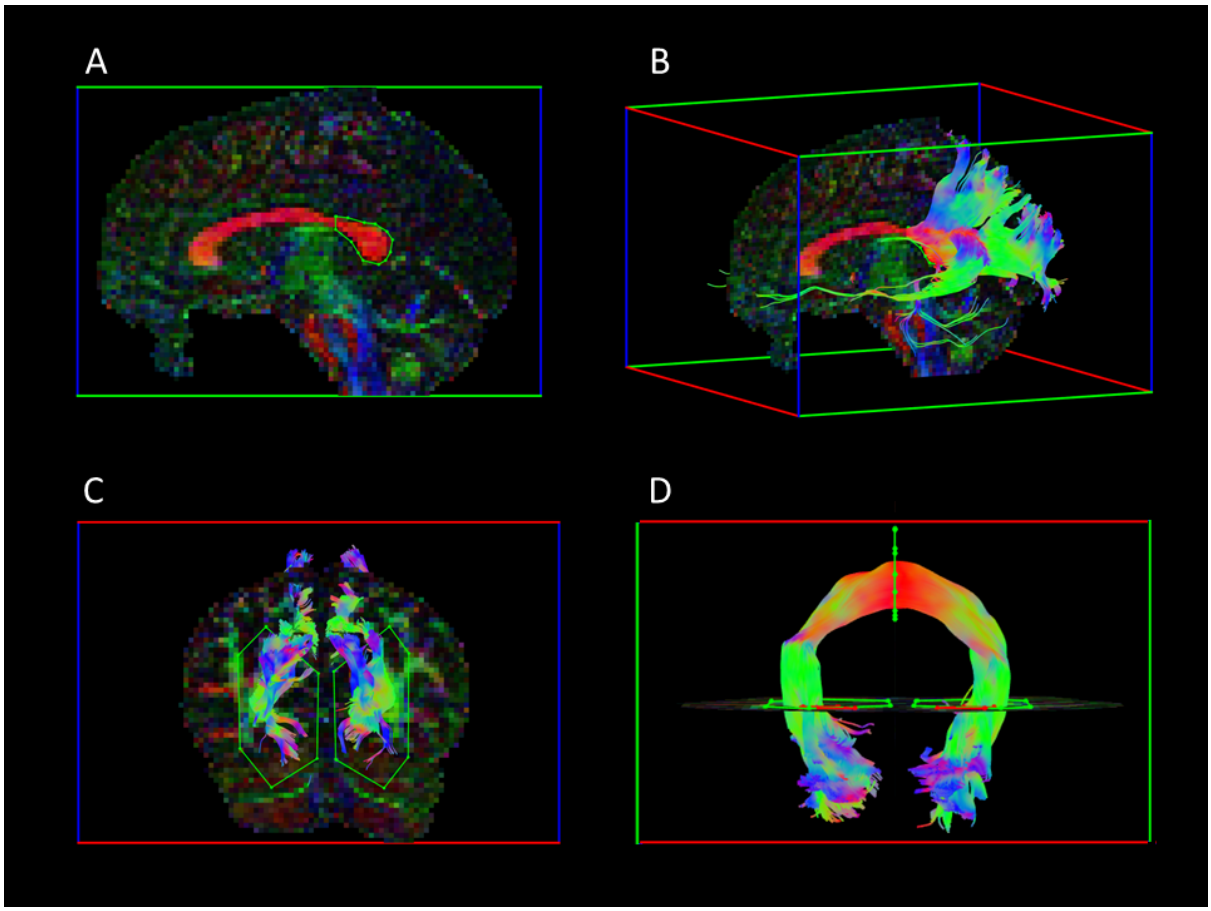

Figure 2-1: Tractography of the CC occipital tracts. (A) Sagittal view of ROI drawn around the splenium on the midsagittal scan. (B) Sagittal view of all tracts traversing the midsagittal ROI. (C) Rear coronal view of ROIs drawn around left and right occipital tract bundles. (D) Axial view of interhemispheric occipital tracts. Tracts are coloured according to direction (red: left-right; blue: top-bottom; green: front-back).

Parietal tracts were selected by replacing the former 'AND' ROIs surrounding the occipital tracts with 'NOT' ROIs (Figure 2-2A) to exclude them. Two more 'NOT' ROIs were drawn on sagittal planes left and right of the midline to exclude tracts that projected to temporal areas (Figure 2-2B). Parietal tracts are illustrated in Figure 2-2C.

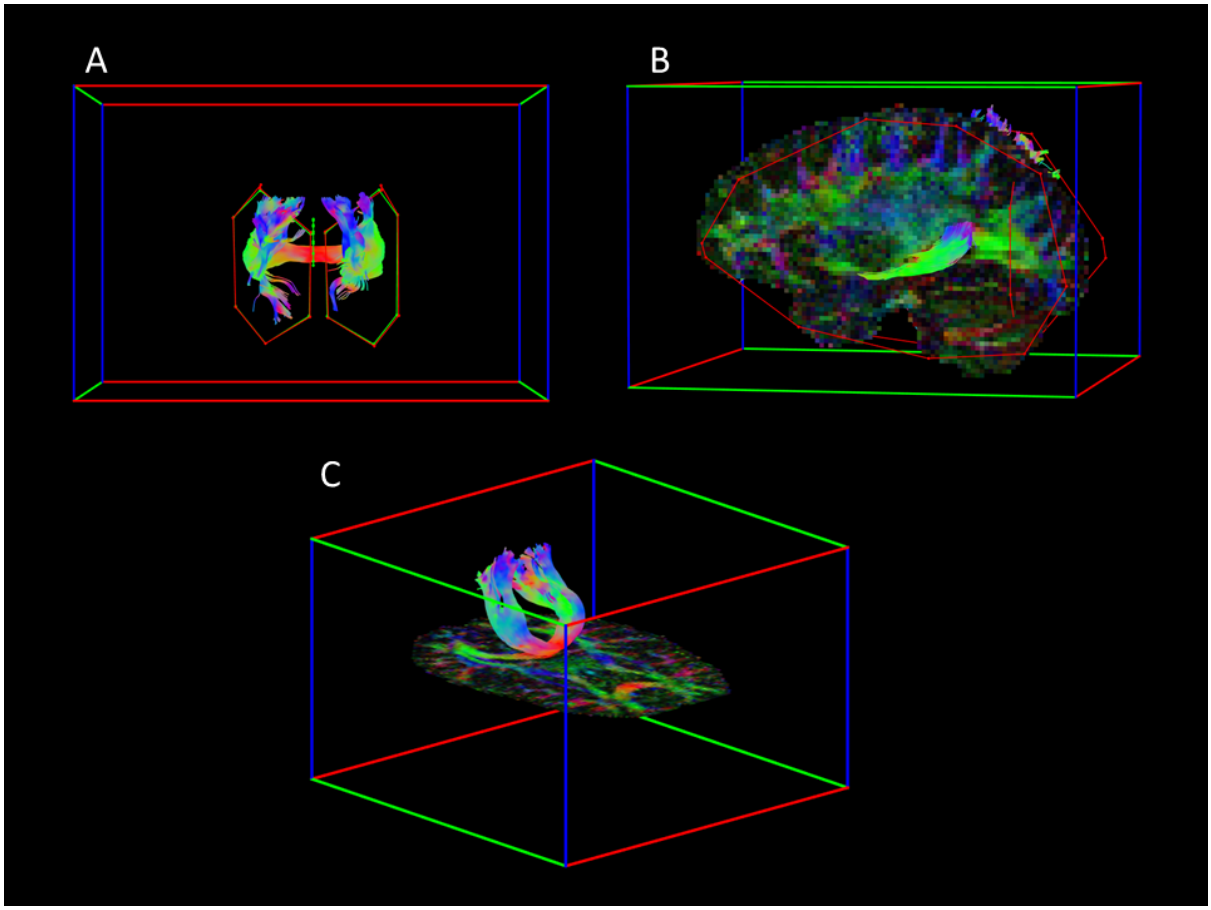

Figure 2-2: Tractography of the CC parietal tracts. (A) Rear coronal view: replacing occipital 'AND' ROIs (green) with 'NOT' ROIs (red) to exclude occipital tracts. (B) Sagittal 'NOT' ROIs drawn either side of the midline to exclude temporal tracts. (C) The resulting interhemispheric parietal tracts.

Tracts that passed through the initial splenium ROI and projected forward to temporal areas were isolated with 'AND' ROIs in the right and left hemisphere on coronal plane (Figure 2-3A & 2-3B).

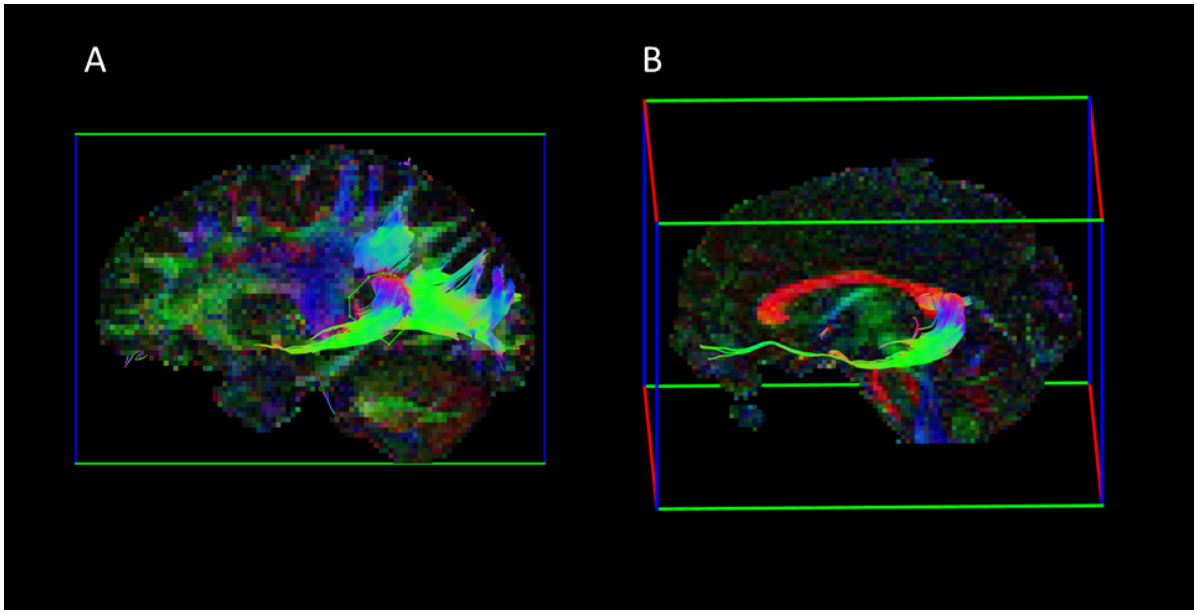

Figure 2-3: Tractography of the CC temporal tracts. (A) Sagittal 'AND' ROIs drawn around left and right temporal projections from the splenium. (B) The isolated interhemispheric temporal tracts. Tracts are coloured according to direction (red: left-right; blue: top-bottom; green: front-back).

Average fractional anisotropy (FA), mean diffusivity (MD), radial diffusivity (RD) and axial diffusivity (DA) metrics were extracted from these tracts of interest and used as dependent variables in the analysis. In addition to the full tract analysis, we segmented each callosal bundle ±6mm (three 2mm slices) either side of the sagittal midline to analyse the midsagittal segments of the CC, and to control for potential confounding effects of tract length or density (Jones, Knösche, & Turner, 2013; Vos, Jones, Viergever, & Leemans, 2011).

2.2.4 Statistical Analysis

DTI tract density has been demonstrated to change in older age and covary with diffusion metrics (Jones et al., 2013; Vos et al., 2011). Tract density is defined as the cumulative density of the voxels that a given reconstructed tract passes through. We first tested for group differences in the approximate tract density (as outputted by ExploreDTI) of each tract bundle using one-way ANCOVA models with Group (young/older) as the independent variable, and sex as a covariate, for each level of ROI. To statistically account for the potential influence of tract density on diffusion properties, we held tract density constant for the between-group tests of diffusion tensor parameters (FA, MD, DA, RD). We used a series of ANCOVA models with Group (young/older adults) as the independent variable and tract density and sex as nuisance covariates, to test for age group differences in the DTI parameters at each level of ROI (occipital/parietal/temporal). The false discovery rate was used to adjust *p*-values for multiple comparisons. This was implemented across the 12 models (for each combination of ROI and DTI metric). This analysis protocol was conducted for both the full and segmented tracts. For display purposes, MD and RD values were scaled by a factor of 1000, and DA values by a factor of 100.

2.3. Results – Study A

2.3.1 Full tract analysis

There was a main effect of age group on occipital, $F(1,22) = 11.70$, *adjusted* $p = .002$, n_p^2 $n_p^2 = 0.33$, parietal, $F(1,22) = 20.69$, *adjusted* $p < .001$, $n_p^2 = 0.46$, and temporal tract density, $F(1,22) = 13.27$, *adjusted* $p = .002$, $n_p^2 = 0.37$. Young adults had higher density in occipital and parietal tracts, whereas older adults had higher temporal tract density than young adults (Figure 2-4).

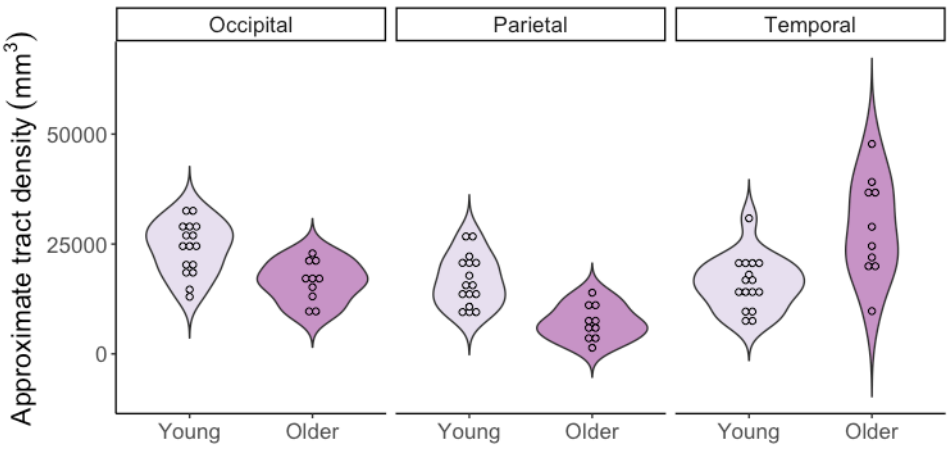

Figure 2-4: Violin plot illustrating the distribution of tract density values across the full splenium tracts in young and older adults. Each circle represents an individual participant.

Main effects of Group on the DTI parameters from the ANCOVA models are presented in Table 2-1. Young adults had significantly higher FA in parietal tracts than older adults. Young adults had significantly lower parietal MD and RD than older adults (Figure 2-5).

Table 2-1: Between-group analysis of full tract bundles

ROI	DTI Metric	Mean Young	*SD* Young	Mean Older	*SD* Older	*F*	df	*p*	*p corrected*	n_p^2
Occipital	FA	0.61	0.02	0.58	0.04	4.95	(1,22)	.036	.108	0.12
	MD	0.85	0.04	0.89	0.07	3.53	(1,22)	.073	.146	0.04
	DA	0.15	0.01	0.16	0.01	1.60	(1,22)	.219	.292	0.01
	RD	0.51	0.04	0.55	0.08	4.04	(1,22)	.056	.135	0.07
Parietal	FA	0.56	0.03	0.50	0.04	17.16	(1,22)	.000	.002**	0.13
	MD	0.79	0.03	0.84	0.03	21.54	(1,22)	.000	.001**	0.20
	DA	0.14	0.01	0.14	0.00	0.01	(1,22)	.916	.916	0.00
	RD	0.49	0.04	0.57	0.05	24.00	(1,22)	.000	.001**	0.20
Temporal	FA	0.53	0.02	0.52	0.02	2.51	(1,22)	.127	.217	0.05
	MD	0.92	0.05	0.94	0.06	1.38	(1,22)	.252	.303	0.09
	DA	0.15	0.01	0.15	0.01	0.52	(1,22)	.479	.523	0.06
	RD	0.62	0.04	0.64	0.05	2.18	(1,22)	.153	.230	0.11

*Note: **p < .01*

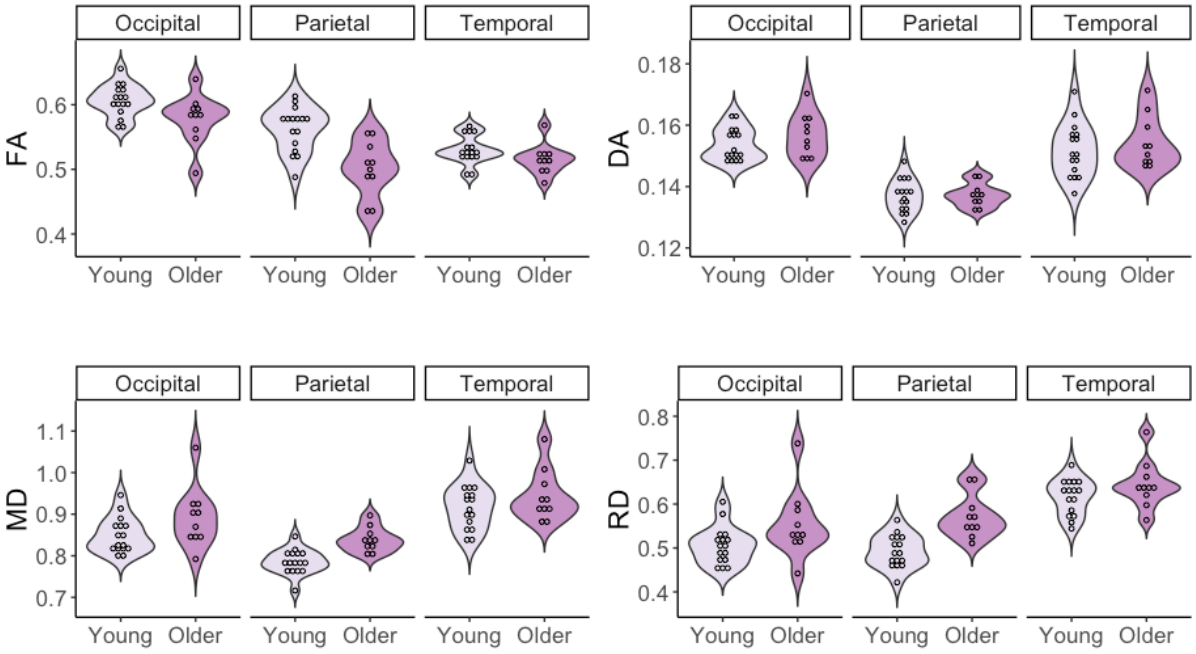

Figure 2-5: Violin plots illustrating the distribution of FA, MD, RD and DA values across the full splenium tracts in young and older adults. Each circle represents an individual participant.

2.3.2 Segmented tract analysis

For the segmented tract analysis, there was an effect of age group on tract density for each of the tract bundles: Occipital, $F(1,22) = 10.05$, *adjusted* $p = .006$, $n_p^2 = 0.30$, parietal, $F(1,22) = 12.72$, *adjusted* $p = .005$, $n_p^2 = 0.35$, and temporal, $F(1,22) = 5.60$, *adjusted* $p = .026$, $n_p^2 = 0.19$. Young adults had higher tract density on average in occipital and parietal tracts than older adults, whereas the reverse was seen for temporal tracts (Figure 2-6).

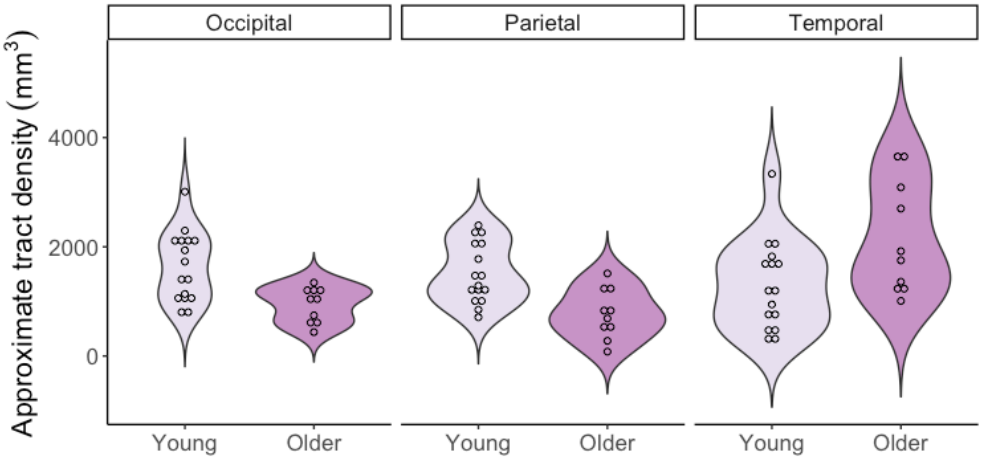

Figure 2-6: Violin plot illustrating the distribution of tract density values across the segmented splenium tracts in young and older adults. Each circle represents an individual participant.

Young adults had significantly higher FA, and significantly lower MD and RD in the parietal tracts (Table 2-2). Furthermore, young adults had significantly higher FA and lower RD in splenium tracts that projected to temporal areas. No differences were observed for occipital tracts (Figure 2-7).

Table 2-2: Between-group analysis of segmented tract bundles

ROI	DTI Metric	Mean Young	*SD* Young	Mean Older	*SD* Older	*F*	df	*p*	*p corrected*	n_p^2
Occipital	FA	0.74	0.03	0.74	0.04	0.27	(1,22)	.606	.909	0.01
	MD	0.86	0.07	0.86	0.07	0.04	(1,22)	.839	.915	0.02
	DA	0.18	0.01	0.18	0.02	0.07	(1,22)	.800	.915	0.01
	RD	0.41	0.05	0.41	0.05	0.00	(1,22)	.963	.963	0.00
Parietal	FA	0.74	0.05	0.63	0.11	13.00	(1,22)	.001	.012*	0.20
	MD	0.83	0.06	0.94	0.13	9.81	(1,22)	.005	.014*	0.14
	DA	0.17	0.01	0.17	0.01	0.04	(1,22)	.837	.915	0.00
	RD	0.38	0.07	0.55	0.17	12.05	(1,22)	.002	.012*	0.18
Temporal	FA	0.77	0.05	0.71	0.05	10.29	(1,22)	.004	.014*	0.20
	MD	0.81	0.08	0.89	0.12	4.72	(1,22)	.040	.081	0.13
	DA	0.17	0.01	0.18	0.01	0.54	(1,22)	.470	.806	0.03
	RD	0.35	0.08	0.46	0.12	7.75	(1,22)	.011	.025*	0.18

*Note: *p < .05*

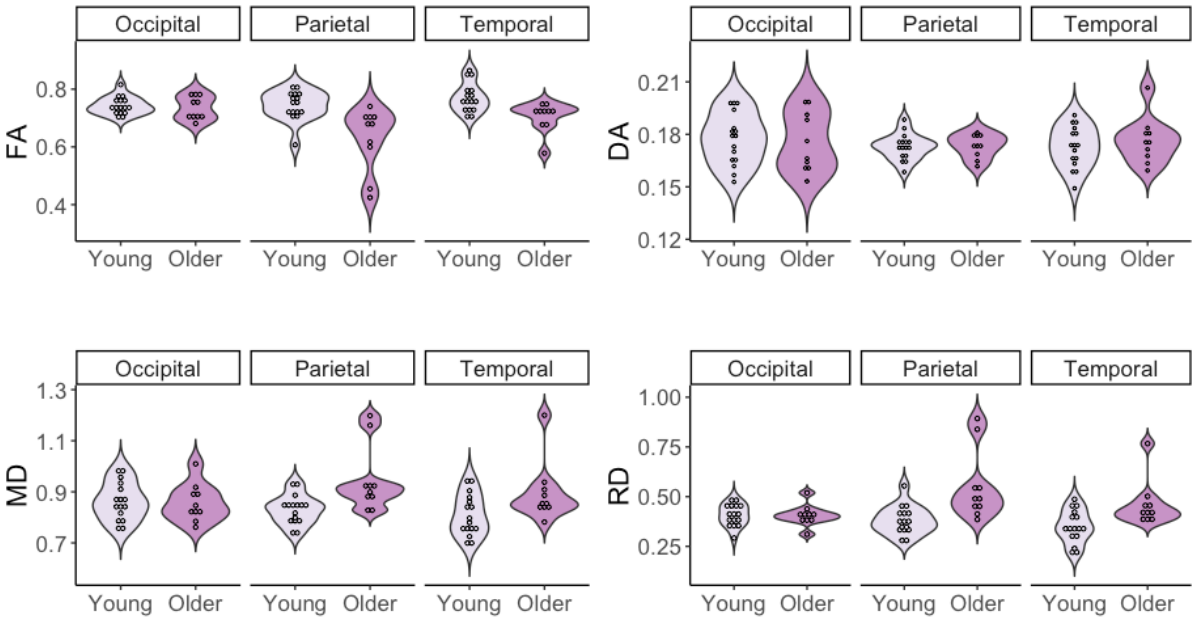

Figure 2-7: Violin plots illustrating the distribution of FA, MD, RD and DA values across the segmented splenium tracts in young and older adults. Each circle represents an individual participant.

2.4 Summary of results – Study A

The analysis of the diffusion parameters of the white matter tract bundles that pass through the CC splenium showed that differential spatial patterns of degeneration occur in older age. We considered firstly the diffusion parameters across the full non-segmented tracts. The analysis revealed that older adults had significantly reduced FA in parietal tracts, but not in occipital or temporal tract bundles. Parietal MD and RD were also compromised in older age. We then segmented each tract bundle at +/- 6mm of the sagittal midline to examine age differences in these tract bundles within the CC splenium itself. An age-related reduction of FA in the temporal and parietal CC segments was observed, while the occipital segments were again preserved in older age. Similarly, older adults had increased MD and RD in parietal and temporal segments compared to young adults, while diffusivity of occipital segments was equivalent between the groups. No group differences were observed in DA across any of the CC bundle segments, again suggesting that it is unlikely that the observed effects are caused by damage to the axons of the tracts. The present analysis includes young and older adult groups comparable to many of the between-group investigations of white matter integrity in the literature (Bennett, Madden, Vaidya, Howard, & Howard, 2010; Davis, Kragel, Madden, & Cabeza, 2012; Madden et al., 2004, 2009). However, lifespan data suggest that many white matter structures do not peak in development until around age 30, and significant decline in some structures may not be observed until later adulthood (Hasan et al., 2009; Lebel, Caverhill-Godkewitsch, & Beaulieu, 2010; Westlye et al., 2010). Therefore, in Study 1B, we set out to replicate this analysis using an independent dataset with more mature young adult (mean age 30 years) and older adult (mean age 80 years) participant groups.

2.5 Method – Study B

2.5.1 Participants

The data used in Study B were collected and provided by the Cambridge Centre for Ageing and Neuroscience (CamCAN) database (Taylor et al., 2016, Shafto et al., 2015; available at http://www.mrc-cbu.cam.ac.uk/datasets/camcan/). CamCAN is funded by the UK Biotechnology and Biological Sciences Research Council (grant number BB/H008217/1), with the support of the UK Medical Research Council and University of Cambridge, UK. The CamCAN database consists of ~700 participants ranging from 18-88 years of age. All participants were classified as being cognitively healthy (MMSE > 24), monolingual from birth (English), and free from neurological disease, high blood pressure, and psychiatric conditions (see Shafto et al., 2014, for a more detailed description of the exclusion criteria). Edinburgh Handedness Inventory (Oldfield, 1971) scores were used to select only fully right-handed participants for the present study. From the remaining participants, 20 young adults and 20 older adults were selectively sampled to have mean group ages of 30 (young adults) and 80 (older adults). Age 30 corresponds to peak maturation of CC tracts according to Lebel et al. (2010), whereas older adults with a mean age of 80 may experience more degeneration than the older adult group in Study 1A (mean age = 68.33). One participant (male, age 85) was omitted from the analysis as parietal tracts could not be detected. The final groups consisted of 20 younger adults (mean age = 30.75, SD = 4.7, range = 23-37, females = 10) and 19 older adults (mean age = 80.21, SD = 2.89, range = 76-86, females = 10; see Appendix A for the ID codes, age and sex characteristics of the participants used in this analysis).

2.5.2 DTI acquisition and pre-processing

Detailed parameters for diffusion tensor imaging are described by Taylor et al. (2017) and Shafto et al. (2014). All participants were scanned for at least ten minutes using a 3T Siemens TIM Trio scanner (Siemens Medical Systems, Germany). Diffusion weighted images were acquired using an echo-planar imaging sequence (30 directions for b-values of 1000 and 2000 s/mm^2, 3 scans at b = 0, TR = 9100 ms, TE = 104 ms, voxel size = 2 mm isotropic, FOV = 192 mm^2, 66 axial slices, averages = 1). DTI data were pre-processed with tools from the FMRIB Software Library (FSL; FMRIB Analysis Group, Oxford, UK). The DTI images were skull-stripped using the Brain Extraction Tool (BET). Corrections for eddy-current-induced distortions were made using the EDDY tool.

2.5.3 Tractography & statistical analysis

The tractography protocol and statistical analyses were identical to that of Study A.

2.6. Results – Study B

2.6.1 Full tract analysis

There were significant between-group differences in full tract density (Figure 2-8). Young adults had higher tract density than older adults in occipital, $F(1,36) = 11.16$, *adjusted* $p = .003$, $n_p^2 = 0.23$, and parietal tracts, $F(1,36) = 5.32$, *adjusted* $p = .003$, $n_p^2 = 0.22$. Older adults had higher temporal tract density than younger adults, $F(1,36) = 47.21$, *adjusted* $p < .001$, $n_p^2 = 0.56$.

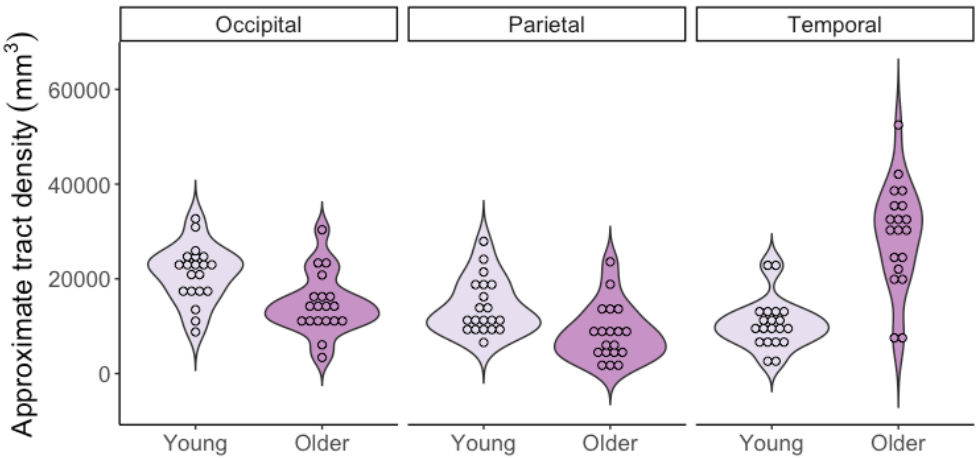

Figure 2-8: Violin plot illustrating the distribution of tract density values across the full splenium tracts in young and older adults from the CamCAN dataset. Each circle represents an individual participant.

Significant age differences were observed across all full tracts and metrics in the CamCAN dataset, with the exception of temporal tract FA (Table 2-3; Figure 2-9).

Table 2-3. Results of CamCAN DTI analysis of full tracts

ROI	DTI Metric	Mean Young	*SD* Young	Mean Older	*SD* Older	*F*	df	*p*	*p corrected*	n_p^2
Occipital	FA	0.63	0.02	0.60	0.04	13.42	(1,36)	.001	.001**	0.10
	MD	0.58	0.03	0.65	0.05	30.97	(1,36)	.000	.000***	0.23
	DA	0.11	0.01	0.12	0.01	17.35	(1,36)	.000	.000***	0.16
	RD	0.34	0.02	0.40	0.06	28.12	(1,36)	.000	.000***	0.21
Parietal	FA	0.57	0.03	0.54	0.04	8.12	(1,36)	.007	.008**	0.05
	MD	0.57	0.02	0.65	0.07	27.74	(1,36)	.000	.000***	0.30
	DA	0.10	0.00	0.11	0.01	15.73	(1,36)	.000	.000***	0.23
	RD	0.36	0.02	0.43	0.06	29.53	(1,36)	.000	.000***	0.28
Temporal	FA	0.54	0.02	0.54	0.03	0.02	(1,36)	.877	.877	0.13
	MD	0.59	0.03	0.65	0.05	24.19	(1,36)	.000	.000***	0.40
	DA	0.10	0.01	0.11	0.01	29.94	(1,36)	.000	.000***	0.34
	RD	0.39	0.03	0.43	0.04	13.68	(1,36)	.001	.001**	0.39

*Note: **p < .01, ***p < .001*

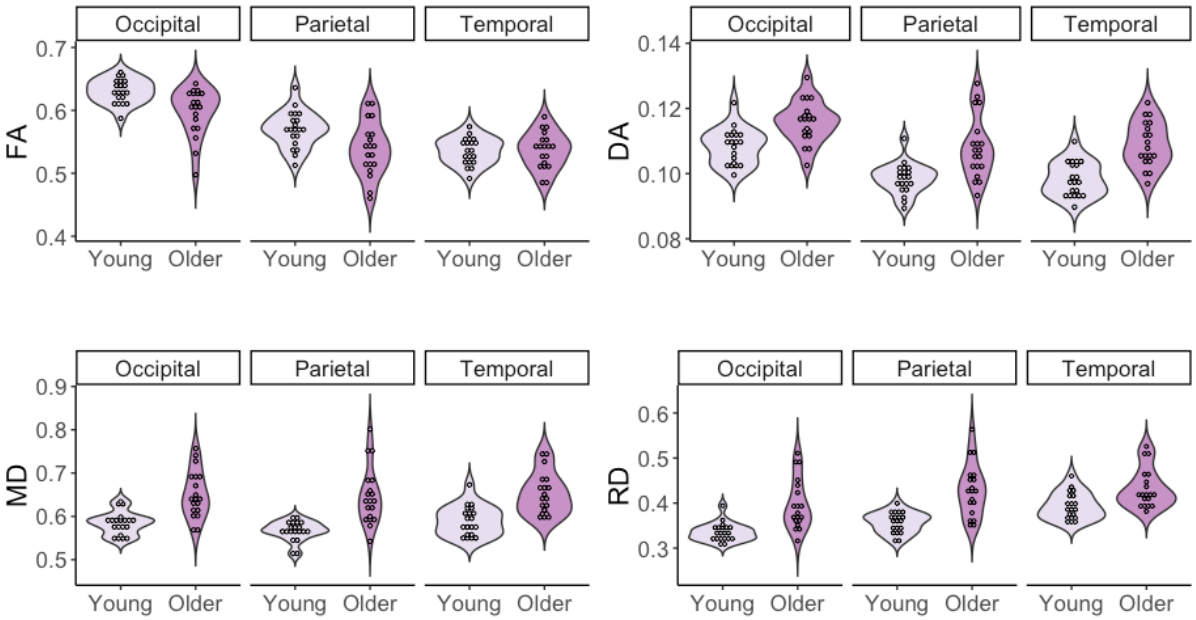

Figure 2-9: Violin plots illustrating the distribution of FA, MD, RD and DA values across the full splenium tracts in young and older adults. Each circle represents an individual participant.

2.6.2 Segmented tract analysis

For the segmented tract density in the CamCAN dataset, group differences were detected in occipital, $F(1,36) = 16.44$, *adjusted* $p < .001$, $n_p^2 = 0.31$, parietal, $F(1,36) = 20.31$, *adjusted* $p < .001$, $n_p^2 = 0.35$, and temporal tracts, $F(1,36) = 26.02$, *adjusted* $p < .001$, $n_p^2 = 0.41$. Young adults had higher density in occipital and parietal tract segments, whereas density was higher in older adults in temporal segments (Figure 2-10).

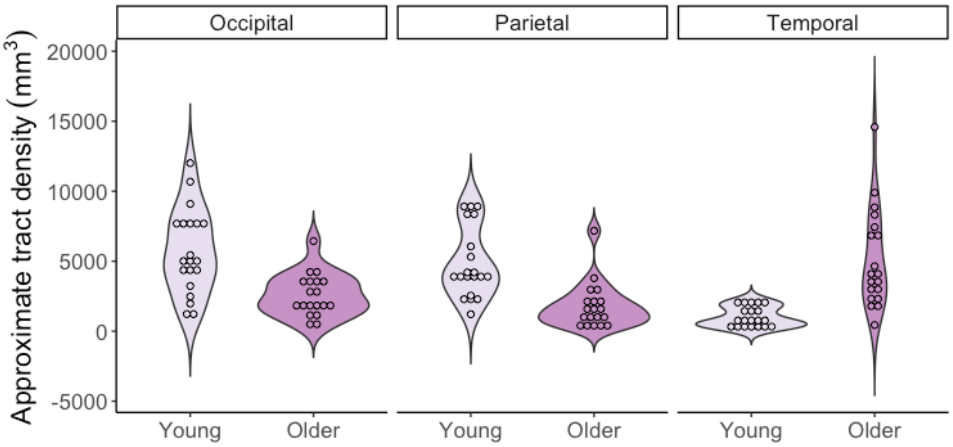

Figure 2-10: Violin plot illustrating the distribution of approximate tract density values across the segmented splenium tracts in young and older adults. Each circle represents an individual participant.

Older adults exhibited increased MD, DA and RD in the parietal segments and increased temporal FA, MD and RD in comparison to young adults (Table 2-4; Figure 2-11). The occipital segments were equivalent across young and older adults.

Table 2-4. Results of CamCAN DTI analysis of segmented tracts

ROI	DTI Metric	Mean Young	*SD* Young	Mean Older	*SD* Older	*F*	df	*p*	*p corrected*	n_p^2
Occipital	FA	0.72	0.05	0.71	0.07	0.08	(1,36)	.780	.780	0.04
	MD	0.53	0.03	0.56	0.05	3.72	(1,36)	.062	.093	0.13
	DA	0.11	0.01	0.11	0.01	3.08	(1,36)	.088	.117	0.06
	RD	0.26	0.04	0.27	0.06	1.13	(1,36)	.295	.354	0.08
Parietal	FA	0.62	0.05	0.60	0.07	0.64	(1,36)	.430	.469	0.01
	MD	0.55	0.03	0.61	0.06	13.73	(1,36)	.001	.003**	0.14
	DA	0.1	0.01	0.11	0.01	10.89	(1,36)	.002	.007**	0.10
	RD	0.32	0.04	0.37	0.07	6.71	(1,36)	.014	.033*	0.08
Temporal	FA	0.76	0.07	0.71	0.06	5.50	(1,36)	.025	.049*	0.01
	MD	0.51	0.04	0.56	0.04	22.67	(1,36)	.000	.000***	0.14
	DA	0.11	0.01	0.11	0.01	4.63	(1,36)	.038	.065	0.06
	RD	0.22	0.05	0.28	0.05	14.64	(1,36)	.000	.003**	0.06

*Note: *p < .05, **p < .01, ***p < .001*

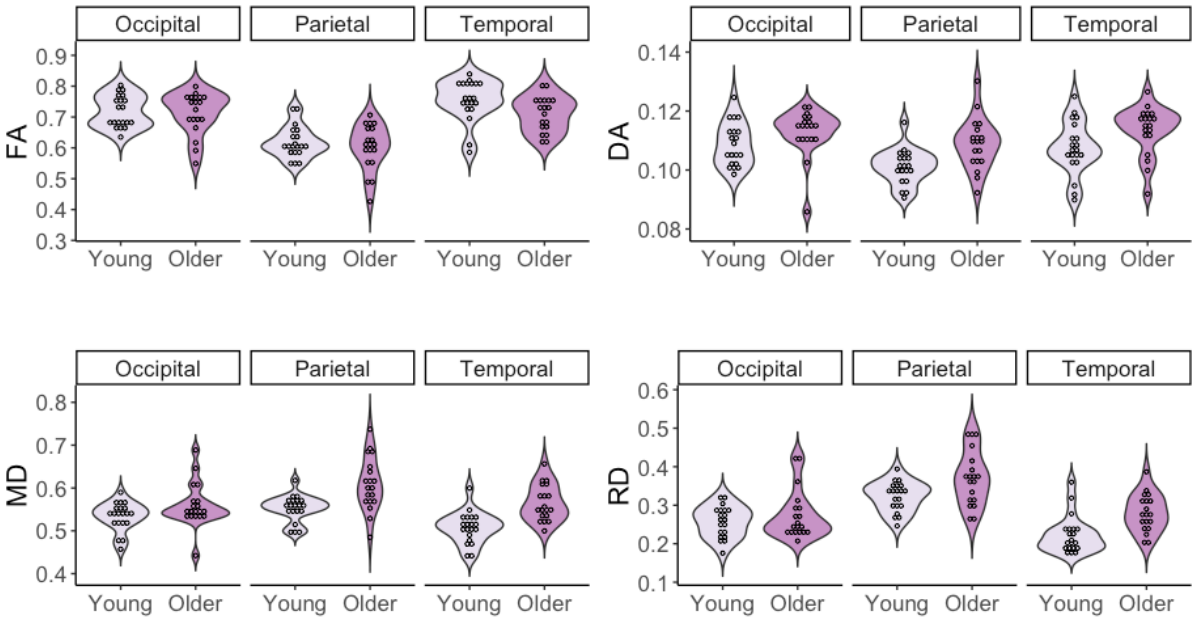

Figure 2-11: Violin plots illustrating the distribution of FA, MD, RD and DA values across the segmented splenium tracts in young and older adults. Each circle represents an individual participant.

2.7 Summary of results – Study B

In the CamCAN sample we attempted to replicate the patterns of age differences observed in Study A with slightly older participant samples. The analysis of the full tracts suggested that age-related differences in all diffusion metrics (except temporal FA) were apparent across each of the ROIs. Specifically, older adults exhibited significant increases in MD and RD, and decreases in FA, that are consistent with an interpretation of reduced white matter integrity in older adults (Van Camp et al., 2012; Wei et al., 2013). However, older adults also exhibited increased DA in all tracts, indicating increased diffusivity along the first eigenvector of the diffusion tensor model, which is usually interpreted as increased axonal integrity (Concha, Gross, Wheatley, & Beaulieu, 2006; Wei et al., 2013). Therefore,

increased DA in older age may reflect continuous axonal maturation with age. In the analysis of segmented tract bundles, effects of age were restricted to the parietal and temporal tracts, similar to the results obtained in Study A. Consistent with the full tract analysis, parietal segment MD, RD and DA were increased in older adults. Temporal tract MD and RD were greater in older adults, but DA was equivalent between the groups.

2.8 General Discussion

The two cross-sectional studies reported above aimed to test whether distinct tract bundles of the CC splenium were differentially affected by age in groups of older adults compared to young adults. Interestingly, results of the full unsegmented tract bundle analysis diverged between studies: Age-related decline of full tracts in Study A was restricted to interhemispheric parietal tracts, whereas the age-related decline of full tracts in Study B was evident in all ROIs. Differences in the ages of the young and older samples between Study A and Study B may provide an explanation for this discrepancy, considering that the samples of Study A were younger than that of Study B. Lebel et al. (2010) presented data demonstrating that while the occipital splenium tracts peak in diffusivity at age 23, parietal and temporal projections peak later in development at ages 29-30. Therefore, the young adults of Study B may have had more developed tracts with higher levels of integrity than the young adults of Study A, on average. Furthermore, very little age-related deficit was observed by age 60 in the data of Lebel et al. (2010). The voxel-wise rather than tractography approach employed by Westlye et al. (2010) suggested that a steep rate of decline occurs only after the age of 60 into later adulthood, although the independent bundles of splenium tracts were not specifically addressed in this study. The discrepancy of age effects between Study A and B could therefore be

attributed to more mature tracts of the younger adult group and more deteriorated tracts in the older adult group of Study B. Additionally, the sample size of Study A was limited compared to Study B, which may have contributed to the disparity of results.

Despite the discrepancy in results of the full tract analysis between Studies A and B, the results of the segmented tract analyses were relatively consistent across both samples, where age-related effects were confined to the parietal and temporal splenium segments. In contrast, the integrity of tracts projecting to the occipital cortices was retained in older adults. These findings support our hypothesis that older adults would experience integrity reductions in splenium connections that project to the areas of cortex that tend to be functionally disrupted during healthy ageing: Parietal and temporal areas. Although this hypothesis is supported, few studies have explicitly investigated the link between parietal and temporal tract bundles and cognitive decline in older age, so the functional implications of decline in these tracts is unknown. Further investigations of possible functions attributed to these tracts are necessary to understand how these changes in white matter integrity may be important for cognitive ageing.

Interestingly, older adults were associated with higher DA than young adults in all full tracts and parietal segmented tracts in Study B. As mentioned, increased DA is consistent with an interpretation of increased diffusivity along the axon. This increase in older adults may therefore reflect continued axonal maturation in older age that coincides with reductions in MD and RD-based integrity, which has been linked to myelination (Wei et al., 2013). Similar patterns have been reported in the CC genu (Bennett et al., 2010; Sullivan, Adalsteinsson, & Pfefferbaum, 2006; Zahr et al., 2009), fornix and external capsule (Bennett et al., 2010; Zahr et al., 2009). The age trends of DA in 5-59 year olds reported by Lebel et al. (2010) also seem to increase as a function of age for occipital, temporal and parietal CC tracts. Bennett et al. (2010) demonstrated that

white matter structures that exhibited age-related increases in RD and DA were structures that showed the largest between-group differences in RD. They suggested that areas that experience simultaneous RD/DA increases may be areas that suffer from age-induced reductions of axonal packing density (i.e. contain fibres of thin diameter), which could drive increases in DA. In line with this hypothesis, studies of fibre composition of the CC indicate that temporal and parietal projections through the CC are thinner in diameter than occipital fibres (Aboitiz, López, & Montiel, 2003; Aboitiz, Rodriguez, Olivares, & Zaidel, 1996; Aboitiz et al., 1992; Caminiti et al., 2013), which may explain our reported age-related increases in DA for segmented parietal tract segments, but not for occipital and temporal tract segments in Study B. The lack of this finding in Study A may again be attributed to the ages of the sample groups.

In both datasets, we investigated differences in approximate tract density between young and older adults. Tract density has been shown to correlate with diffusion metrics, such that it may confound the analysis of diffusivity if not adequately controlled for (Jones, 2010; Jones et al., 2013; Klawiter et al., 2011). This analysis revealed that older adults had lower tract density than young adults in occipital and parietal tracts, whereas temporal tract density was higher in older than in young adults. This robust pattern was stable and consistent across both datasets in the present study. The reductions of parietal tract density in older adults are consistent with the reported effects of age on the diffusion parameters, suggesting that reductions in both density and diffusion co-occur with advancing age. However, age-related reductions in occipital tract density seem to be independent of occipital tract integrity (with the exception of the full tract analysis in Study B), suggesting that ageing may be associated with a reduction in the quantity of occipital splenium tracts, while tract quality is maintained. The finding of increased temporal tract density with a reduction of temporal tract integrity in older adults was

unexpected. A possible explanation is that the interhemispheric temporal tracts continue to generate beyond the peak developmental stage of tract integrity, while the newly generated tracts simultaneously decline in terms of tract integrity. Longitudinal investigations will be necessary to confirm this interpretation, by demonstrating increased density and reduced integrity within participants over time. It should be stressed that quantification of reconstructed tracts must be interpreted with caution. Tract count and density measures are insufficient in quantifying the number or volume of actual axonal fibres that DTI tractography attempts to reconstruct, as tract density metrics may be influenced by other factors such as tract curvature, length, packing density and diameter (Jones et al., 2013). Nonetheless, in our analysis of midsagittal CC segments, many of these features were controlled for.

We have interpreted age differences in the microstructural properties of reconstructed white matter tracts as a difference in the "integrity" of the targeted white matter fibres. Given the context of the study and the assumption that white matter microstructure does indeed deteriorate with age (Bowley, Cabral, Rosene, & Peters, 2010; Peters & Sethares, 2002; Alan Peters, 2002; Wiggins et al., 1988), this interpretation is justified. However, as has been demonstrated and discussed thoroughly (Jones et al., 2013; Takahashi et al., 2002), changes in the microstructural tract properties estimated by DTI may reflect phenomena other than integrity, such as tract density, axon diameter and the presence of crossing tracts (where two or more tracts are imaged within the same voxel). In the present study, we attempted to control for tract density by co-varying for the approximate density of reconstructed tracts. Crossing tracts can lead to the distortion of the tensor model in a given voxel, especially when the crossing tracts diverge in orientation (Jeurissen, Leemans, Tournier, Jones, & Sijbers, 2013), rendering the interpretation of anisotropy and diffusion metrics redundant. As demonstrated by

Jeurissen and colleagues (2013), the CC splenium predominantly consists of voxels with a single (sagittal) fibre orientation, especially in midsagittal segments. Our analysis of the mid-sagittal portion of the posterior CC should therefore have reduced the likelihood of estimating microstructural properties at the locations of crossing tracts, although the analysis of the full tract bundles, which often kink and curve, may be vulnerable to reduced anisotropy caused by crossing tracts.

To summarise, this study identified age-related modulations of the white matter tracts that pass through the splenium of the CC. These modulations were interpreted as a reduction of integrity in the underlying white matter fibres in older age, likely due to demyelination as proposed by prior histological investigations of ageing (Peters & Sethares, 2002; Peters, Moss, & Sethares, 2000; Wiggins et al., 1988). To our knowledge, this is the first study to reveal that older adults experience reduced integrity in midsagittal parietal and temporal commissural segments, while the midsagittal occipital segments are preserved in older age. This effect was replicated and validated in an independent dataset acquired with a different scanner and different scanning parameters. Analyses of the full unsegmented tract bundles were less robust, as the results differed between the two datasets. In one dataset, parietal tracts were exclusively affected by older age. In the second dataset, all tract bundles were significantly affected by older age, which may be attributed to discrepancies in participant group ages between studies. According to our study, the midsagittal portion of interhemispheric parietal tracts may be a robust marker of older age, which is a novel finding. Despite these results, very little research has considered these tracts in isolation, and their functional significance is effectively unknown. Further research is required to identify cognitive tasks that are facilitated by interhemispheric parietal tracts, and to what degree these tasks are affected by healthy normal ageing.

Appendix A – participant codes from CamCAN dataset (for replication)

ID	AGE	HANDEDNESS	SEX	GROUP
CC120727	23	100	FEMALE	YOUNG
CC121194	24	100	FEMALE	YOUNG
CC121317	25	100	FEMALE	YOUNG
CC110319	28	100	FEMALE	YOUNG
CC221033	28	100	FEMALE	YOUNG
CC221580	31	100	FEMALE	YOUNG
CC222956	32	100	FEMALE	YOUNG
CC220828	33	100	FEMALE	YOUNG
CC220901	35	100	FEMALE	YOUNG
CC220635	36	100	FEMALE	YOUNG
CC110098	23	100	MALE	YOUNG
CC121397	27	100	MALE	YOUNG
CC120264	28	100	MALE	YOUNG
CC220132	31	100	MALE	YOUNG
CC220223	33	100	MALE	YOUNG
CC210422	34	100	MALE	YOUNG
CC222125	34	100	MALE	YOUNG
CC221040	36	100	MALE	YOUNG
CC210526	37	100	MALE	YOUNG
CC221977	37	100	MALE	YOUNG
CC610146	76	100	FEMALE	OLDER
CC610212	77	100	FEMALE	OLDER
CC620572	78	100	FEMALE	OLDER
CC721107	79	100	FEMALE	OLDER
CC722421	79	100	FEMALE	OLDER
CC721648	80	100	FEMALE	OLDER
CC720622	81	100	FEMALE	OLDER
CC721704	82	100	FEMALE	OLDER
CC710099	85	100	FEMALE	OLDER
CC720400	86	100	FEMALE	OLDER
CC620610	76	100	MALE	OLDER
CC610658	78	100	MALE	OLDER
CC720188	78	100	MALE	OLDER
CC720511	79	100	MALE	OLDER
CC711128	80	100	MALE	OLDER
CC710350	81	100	MALE	OLDER
CC721504	82	100	MALE	OLDER
CC710548	83	100	MALE	OLDER
CC720290	84	100	MALE	OLDER
CC710551 (removed)	85	100	MALE	OLDER

Chapter 3

3. Study 2: Differential effects of Alzheimer's Disease and Mild Cognitive Impairment on the white matter tracts of the corpus callosum splenium

3.1 Introduction

For years, research has considered how the white matter pathways of the brain are affected by Alzheimer's Disease (AD). Previously described as a disease of the grey matter localised in the hippocampus (Ball et al., 1985), it is now widely accepted that AD is associated with significant atrophy to white matter tissues of the brain (Delbeuck, Van der Linden, Collette, & Linden, 2003; Madhavan et al., 2016; Takahashi et al., 2002). Many studies have demonstrated that parameters extracted from white matter tracts in diffusion tensor imaging (DTI) scans yield highly accurate metrics for classifying groups of AD patients against groups of healthy controls. Oishi, Mielke, Albert, Lyketsos and Mori (2012) found that fractional anisotropy (FA; a measure describing the degree of directionality of a reconstructed white matter tract within a voxel) of the fornix was 81% accurate in classifying individuals with AD. Bozoki, Korolev, Davis, Hoisington and Berger (2012) reported classification accuracies of between 80-86% for FA of the fornix, parietal projection fibres and descending cingulum tracts. Fieremans et al. (2013) found high accuracy for radial diffusivity (RD; the average of the second and third eigenvectors of the diffusion tensor model, often linked to myelination) of the genu (91%), midbody (80%) and splenium (93%) of the corpus callosum (CC) in classifying AD patients against controls.

Whether changes in microstructural white matter integrity are evident during preclinical and prodromal stages of AD is of particular interest for detecting and classifying individuals in the early stages of the disease. Early identification and intervention is thought necessary in order to have significant impact on disease progression (Cummings, Doody, & Clark, 2007). Amnestic mild cognitive impairment (MCI) has been the target of many research initiatives that aim to alleviate AD symptomology (Sherman, Mauser, Nuno, & Sherzai, 2017). The fundamental pathophysiology of MCI is typical of AD symptomology, and is classified via neuropsychological assessment as an isolated and unambiguous memory deficit, but with preserved abilities of independent daily living (Petersen, 2004). Accuracy of white matter tract diffusion tensor parameters has also been assessed in MCI patients. van Bruggen et al. (2012) reported high accuracy values for classifying MCI patients who converted to AD against MCI patients that did not convert, using reductions in FA of the CC (94%), fornix (71%), left cingulum (94%) and right cingulum (85%). Furthermore, Fieremans et al. (2013) found that reductions in diffusion tensor parameters of CC subdivisions was a highly accurate classifier of MCI patients against normal controls, reporting 91% for RD of the genu tracts, 88% for the midbody, and 87% for the splenium.

Other studies that have not reported classification statistics have found significant differences between normal controls and MCI/AD patients in diffusion tensor parameters extracted from the CC splenium, which indicate a reduction of white matter integrity with disease (Agosta et al., 2011; Alves et al., 2012; Hanyu et al., 1999; Naggara et al., 2006; Nowrangi et al., 2013; Parente et al., 2008; Ukmar et al., 2008). The label *splenium* is typically applied to the posterior quarter of the CC, which consists of white matter projections to bilateral occipital, posterior parietal and temporal lobes (Hofer & Frahm,

2006). Acosta-Cabronero, Williams, Pengas and Nestor (2010) demonstrated that splenium FA and RD were correlated with scores on the Addenbrooke's Cognitive Examination, a widely used test of cognitive impairment typical of AD. Clerx, Visser, Verhey and Aalten (2012) conducted a meta-analysis of DTI biomarkers for AD in 55 studies, comprising of 2,791 individuals, finding a large effect size for mean diffusivity (MD; the average of all eigenvectors of the diffusion tensor model) of the splenium in AD and a smaller effect for MCI patients. Preti et al. (2012) found significant reductions of FA in each of the CC subsections in AD patients compared to controls. Furthermore, they found that exclusively the occipital, left temporal and parietal CC tract FA were significantly affected in MCI patients, suggesting that posterior sections of the CC may be targeted at early stages of the AD continuum. Importantly, the splenium seems to be less affected in older age than other sections of the CC, in particular the anterior sections (Bennett, Madden, Vaidya, Howard, & Howard, 2010; Hasan et al., 2009; Kennedy & Raz, 2009; Lebel et al., 2012; Lebel, Caverhill-Godkewitsch, & Beaulieu, 2010). If the splenium is specifically affected by AD, and relatively unaffected by healthy ageing, diffusion tensor parameters of the splenium may be a particularly informative disease marker.

Despite the high classification accuracy of the CC splenium for both AD and MCI (Fieremans et al., 2013), few explicit investigations of the distinct occipital, parietal and temporal tract bundles that pass through the splenium have been conducted. Preti et al. (2012) did look at sub-tracts of the splenium but reported solely on the FA parameter. By considering the splenium bundles in isolation, classification accuracy may be improved and novel insight into the white matter pathways that are targeted by AD will be acquired. The present study aimed to address whether the distinct tract bundles that traverse the CC splenium were compromised in MCI and AD compared to healthy older controls. We

implemented DTI tractography to reconstruct the splenium tract bundles in DTI scans submitted to the National Alzheimer's Coordinating Center database (USA; Beekly et al., 2007; Heller et al., 2014). We compared a group of MCI patients and a group of AD patients to normal healthy controls to determine if the splenium tract bundles were differentially affected by AD neuropathology.

3.2 Method

3.2.1 Participants

Data for the present study were obtained from the National Alzheimer's Coordinating Centre (NACC) repository (Beekly et al., 2007; Heller et al., 2014), funded by the National Institute of Aging (USA). The NACC comprises of demographic, neurocognitive and clinical data, as well as genetic biomarker information and neuroimaging data from individuals seen at 34 Alzheimer's Disease Centres (ADCs) in the United States. From this database we aimed to extract DTI scans from a group of healthy older adults, MCI patients and AD patients.

Scans that were performed within +/- 1 year of an individual's visit to an ADC were obtained from the NACC database. ADC clinical judgements of cognitive status (item NACCUDSD) and underlying aetiology (item NACCALZP) were used to identify cognitively normal, MCI and AD individuals. Cognitively normal individuals were identified as having no cognitive symptoms (NACCUDSD = 1) and no suspected underlying aetiology of AD (NACCALZP = 0). MCI patients were identified as having a clinically judged cognitive status consistent with MCI (NACCUDSD = 3) and a suspected primary aetiology of AD (NACCALZP = 1). AD patients were identified as having a clinically judged cognitive status

consistent with AD (NACCUDSD = 4) and a suspected primary aetiology of AD (NACCALZP = 1). This yielded a total of 403 individuals. To avoid between-site effects we chose participants originating from a single ADC. The ADC containing the largest number of participants with consistent scanning parameters was selected, which yielded 86 participants (35 controls, 20 MCI, 31 AD). As there were fewest individuals in the MCI group, healthy individuals and AD patients were selected to accurately match the age and sex distribution of the MCI group. The age and sex characteristics of the final sample are outlined in Table 3-1.

Table 3-1: Demographic characteristics of NACC sample

Group	Age (mean)	Age (SD)	Sex (M/F)
Normal	75.45	3.80	(10/10)
MCI	75.45	3.91	(10/10)
AD	75.95	3.72	(11/9)

3.2.2 DTI acquisition and pre-processing

MRI parameters for images submitted to the NACC database vary by ADC, and some acquisition information, such as echo time and repetition time, were unavailable. Descriptions of the scan parameters are as follows: 40 directions for b-values of 1000 s/mm^2, 8 scans at b = 0, voxel size = 1 x 1 x 2.5mm^3, FOV = 255 mm^2, 52 axial slices, matrix size = 255 x 255. Corrections for DWI signal drift, subject motion and eddy-current-induced distortions were made using the ExploreDTI software (Leemans et al., 2009). Brain extraction was also implemented by ExploreDTI.

3.2.3 DTI tractography

The tractography protocol was identical to that of the protocol used in Study 1 (Chapter 2). Tract bundles that passed through the CC and projected to temporal, parietal or occipital areas were isolated. Diffusion tensor parameters FA, MD, RD and DA (axial diffusivity: diffusion along the first eigenvector of the diffusion tensor model, often related to axonal integrity) were extracted from each bundle for each participant. Each bundle was segmented at +/- 6mm each side of the midsagittal plane. Analysis was conducted on the full and segmented tract bundles in order to determine whether effects were evident at the midline, where much research has focused.

3.2.4 Statistical analysis

We aimed to test for group differences in FA, MD, RD and DA of the occipital, parietal and temporal bundles of the CC splenium. Since quantitative tract measures have been shown to covary with DTI scalars (Jones et al., 2013; Vos et al., 2011), we first examined group differences in approximate tract density. Tract density is defined as the cumulative density of the voxels that a given reconstructed tract passes through. We first tested for group differences in the approximate tract density of each tract bundle using one-way ANCOVA models, with Group as the independent variable and age and sex as covariates, for each ROI. Participants with tract density of 0 (i.e. missing tracts) were identified and removed from analysis of the DTI metrics. We then tested for group differences in the diffusion tract parameters: ANCOVA models with a between-subjects factor Group and covariates of tract density, age and sex were used to test for group differences in FA/MD/RD/DA at each ROI. Effect sizes were reported in the form of partial eta squared. In the interest of preserving statistical power, and because we were interested in

differences between Normal-MCI, and Normal-AD groups, but not interested in differences between MCI-AD, we ran separate models to compare these pairs of groups directly. False discovery rate (FDR) adjustments to *p*-values for multiple comparisons were implemented across the models for each combination of ROI, DTI metric and Group. The same analysis protocol was conducted for both the full tract and segmented tract analysis. For display purposes, MD and RD values were scaled by a factor of 1000, and DA values by a factor of 100. We also carried out receiver operator characteristic (ROC) analysis to determine the accuracy of each tract and diffusion parameter for distinguishing MCI and AD groups from controls. For a given DTI parameter, ROC analysis determines the sensitivity, specificity and accuracy of that parameter for classifying a group of interest at different thresholds of that measure. Here we report ROC statistics for the optimum threshold. Accuracy is provided using the area under the curve (AUC) measure, expressed as a percentage. Sensitivity and specificity values for the optimum threshold are also presented, which describe the ability to correctly detect disease states and non-disease states, respectively.

3.3 Results

3.3.1 Full tract analysis

There were no significant differences in tract density between controls and MCI individuals. AD patients had significantly reduced tract density compared to controls in the occipital and parietal tract bundles (Figure 3-1; Table 3-2). Both occipital and parietal tract density were good classifiers of AD (AUC > 80%). As one control participant, one

MCI patient and five AD patients were missing parietal tracts (Figure 3-1), they were omitted from the subsequent analysis of diffusion tensor metrics.

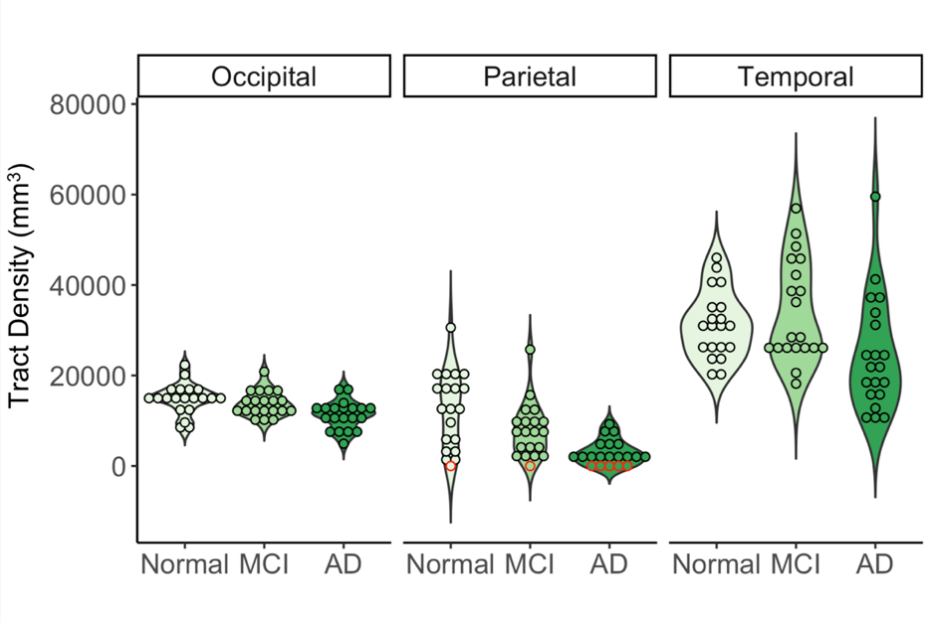

Figure 3-1: Group distributions in diffusion tensor metrics across full tract bundles. Circles represent individual data points. Red circles represent a value of zero, indicating the absence of tracts.

Table 3-2: Group comparisons of full bundle tract density

		Controls vs. MCI						Controls vs. AD					
ROI	**Metric**	***F***	p_{FDR}	n_p^2	***AUC***	***Sens***	***Spec***	***F***	p_{FDR}	n_p^2	***AUC***	***Sens***	***Spec***
Occipital	Density	1.33	.308	0.03	64	70	75	12.83	.003**	0.25	80.50	90	75
Parietal	Density	3.91	.083	0.09	66.63	85	60	22.95	.000***	0.38	83.63	100	65
Temporal	Density	0.95	.336	0.02	44.75	55	60	4.25	.083	0.10	72.75	70	80

*Note: **p < .01, ***p < .001, p_{FDR} = p-values adjusted with the false discovery rate. AUC = area under the ROC curve. Sens = Sensitivity. Spec = Specificity.*

There were no significant differences in full tract diffusion tensor parameters between controls and MCI patients that withstood the FDR correction. However, significant differences in parietal tract MD and RD were apparent between normal older adults and

AD patients (Figure 3-2**,** Table 3-3). Parietal MD was the best classifier of AD against controls, with an AUC of 82.81%.

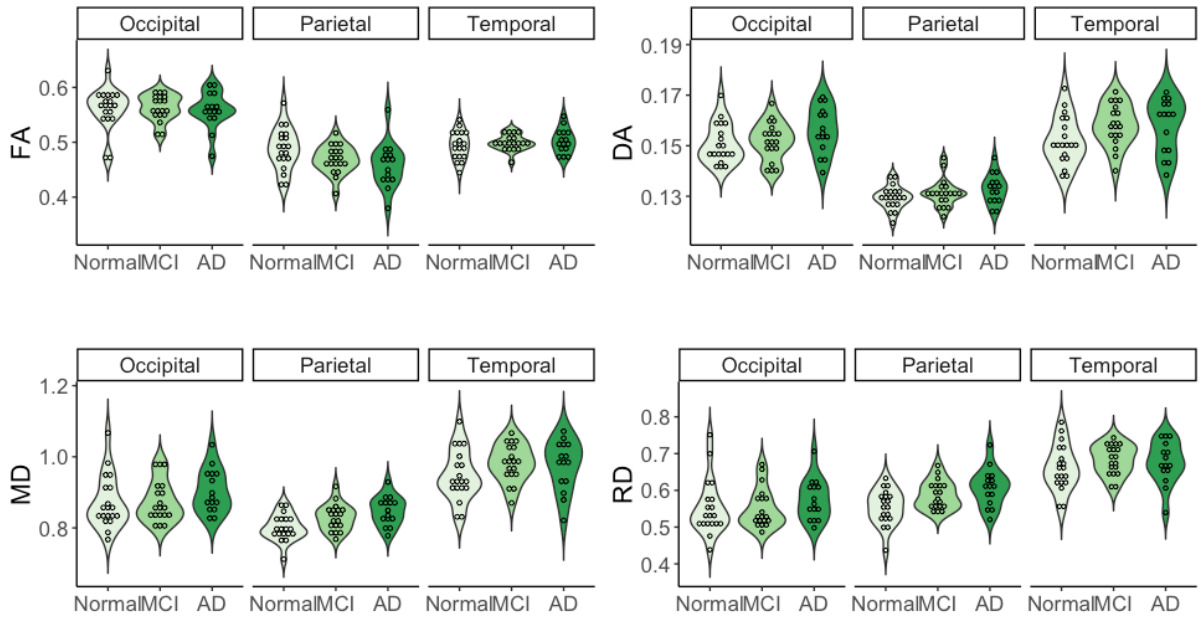

Figure 3-2: Group distributions of diffusion tensor metrics across full tract bundles. Circles represent individual data points.

Table 3-3: Group comparisons of full bundle diffusion tensor metrics

		Controls vs. MCI						Controls vs. AD					
ROI	**Metric**	***F***	p_{FDR}	n_p^2	***AUC***	***Sens***	***Spec***	***F***	p_{FDR}	n_p^2	***AUC***	***Sens***	***Spec***
Occipital	FA	0.02	.917	0.01	50.14	52.63	63.16	0.06	.917	0.04	54.04	73.33	52.63
	MD	0.01	.917	0.00	54.29	78.95	42.11	2.05	.299	0.00	68.07	73.33	68.42
	DA	0.24	.756	0.00	56.23	78.95	52.63	3.41	.178	0.03	67.37	73.33	68.42
	RD	0.02	.917	0.01	48.48	100	10.53	0.95	.477	0.01	64.56	93.33	42.11
Parietal	FA	4.03	.157	0.02	66.20	94.74	36.84	5.78	.117	0.00	73.33	80.00	63.16
	MD	5.53	.117	0.12	70.08	78.95	63.16	12.36	.033*	0.18	82.81	73.33	84.21
	DA	1.44	.405	0.09	59.83	68.42	57.89	4.31	.157	0.23	66.67	60.00	78.95
	RD	6.04	.117	0.08	69.53	100	42.11	10.34	.036*	0.08	77.54	73.33	78.95
Temporal	FA	0.69	.551	0.01	56.23	94.74	31.58	1.26	.405	0.13	58.60	93.33	26.32
	MD	3.71	.166	0.13	66.48	84.21	57.89	1.35	.405	0.03	63.51	66.67	73.68
	DA	5.17	.117	0.15	70.36	84.21	63.16	2.69	.242	0.08	64.91	60.00	78.95
	RD	2.08	.299	0.09	62.33	68.42	57.89	0.47	.630	0.00	59.30	80.00	47.37

*Note: *p < .05, p_{FDR} = p-values adjusted with the false discovery rate. AUC = area under the ROC curve. Sens = Sensitivity. Spec = Specificity.*

3.3.2 Segmented tract analysis

For the segmented tract bundles, there were no differences in tract density between normal adults and MCI. AD patients had significantly reduced tract density compared to normal older adults in the occipital and parietal tract segments (Figure 3-3**,** Table 3-4). Parietal tract density was the best classifier of AD against controls (AUC = 87.63%).

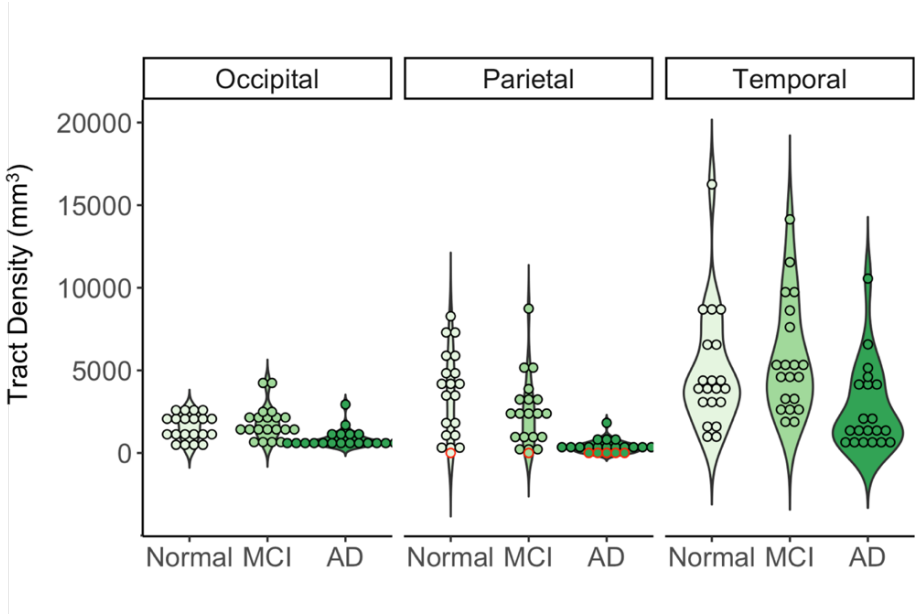

Figure 3-3: Group distributions of tract density across segmented tract bundles. Circles represent individual data points. Red circles represent a value of zero, indicating the absence of tracts.

Table 3-4: Group comparisons of segmented bundle tract density

		Controls vs. MCI						Controls vs. AD					
ROI	**Metric**	***F***	p_{FDR}	n_p^2	***AUC***	***Sens***	***Spec***	***F***	p_{FDR}	n_p^2	***AUC***	***Sens***	***Spec***
Occipital	Density	0.81	.449	0.17	44.7	90	15	9.20	.013*	0.19	75.75	85	75
Parietal	Density	2.18	.222	0.83	63.13	80	60	28.39	.000***	0.43	87.63	95	75
Temporal	Density	0.56	.457	0.98	59.75	60	70	4.96	.064	0.12	70.75	65	80

*Note: *p < .05, ***p < .001, p_{FDR} = p-values adjusted with the false discovery rate. AUC = area under the ROC curve. Sens = Sensitivity. Spec = Specificity.*

Compared to normal older adults, MCI patients had significantly increased MD and RD in parietal tract segments. Both parameters had perfect sensitivity for detecting MCI, but poor specificity, misclassifying up to 63% of controls. Effects of AD were widespread. At occipital segments there were some small effects, whereby AD patients had significantly higher FA and higher DA than controls. In temporal segments, AD patients had significantly higher FA and DA, but lower RD than controls. In parietal segments, AD

patients had higher MD, RD and DA than controls (Figure 3-4, Table 3-5). Parietal DA was the best classifier of AD against controls (AUC = 98.95%), with high sensitivity (100%) and high specificity (94.74%).

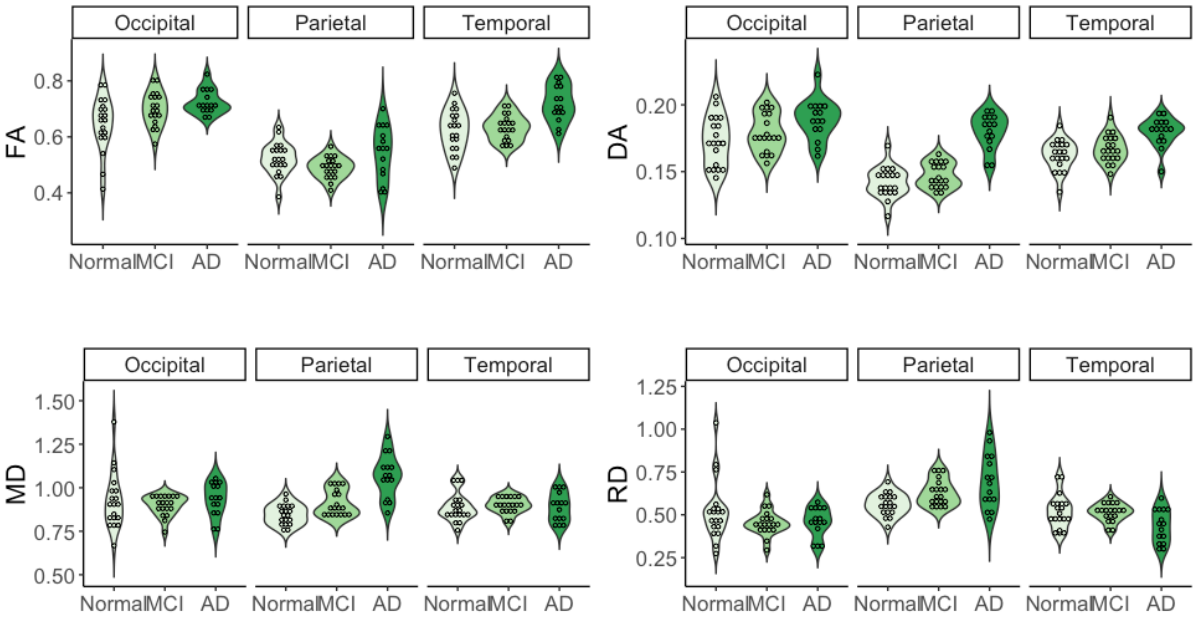

Figure 3-4: Group distributions of diffusion tensor metrics across segmented tract bundles. Circles represent individual data points.

Table 3-5: Group comparisons of segmented bundle diffusion tensor metrics

		Controls vs. MCI						Controls vs. AD					
ROI	**Metric**	***F***	p_{FDR}	n_p^2	***AUC***	***Sens***	***Spec***	***F***	p_{FDR}	n_p^2	***AUC***	***Sens***	***Spec***
Occipital	FA	3.94	.110	0.11	67.59	94.74	36.84	8.09	.023*	0.22	76.49	100	52.63
	MD	0.41	.662	0.01	49.58	89.47	31.58	0.06	.853	0.00	58.60	86.67	42.11
	DA	1.69	.287	0.07	62.33	100	31.58	7.60	.026*	0.14	73.68	80.00	63.16
	RD	2.50	.210	0.06	63.16	84.21	52.63	1.69	.287	0.08	55.79	66.67	52.63
Parietal	FA	4.49	.090	0.08	69.81	94.74	42.11	0.71	.541	0.05	60.35	60.00	73.68
	MD	8.77	.019**	0.16	73.41	100	47.37	45.23	.000***	0.41	95.09	93.33	89.47
	DA	2.52	.210	0.06	65.37	84.21	52.63	79.63	.000***	0.59	98.95	100	94.74
	RD	9.53	.016*	0.17	75.35	100	36.84	11.45	.009**	0.12	75.79	60.00	89.47
Temporal	FA	0.26	.703	0.01	46.81	100	10.53	20.11	.001**	0.27	84.21	80.00	78.95
	MD	0.29	.703	0.01	63.16	89.47	47.37	0.00	.973	0.00	49.47	53.33	68.42
	DA	1.88	.286	0.06	60.39	31.58	94.74	20.05	.001**	0.33	88.07	86.67	84.21
	RD	0.05	.853	0.00	51.25	78.95	42.11	6.86	.033*	0.10	73.68	66.67	73.68

*Note: *p < .05, **p < .01, ***p < .001, p_{FDR} = p-values adjusted with the false discovery rate. AUC = area under the ROC curve. Sens = Sensitivity. Spec = Specificity.*

3.4 Discussion

In the present study we used DTI tractography to examine differences in the occipital, parietal and temporal tract bundles of the CC splenium between cognitively normal older adults and adults with MCI or AD. We found significant differences in occipital and parietal tract density between AD and normal individuals in both the full and segmented tract bundles, but no modulations of tract density were seen in MCI patients. Significant increases in parietal tract MD and RD were evident for AD patients in the analysis of full unsegmented tracts. The analysis of segmented tract bundles yielded differences in AD patients at all ROIs, with the strongest effects observed in parietal segments. In contrast, differences in segmented tract diffusivity between controls and MCI patients were apparent only at parietal tract MD and RD. Increased DA of the parietal CC segments was the best classifier of AD against controls, with an AUD of 98.95%, sensitivity of 100% and

specificity of 94.74%. The best performing classifier for distinguishing MCI patients from controls was RD of the parietal CC segment (AUC = 75.35%), which had perfect sensitivity (100%) but poor specificity (36.84%).

3.4.1 Differences in AD

A number of differences were observed at different ROIs between AD patients and control participants. Increases in MD and RD have been linked to demyelination of white matter tracts in histological studies (Janve et al., 2013; Song et al., 2005), while reductions in DA are linked to axonal damage (Budde, Xie, Cross, & Song, 2009). Both types of atrophy have been demonstrated to occur in AD (Englund & Brun, 1990; Mitew et al., 2010; Sachdev et al., 2013). The strongest between-group effects and highest classification accuracies were evident in the parietal tracts of AD patients, particularly for parietal MD, DA and RD, while effects of FA were absent. To our knowledge, Preti et al. (2012) provided the only other report of reduced parietal tract integrity in AD using the tractography approach. However, they reported significant reductions of FA in unsegmented posterior parietal tracts of the CC in both AD and MCI groups, while differences in MD, RD and DA were not investigated. This pattern was not replicated in the present study, which revealed no group differences in parietal FA for either MCI or AD patients.

Interestingly, some of the differences we observed between AD and controls were consistent with an interpretation of higher white matter integrity in the AD group. For example, AD patients expressed increased DA in each ROI compared to controls, as well as increased FA in both the occipital and temporal tracts. High DA is often linked to high axonal integrity. For example, Concha, Gross, Wheatley and Beaulieu (2006) demonstrated significant DA reductions in three patients that underwent callosotomy,

compared to DA pre-surgery. However, the present finding of increased axonal integrity in AD is incompatible with preclinical studies that have demonstrated axonal damage due to AD (Sachdev et al., 2013). Increased DA in the posterior CC of AD patients has been observed previously (Acosta-Cabronero, Alley, Williams, Pengas, & Nestor, 2012; Acosta-Cabronero et al., 2010; Huang et al., 2012), validating the current results, though the mechanisms by which these microstructural changes occur are unknown. Acosta-Cabronero et al. (2012) suggested that increased DA may be a "state-specific" biomarker, as the level of integrity remained stationary over the course of one year. Aung, Mar and Benzinger (2013) suggested that increased DA may reflect a process known as reactive astrogliosis. Reactive astrogliosis refers to the abnormal generation of glial cells, known as astrocytes, in response to the degeneration of neurons in neurodegenerative disorders. While this process is known to occur in AD (Jain, Kumar Wadhwa, & Ramanlal Jadhav, 2015), the relationship with DTI parameters is yet to be verified in preclinical models of AD or in post-mortem studies of humans, as *in vitro* imaging is required to examine astrogliosis. Bennett et al. (2010) and Zahr, Rohlfing, Pfefferbaum and Sullivan (2009) reported increased DA and increased RD in the CC of older adults compared to young adults, and regions consistent with this pattern had the strongest age differences in RD (Bennett et al., 2010). They hypothesised that simultaneous increases in DA and RD are due to reduced axonal packing density in regions where fibres are of thin diameter, such as the CC genu (Bennett et al., 2010). Our observation of increased DA in AD patients at parietal and temporal CC segments may indeed reflect reduced packing density; these fibres are known to have thinner and less myelinated fibres compared to occipital fibres (Aboitiz et al., 2003, 1992). Thus, AD may be associated with an accelerated reduction of axonal packing density in CC regions that contain small-diameter fibres. Interestingly, increased DA in parietal tracts was the strongest classifier of AD in the present study.

Further multimodal histological/DTI studies are necessary to understand the underpinning of simultaneous increases in DA and RD in ageing and AD.

Similarly, higher FA is generally associated with increased white matter tract integrity. The FA metric can be difficult to interpret because FA is mathematically constructed from a combination of the other diffusion parameters (O'Donnell & Westin, 2011). Specifically, FA characterises the disproportion between DA and RD, and can be inflated due to facilitated DA or restricted RD (Scholz, Tomassini, & Johansen-Berg, 2013). We propose that this effect was driven by the increases in DA observed in AD patients in the present study, and reject the interpretation that AD patients are experiencing significantly improved white matter integrity compared to healthy counterparts.

MD and RD were also significantly elevated in AD patients in both the full and segmented parietal tract bundles. RD has been linked to myelination in animal models (Sun et al., 2006; Wei et al., 2013), with an increase in RD corresponding to demyelination. Like FA, MD is another composite measure, averaging the information from both RD and DA. Some have reported higher correlations between RD and MD than between DA and MD, and MD correlates with the same histological features as RD, suggesting it is sensitive to myelination (Wei et al., 2013). Therefore, increased MD and RD in parietal tracts of AD patients likely represents demyelination, a well-documented feature of AD (Bronge et al., 2002; Brun & Englund, 1986).

Parietal tract density was significantly lower in AD patients compared to controls. It has been discussed thoroughly that tract quantification cannot be directly interpreted as a 'count' of the anatomical white matter fibres (Jones, 2010; Jones et al., 2013). However, the measure seems to be indicative of AD and should not be discounted by initiatives that wish to classify AD neuropathology. Interestingly, seven individuals, including five AD patients, were devoid of reconstructed parietal commissural tracts

during the analysis, whereas there were no missing occipital or temporal tracts across the entire sample. Future work is necessary to determine if missing parietal tracts could be a clinically or functionally relevant feature of normal ageing or AD pathology. In Chapter 2 (Study 1), increases of parietal tract DA were evident in older adults compared to young adults. Currently it is not possible to distinguish between axonal maturation and a process like astrogliosis using a single measure like DA. Altered commissural parietal tract integrity is therefore not specific to AD, and the deterioration of integrity in AD likely reflects an exacerbation of the deterioration observed in normal ageing. To our knowledge, the present study is the only study to report significant alterations of MD, RD, DA and tract density from interhemispheric parietal tracts in AD patients. Interhemispheric parietal tract parameters could be included as features in predictive algorithms to classify AD in future initiatives.

3.4.2 Differences in MCI

We observed surprisingly few differences between MCI patients and controls, where effects were limited to weak increases in MD and RD of the interhemispheric parietal tracts, likely indicating demyelination (Bronge et al., 2002; Brun & Englund, 1986). Preti et al. (2012) reported that parietal, occipital and left temporal tract FA were compromised in MCI patients compared to controls, inconsistent with the lack of significant FA effects presented here. Preti et al. (2012) did not report on other diffusion metrics, so it is unclear if our MD and RD differences were evident in their sample. In this study, MCI patients did not exhibit an increase in DA like the AD group, although there was a trend towards elevated DA in MCI participants in all ROIs. This is in line with Acosta-Cabronero et al. (2012)'s interpretation of increased DA as a "state-specific"

rather than "stage-specific" marker of AD, and suggests that these microstructural changes may only be evident in later stages of the disease. Future studies should investigate if increased DA is a useful marker of conversion from MCI to AD.

Many studies have found no differences between MCI and controls in the tracts of the entire posterior CC (Alves et al., 2012; M Di Paola, Spalletta, et al., 2010; Nikki H Stricker et al., 2016). It is likely that there is high variability between study samples, especially when information about symptom onset, severity and stability within the MCI category are not taken into account (Albert et al., 2011; Ellendt et al., 2017; Petersen, 2004). Koepsell & Monsell, (2012) reported that 16% of patients in the NACC database with a diagnosis of MCI return to normal within one year. Ellendt et al. (2017) found that remission from MCI was predicted by single domain impairment, whereas individuals with deficits in multiple domains were more likely to convert to full AD. These factors may lead to the detection of fewer differences between MCI patients and controls in neuroimaging studies. Alternatively, noticeable differences in posterior CC tracts may not be evident at this early stage of the disease trajectory.

3.4.3 Future directions and caveats

The present study benefitted from samples of MCI and AD patients recruited in a clinical setting, in which expert clinical judgements about symptom aetiology were available to categorise individuals into the respective study groups. Additionally, the groups were carefully matched to avoid confounding effects of age and sex. One limitation of the study is that participants were not matched for level of educational attainment or cognitive reserve, which some studies have suggested might modulate both white matter integrity (Teipel, Meindl, et al., 2009) and the risk of AD (Meng & D'Arcy, 2012; Sharp & Gatz, 2011;

Valenzuela & Sachdev, 2006). Similarly, evidence of stability or worsening of symptoms over time would have been useful to ensure the MCI group were not liable to return to normal cognitive status. The DTI tractography method itself is associated with various limitations. Anisotropy cannot be correctly estimated at voxels where independent DTI tracts diverge (Lee, Park, Park, & Hong, 2015). However, commissural tracts of the midsagittal CC are unidirectional and uninfluenced by crossing fibres (Acosta-Cabronero et al., 2012), and therefore our analysis of the segmented tract bundles will have avoided any influence of crossing tracts. Diffusion tensor parameters may also be influenced by factors such as tract density (Jones et al., 2013), diameter and packing density of the anatomical fibres (Takahashi et al., 2002), especially in studies of neurodegeneration (Bennett et al., 2010). In the present study we attempted to control for group differences in tract density in our statistical analysis. Quantification of axon diameter and packing density were not accessible using the DTI method. Although it is unknown if AD modulates these features, the group differences in diffusion tensor scalars observed in this study may reflect underlying group differences in fibre diameter or packing density. To preserve statistical power, we did not examine group differences in the left and right projections of the CC tract bundles. Fibres of the CC are naturally asymmetrical, although this may be influenced by factors like sex, handedness and individual differences (Aboitiz et al., 1992; Dorion et al., 2000; Luders et al., 2006). Left or right tract segments could potentially be differentially affected by ageing and AD pathology. Future work could benefit from examining lateralisation effects in healthy older adults and individuals with AD symptoms.

To conclude, this study has determined that the parietal commissural tracts of the CC are a highly predictive feature of AD, and moderately indicative of MCI. Increased parietal tract DA was the most accurate classifier of AD patients against controls

(98.95%). Further work is necessary to determine the functional specificity of interhemispheric parietal white matter tracts, which according to the literature are a largely understudied pathway of the brain. Furthermore, the underpinnings of DA increases at parietal and temporal CC regions in AD patients warrants further exploration, as there is currently no consensus as to what microstructural change is being indexed. Future investigations that classify AD patients using DTI scans would benefit from the inclusion of segmented parietal interhemispheric tract parameters.

Chapter 4

4. Study 3: Visual and visuomotor interhemispheric transfer time in healthy ageing (Scally et al., 2018b, *Neurobiology of Aging*)

4.1 Introduction

Aging is associated with white matter degeneration in the brain (Barrick, Charlton, Clark, & Markus, 2010; Bastin et al., 2010; Davis et al., 2009; Tang, Nyengaard, Pakkenberg, & Gundersen, 1997). In particular, damage to the structure known as the corpus callosum (CC) is a strong predictor of global cognitive and motor deterioration in later life (Frederiksen et al., 2012; Jokinen et al., 2007; Penke et al., 2010; Ryberg et al., 2011). The evidence from neuroimaging suggests that differential patterns of degeneration in the CC may be related to typical and pathological aging (Bastin et al., 2010; Penke et al., 2010; Salat et al., 2005). For example, white matter integrity in the posterior section of the CC has been related to processing speed, hypertension and cognitive abilities in older adults (Penke et al., 2010; Wong et al., 2017). Therefore, rigorous measurement of the CC and its associated functions has the potential to provide important information about how the brain ages successfully and unsuccessfully.

Neuroimaging has provided valuable insight into how the structure of the CC is affected by aging (Frederiksen et al., 2012; Sullivan et al., 2010). It has increasingly been shown that white matter integrity in the aging CC follows an anterior-posterior gradient of decline. Age-related degeneration of CC fibres occur primarily in the anterior section known as the genu (Bastin et al., 2008, 2010; Hou et al., 2012; Madden et al., 2009; Salat et al., 2005), which consists of small-diameter fibres that connect the frontal lobes. In

contrast, the more posterior splenium, which connects the occipital lobes, appears to be spared in older adults (Bastin et al., 2010; Hou & Pakkenberg, 2012; Salat et al., 2005). While these specific patterns have been well documented and replicated, less emphasis has been placed on the assessment of functions that may be targeted by age-induced alterations to specific CC subsections. A primary function of the CC is to facilitate information transfer between hemispheres (Bloom & Hynd, 2005; Brown, Bjerke, & Galbraith, 1998; Rugg, Milner, & Lines, 1985), a process known as interhemispheric transfer. For example, a stimulus observed through the left visual hemifield, and therefore processed by the contralateral right hemisphere, needs to be transferred to the left hemisphere before making a right hand response to that stimulus. This process was exploited in a classic paradigm pioneered by Poffenberger (1912), which attempts to measure interhemispheric transfer time (IHTT). The paradigm considers the difference in reaction times (RTs) through the interhemispheric (crossed; e.g. left hemifield - right hand) and intrahemispheric (uncrossed; e.g. left hemifield - left hand) response pathways, known as the crossed-uncrossed difference (CUD). IHTT can also be measured via the lag between ipsilateral and contralateral event-related potentials (ERP) that are evoked in response to the Poffenberger stimulus (Saron & Davidson, 1989b). Surgical sectioning or under-development of the CC is associated with slower IHTT (Brown et al., 1998; van der Knaap & van der Ham, 2011), suggesting that white matter degeneration in aging may also increase estimates of IHTT.

Despite the preservation of the splenium fibres, a number of studies have reported that IHTT is lengthened in older adults. This has been widely described by studies employing the CUD measure (Bellis & Wilber, 2001; Davis, Kragel, Madden, & Cabeza, 2012; Jeeves & Moes, 1996; Reuter-Lorenz & Stanczak, 2000), though others have failed

to observe any aging effects (Linnet & Roser, 2012; Schulte et al., 2013). For the ERP measure, Curran et al. (2001) reported an increase in the latency of the ipsilateral P1 component in older adults, indicating an increase in IHTT. Hoptman et al. (1996) contrarily reported no difference in the latency of ipsilateral components between young and older groups, although there was a trend towards an elongated IHTT for older adults.

Inconsistent age effects and lack of correlations between the CUD and ERP (Saron et al., 1989) could be explained by the idea that behavioural and ERP measures describe IHTT through independent callosal pathways. Much evidence suggests that the CUD may rely on transfer through more anterior CC regions, such as the CC midbody or even genu, rather than splenial fibres. Tomaiuolo, Nocentini, Grammaldo and Caltagirone (2001) reported that the CUD (measured across > 2000 trials) was elongated in a patient with anterior lesions to the CC, while the splenium and rostrum were still intact. Similarly, Di Stefano, Sauerwein and Lassonde (1992) found an increased CUD in two acallosal patients and one patient with anterior CC lesions. In contrast, Tassinari et al. (1994) did not observe an elongated IHTT in six patients with exclusively anterior or posterior regions. However, as evident in their report, midbody fibres were preserved in at least four of these patients, which may have protected their CUD estimates (Zaidel & Iacoboni, 2003). In healthy participants, Schulte et al (2005) observed that the CUD was significantly correlated with the genu and marginally with the splenium in healthy adults, indicating that the genu may be the more involved region. Furthermore, investigations of the Poffenberger paradigm using fMRI have yielded premotor, sensorimotor and prefrontal activations (Iacoboni & Zaidel, 2004; Tettamanti et al., 2002), as well as activations in the CC genu (Gawryluk, D'Arcy, Mazerolle, Brewer, & Beyea, 2011; Omura et al., 2004; Tettamanti et al., 2002; Weber et al., 2005) and the CC midbody (Gawryluk et

al., 2011), supporting a lack of involvement of posterior regions. Iacoboni & Zaidel (2004) found a strong correlation (r = 0.9) between the CUD and BOLD activity in the right superior parietal cortex, indicating that transfer as measured by the CUD may depend on CC midbody fibres that connect sensorimotor areas, rather than on the genu or splenium.

The possible dependence of the CUD on anterior interhemispheric pathways, coupled with age-related decline in the CC genu, may account for the reports of an increased CUD in older adults. However, these findings are less able to explain the reports of older age IHTT as measured by visual ERPs (Curran et al., 2001). Westerhausen et al. (2006) demonstrated that IHTT between contralateral and ipsilateral P1 peaks was correlated with posterior CC integrity, indicating that the splenium fibres are the most likely pathway for visual transfer. Further investigations are clearly necessary to untangle which specific functions of the CC are affected by older age. In this paper we review the traditional measures of IHTT and propose a constrained ERP approach in order to revisit the issue of how IHTT is affected by aging.

Despite being widely used, the CUD and ERP measures are associated with various shortcomings. CUD estimates can be as low as 2ms (Iacoboni & Zaidel, 2000; Marzi, Bisiacchi, & Nicoletti, 1991), which is quicker than the conduction velocity of the largest callosal fibres (Aboitiz, Scheibel, Fisher, & Zaidel, 1992). Furthermore, the CUD often takes a negative value (e.g. Braun, Villeneuve, & Achim, 1996; Marzi et al., 1991; Tettamanti et al., 2002), unintuitively suggesting that there is no temporal cost associated with interhemispheric transfer. To date, nobody has been able to fully account for the negative CUD (Chaumillon, Blouin, & Guillaume, 2014; Derakhshan, 2006). Similarly, ERP estimates of IHTT can be negative. For instance, Saron et al. (2003) reported that peak latency measures of IHTT were in the anatomically predicted direction in only 80% of

participants. The ERP approach requires the selection of peak latencies at the single-subject average level, which involves defining a time window around the component of interest and selecting the latency of the most prominent positive or negative peak. Single-subject averages do not always have an clear morphology (see e.g. Li, Bin, Hong, & Gao, 2010), likely due to trial-by-trial variability in the P1/N1 latencies. Ambiguity in peaks may lead to skewed estimates of the component latencies, thus conflating the estimate of IHTT.

Recent studies have demonstrated that visual evoked potentials like the P1 and N1 arise from event-related phase synchronisation of ongoing EEG oscillations in the theta (4-8 Hz) and alpha (9-14 Hz) frequency bands (Freunberger et al., 2008; Gruber et al., 2014; Gruber, Klimesch, Sauseng, & Doppelmayr, 2005; Klimesch et al., 2004). Gruber et al. (2014) provided compelling evidence that for a given participant, the grand average P1 includes trials which do, and do not have positive-going alpha phase during the P1 time window. When there was negative going alpha phase in this time window, the P1 potential was not elicited in response to the stimulus, and behavioural responses to these stimuli were more delayed. This suggests that to obtain a true measure of the P1 component, trials with negative going phase during the P1 time window should be removed from the dataset.

In the present paper, we apply this logic to ERPs acquired during the Poffenberger paradigm by firstly analysing IHTT in distinct alpha and theta frequency bands (since these are the frequencies of interest for the P1 and N1 components) and secondly filtering out trials where the phase of the theta or alpha oscillation is in the opposite direction to that of the expected component (i.e. negative phase during the P1 time window; positive phase during the N1 time window). Our hypothesis is that, consistent with the

preservation of the splenium in aging (Bastin et al., 2008, 2010; Hou et al., 2012; Madden et al., 2009; Salat et al., 2005), IHTT using this constrained ERP approach will be preserved in older adults to the level of young adults. We also calculated the CUD measure using the mean and median of the reaction time distributions to compare between young and older adults.

4.2 Method

4.2.1 Participants

Twenty-three healthy young adults (ages 18-27) and 32 healthy older adults (ages 63-80) participated in this study (see Table 4-1). All participants were right handed (self-reported) and had normal or corrected-to-normal vision, with no history of stroke or other neurological problems. Older adults were screened for Alzheimer-related memory impairment using the Memory Alteration Test (Rami, Molinuevo, Sanchez-Valle, Bosch, & Villar, 2007). No participants were removed based on these scores. Chi-square tests indicated no significant differences between groups across sex, X^2 (1) = 0.09, p = .758. The groups did differ in terms of education, with older adults having slightly more years in education than young adults, t(54.98) = -2.22, p = .03.

Table 4-1: Participant demographics

	Young (n = 23)	**Older (n = 32)**
Age	19.86 (2.15)	69.75 (4.91)
Years of Education	14.95 (2.01)	17.25 (4.50)*
Sex (M/F)	(7/16)	(11/21)^{ns}
M@T	-	45.87 (37-50; cut-off = 37)

Note: *p < .05, ns = non-significant

4.2.2 Behavioural Paradigm

Participants were seated 57cm from a CRT monitor (1024x768 pixel resolution, 75Hz). A black fixation cross was positioned at the centre of a grey background. A 200Hz warning tone preceded a target stimulus by a pseudorandom interval of 500/750/1000ms. The target stimulus consisted of a black and white circular checkerboard with a diameter of 3° of visual angle. The target was presented 4° to the left or right of fixation cross (measured from the centre of the fixation cross to the centre of the target stimulus) for 50ms. The participant was instructed to fixate on the cross, and to quickly make a manual response by pressing a button with their index finger when they detected a checkerboard. A blank screen was presented between trials for either 1250/1500/1750ms to allow for the dissipation of ERP activity between trials.

Participants completed 330 trials of the task, divided into six blocks. Each block contained 25 stimulus presentations to the right (RVF) and left visual field (LVF) in a pseudorandom order. Five catch trials, in which no stimulus appeared, were also included to monitor the attention of the participant. In a given block, participants were asked to respond with a button press using either the left or right hand. The response hand alternated between blocks and the order was counterbalanced across participants. Fixation was monitored using a video-based eye tracker (Eyelink 1000; SR Research) recording at 1000Hz. Trials were rejected if the participant made a saccade outside of a 2x2 degree boundary centered on the fixation cross before they made a manual response.

4.2.3 Reaction time processing

Reaction times below 150ms and above three standard deviations of the single-subject mean RT were omitted from the data. We calculated the mean and median RT across the conditions of hand (left/right) and visual field (LVF/RVF). Raw CUD estimates were calculated by subtracting the mean/median RTs from the uncrossed conditions ((LVF-left hand + RVF-right hand)/2) from the mean/median crossed RTs ((LVF-right hand + RVF-left hand)/2).

4.2.4 EEG acquisition and pre-processing

EEG was recorded via 64 electrodes on a cap, arranged in the international 10-20 system (Jasper, 1958), and amplified using NeuroScan Synamps^2 amplifiers (Compumedics). Bipolar vertical electrooculographic electrodes were placed above and below the centre of the left eye. All leads were checked for proper contact with the scalp by ensuring that the direct current electrode offset was below 10kOhm. Activity was digitized on 24 bits with a sampling rate of 1024 Hz. EEG analysis was conducted using Matlab (Mathworks) and the EEGLAB toolbox (Delorme & Makeig, 2004). Channels were band-pass filtered offline between 1-30 Hz and down-sampled to 256 Hz. Channels containing spurious artefacts were identified by visual inspection and removed. Infomax independent component analysis (ICA) was used to remove eye movements and muscle artefacts from the data. Removed channels were interpolated using spherical spline interpolation. Before extracting epochs, the continuous data was bandpass filtered into the theta (4-8 Hz) and alpha (9-14 Hz) bands with a zero-phase IIR Butterworth filter using the *filtfilt* function in Matlab. Epochs were extracted from the data between -200ms and 700ms

relative to stimulus onset and baseline corrected between -200 and 0ms. Trials that exceeded a ±75 μV amplitude threshold were rejected. The data was re-referenced to the common average and separated into LVF and RVF presentation conditions.

4.2.5 Data reduction and constrained ERP analysis

Our analysis of the EEG was restricted to two regions in the posterior right and left hemisphere, in which the P1 and N1 components are typically evoked. Electrode clusters from left (P3, P5, P7, PO5, PO7) and right hemispheres (P4, P6, P8, PO6, PO8) were averaged to make two composite regions of interest (ROIs). Time windows of interest were defined for the detection of a P1 and N1 component. These were set liberally at 70-200ms for the P1 and 145-280ms for the N1. A custom Matlab script was used to identify trials that contained a negative peak in the contralateral ROI during the P1 time window or a positive peak during the N1 time window at either the alpha or theta frequency bands, and to mark and remove those trials from further analysis. The P1 and N1 peak latencies were calculated in the same time windows in each of the remaining trials (see Figure 4-1). Single-trial peaks were then averaged for each participant (see Figure 4-2 for an example). It is important to clarify that the ERP estimates of IHTT are independent of the crossed and uncrossed conditions of the CUD paradigm because visual transfer occurs automatically for every trial regardless of the manual response, and unlike the CUD, ERP-IHTT can be calculated on a single trial basis.

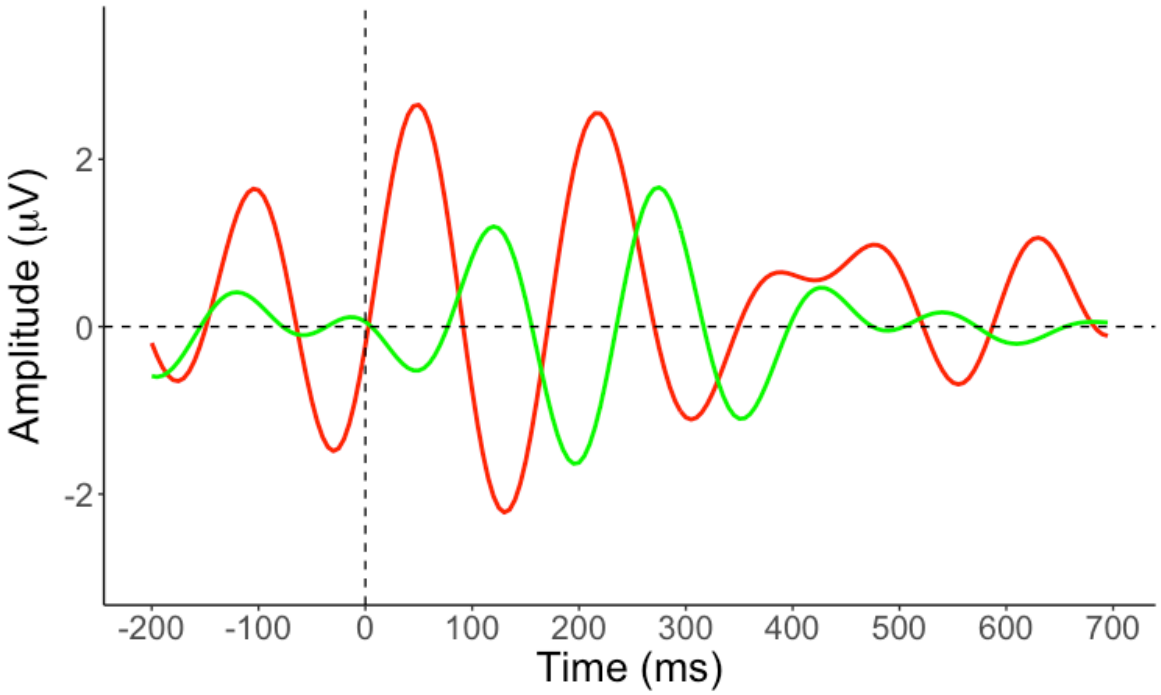

Figure 4-1: Illustration of the constrained ERP approach. Trials with negative going deflections in the P1 time window (70-200ms) and positive-going deflections in the N1 time window (145-280ms) were removed from the data of each subject. The red line reflects the mean signal from rejected trials in one example participant. The green signal represents the mean of the trials selected for analysis. For a similar approach see Gruber et al. (2014).

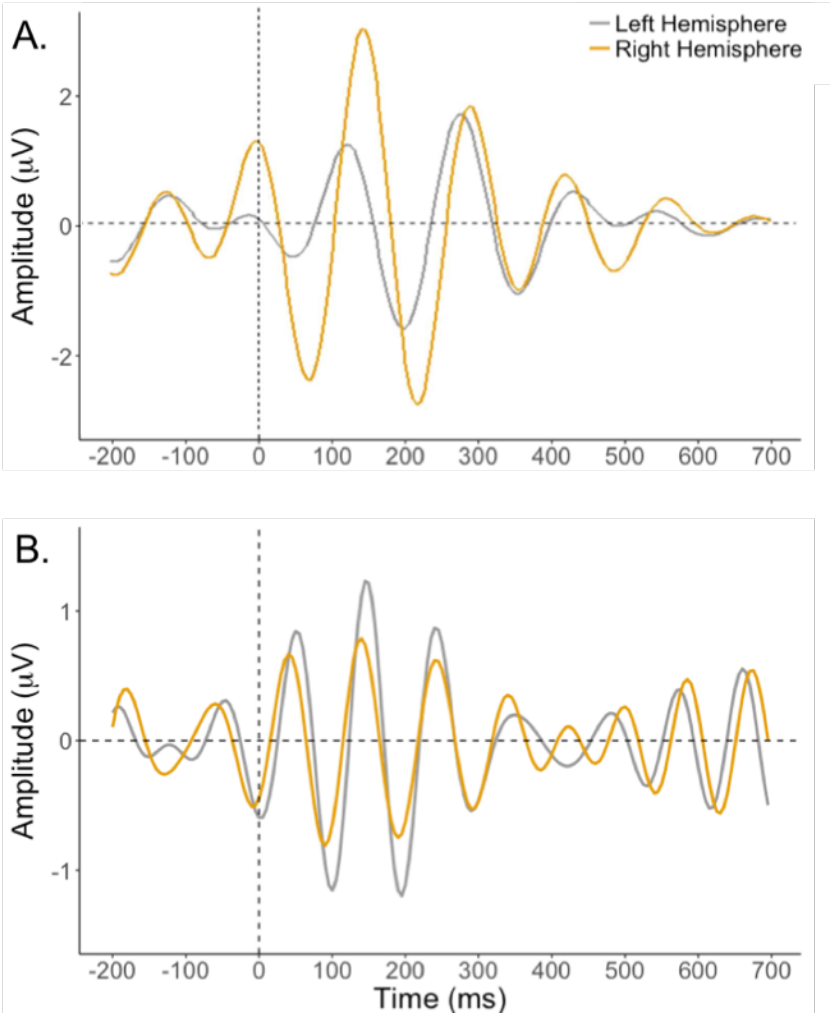

Figure 4-2: Examples of interhemispheric transfer in the theta and alpha bands in a single older adult participant. (A) RVF stimulation with earlier theta P1 and N1 peaks in the left hemisphere. (B) LVF stimulation with earlier alpha P1 and N1 peaks in the right hemisphere.

4.2.6 Data analysis

The reaction time data were analysed using a Condition (crossed/uncrossed) x Group (young/older) ANOVA with mean and median RTs as the dependent variables in separate models. The ERP latencies were analysed in Visual Field (LVF/RVF) x Hemisphere

(left/right) x Group (young/older) ANOVAs for each of the alpha and theta frequency bands separately. For all ANOVAs, effect sizes are reported as generalized eta squared (n_G^2; Bakeman, 2005) whereby an effect of 0.02 is considered small, 0.13 medium, and 0.26 as large. For the ANOVA models conducted on ERP latencies, post-hoc t-tests with Bonferroni-Holm adjustments for multiple comparisons were carried out between groups at each combination of the Visual Field and Hemifield factors (e.g. left hand LVF; left hand RVF; right hand LVF; right hand RVF).

4.3. Results

4.3.1 Behavioural data

On average, 3% of trials were removed due to eye movements away from fixation during stimulus onset. The cut-off criteria for reaction times resulted in the omission of 0.06% of trials on average. The remaining number of RT trials across all participants was 295.6 (SD = 2.97). For mean RT, the main effect of Group was significant, $F(1,53) = 12.43$, $p < .001$, $n_G^2 = 0.20$, indicating that older adults had significantly slower reaction times than young adults. There was a significant main effect of Condition, $F(1,53) = 18.89$, $p < .001$, $n_G^2 = 0.003$, which demonstrated that RTs to the stimulus ipsilateral to the response hand were quicker than RTs to the contralateral stimulus. In other words, the uncrossed RTs were quicker than the crossed RTs, as is traditionally observed. Crucially, there was no interaction between Group and Condition, $F(1,53) = 0.008$, $p = .927$, $n_G^2 < 0.00$, suggesting that the difference between crossed and uncrossed RTs did not vary across groups. The mean CUD value for younger adults was 4.6ms (SD = 7.11) and the mean CUD value for older adults was 4.47ms (SD = 8.37; see Figure 4-3A).

For median RTs, there was a significant main effect of Group, $F(1,53) = 10.51$, $p = .002$, $n_G^2 = 0.17$, and a significant main effect of Condition, $F(1,53) = 35.12$, $p < .001$, $n_G^2 = 0.003$, in the same directions as the mean RT results. No significant Group by Condition effect was observed, $F(1,53) = 0.07$, $p = .788$, $ges < 0.00$. The median CUD value for young adults was -4.47ms (SD = 5.11) and the median value for older adults was -3.98ms (SD = 5.51; see Figure 4-3B).

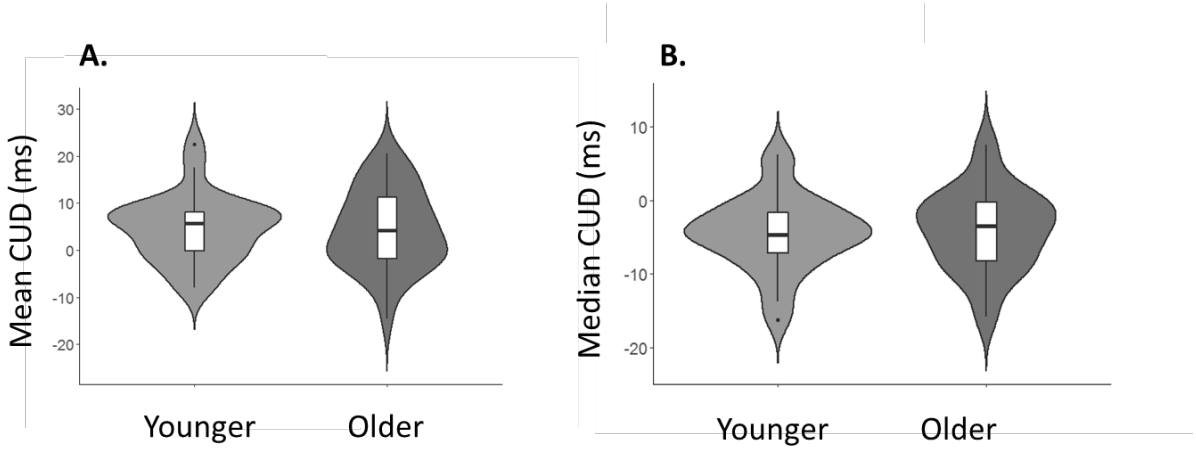

Figure 4-3: Violin boxplots illustrating the distribution of CUD estimates in young and older adults as calculated by the mean (A) and median (B) RTs. The bold horizontal line represents the median of the CUD distributions, while the box edges represent the interquartile range. The whiskers represent 1.5 times the upper and lower quartile, and dots represent outliers.

4.3.2 P1 analysis

On average, 243 trials per participant were included in the ERP analyses after cleaning the data (SD = 38, Range = 143-299). A Group x Visual Field x Hemisphere ANOVA was conducted for P1 latencies in both the theta and alpha bands. In the theta band, the typical

Hemisphere x Visual Field interaction was present, $F(1,53) = 128.41$, $p < .001$, $n_G^2 = 0.37$, suggesting that contralateral latencies were quicker than ipsilateral latencies, such that interhemispheric transfer had occurred. There was a significant three-way interaction, $F(1,53) = 14.96$, $p < .001$, $n_G^2 = 0.06$, suggesting that the groups differed in terms of the Visual Field x Hemisphere interaction. A series of post-hoc Bonferroni-Holm adjusted t-tests were conducted to test for group difference at each level of Hemisphere and Visual Field. There were no differences between groups in P1 latencies at the ipsilateral hemisphere for either the LVF (adjusted $p = .5$) or RVF conditions (adjusted $p = 1$). In the contralateral hemispheres, older adults had significantly quicker latencies in both the LVF (adjusted $p = .005$) and RVF conditions (adjusted $p < .001$), suggesting that older adults had significantly quicker P1 ERPs in the receiving hemispheres, but not in the transferred hemispheres.

For the alpha band, the Group x Visual Field x Hemisphere interaction approached significance, $F(1,53) = 3.699$, $p = .060$, $n_G^2 = .02$. We again tested for group differences at each combination of visual field and hemisphere using t-tests. Older adults had significantly quicker P1 latencies in the hemisphere ipsilateral to the RVF stimulus (adjusted $p = .008$), while a similar trend was evident for latencies in the hemisphere ipsilateral to the LVF stimulus (adjusted $p = .057$). In the contralateral hemispheres, there were no group differences for either the LVF (adjusted $p = 1$) or RVF stimulus (adjusted $p = 1$). Older adults therefore exhibited quicker alpha P1 latencies in the transferred hemisphere (see Figure 4-4).

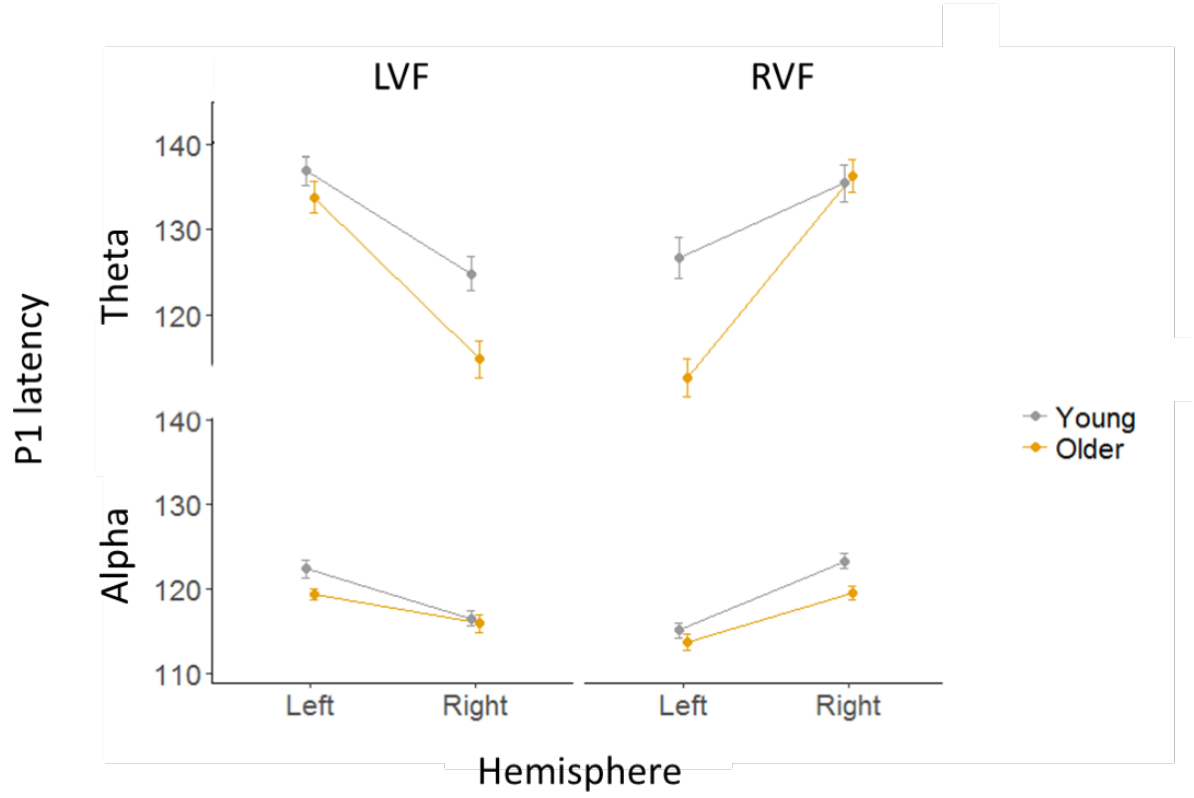

Figure 4-4: P1 latencies in the theta and alpha bands across the levels of Group, Visual Field and Hemisphere. Error bars indicate the standard error of the mean.

4.3.3 N1 analysis

The Group x Visual Field x Hemisphere interaction was significant for N1 latencies in the theta band, $F(1,53) = 19.18$, $p < .001$, $n_G^2 = .06$ (see Figure 4-5). At the ipsilateral hemispheres, there were no significant group differences for the LVF (adjusted $p = 1$) or RVF conditions (adjusted $p = .96$). Group differences were also absent in the hemisphere contralateral to the LVF stimulus (adjusted $p = 0.29$). For the hemisphere contralateral to the RVF stimulus, older adults had significantly quicker N1 latencies (adjusted $p = .001$). In the alpha band, the three-way interaction did not approach significance, $F(1,53) = 0.98$, $p = .326$, $n_G^2 = .004$, and so no post-hoc tests were conducted.

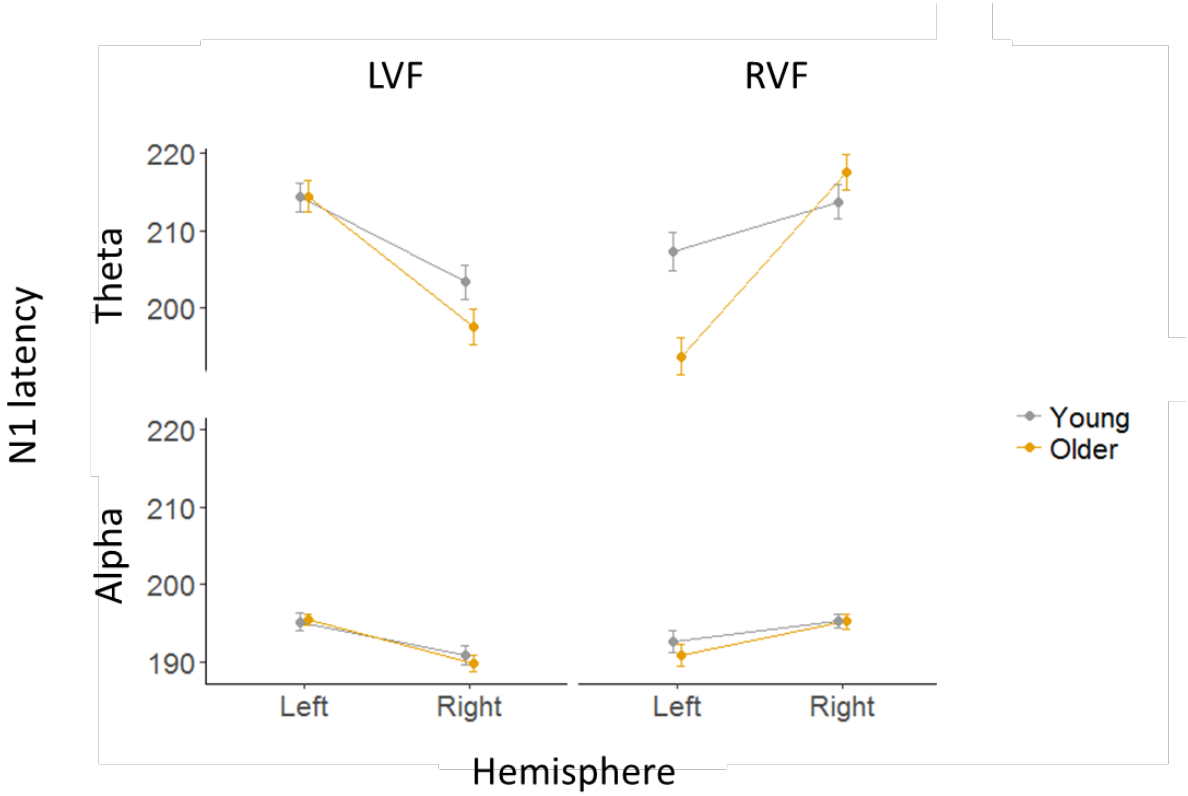

Figure 4-5: N1 latencies in the theta and alpha bands across the levels of Group, Visual Field and Hemisphere. Error bars indicate the standard error of the mean.

4.4 Discussion

This study aimed to test whether interhemispheric transfer is affected in older age. Using a constrained ERP approach, we calculated IHTT from peaks arising during the P1 and N1 time windows which were filtered into either the theta or alpha frequency bands. We assumed that because CC splenium fibres connecting visual areas are spared in healthy aging (Bastin et al., 2008, 2010; Hou et al., 2012; Madden et al., 2009; Salat et al., 2005), IHTT as measured by visual ERP components would not differ between young and older adults. We also calculated the classic CUD measure by subtracting RTs in the uncrossed (ipsilateral response) from the crossed (contralateral response) conditions. Since there

is still debate surrounding which channels of the CC are responsible for the CUD, we had no concrete hypothesis about how aging should affect the CUD. If the CUD operates through the CC genu, we should observe an elongated CUD in older adults, who experience degeneration of genu fibres with advancing age (Bastin et al., 2008, 2010; Hou et al., 2012; Madden et al., 2009; Salat et al., 2005). If the CUD is related to midbody or splenium fibres, there should be no difference between young and older adults.

4.4.1 No age differences in the CUD

There was no detectable difference in CUD estimates between young and older adults on average. This supports the findings of Linnet & Roser (2012) and Schulte et al., (2013) but contradicts the findings of many others (Bellis & Wilber, 2001; Davis et al., 2012; Jeeves & Moes, 1996; Reuter-Lorenz & Stanczak, 2000). The absence of the effect cannot be attributed to the relative youth of the older adults in this study, as Bellis & Wilber (2001) reported that adults as young as 55-60 had longer CUDs compared to 35-45 year olds. Our data suggest that transfer measured by the CUD is likely associated with callosal fibres that do not experience degeneration during healthy aging, such as the midbody fibres. As mentioned, Iacoboni & Zaidel (2004) found that the CUD correlated more strongly with BOLD activity from the superior parietal cortex than with other areas of activation during their fMRI study, in support of this theory. Additionally, it is compatible with the BOLD activation in the CC midbody during the Poffenberger paradigm (Gawryluk et al., 2011). It is, however, incompatible with the observed activation of the CC genu during the task (Gawryluk et al., 2011; Omura et al., 2004; Tettamanti et al., 2002; Weber

et al., 2005), suggesting that while the vascular properties of the genu may be involved in Poffenberger-derived transfer, it may not by crucial for the CUD.

There are other potential explanations for the lack of age differences. Iacoboni & Zaidel (2000) reported that thousands of trials are required to obtain CUD values that reflect true callosal transfer, whereas this study, among others, reported a CUD based on 300 trials. However, Bellis & Wilber (2001) used 320 trials and still reported effects of aging, deeming it unlikely that the discrepancy of between-group effects between our study and others can be solely attributed to the increased variability associated with having an insufficient number of trials. Furthermore, our sample size was comparable to that of other studies who reported an age effect (Jeeves & Moes, 1996; Bellis & Wilber, 2001, Reuter-Lorenz & Stanczak, 2000) suggesting that the power to achieve a between-groups effect was sufficient. We demonstrated that our results were consistent across the mean and median measures of central tendency, the median often being the choice of central tendency for RTs (Bellis & Wilber, 2001; Jeeves & Moes, 1996). Alternatively, the CUD may be sensitive to individual differences and variations in the task design, such as stimulus size, duration or eccentricity, which often vary between studies. It is possible that certain presentation parameters utilised in other studies are more sensitive to aging. Lastly, older adults had a significantly higher level of education than young adults in the present study, which may have reduced the likelihood of detecting a difference in the CUD between young and older adults. While the effect of education on the CUD has not been directly investigated, some studies have associated CC integrity with higher callosal integrity (Luders et al., 2007; Penke et al., 2010), suggesting a possible preservative effect on IHTT for older adults with higher levels of education. However, we acknowledge that level of education is a crude measure of cognitive ability and further research needs to be

conducted to rule out the effects of cognitive ability on transfer speed. Nevertheless, from the data presented here we draw the conclusion that interhemispheric transfer as measured by the CUD is spared in older adults, and likely operates through the CC midbody, which is unaffected by aging.

4.4.2 Age differences in ERP-IHTT

Our ERP analysis deviated from the traditional method of picking latency peaks from the single-subject grand average waveforms. This was possible by considering specific frequency bands of interest, namely the theta and alpha bands, in which the P1 and N1 components are situated according to a large body of literature (Freunberger et al., 2008; Gruber et al., 2014, 2005; Klimesch et al., 2004). In each of the analyses presented here, the typical Visual Field x Hemisphere interaction was highly significant with a large effect size, indicating that interhemispheric transfer was taking place between lateralized visual ERPs in both frequency bands. For both the P1 and N1 components in the theta band, the crucial Group x Visual Field x Hemisphere interaction was present, suggesting that older adults were associated with an elongated IHTT. Surprisingly, this effect was driven by quicker P1 latencies in the hemisphere contralateral to the stimulus, rather than elongated ipsilateral peak latencies in the older adult group. These findings suggest that visual information processing in the theta band is taking place more quickly in older adults than in younger adults, while the transferred signal in older adults reaches the ipsilateral hemisphere at around the same time as young adults. While this presents as an elongated IHTT in older adults, there is not necessarily an advantage for a quicker IHTT in younger adults since the transferred signal reaches the ipsilateral hemisphere at

the same time. This calls into question the validity of ERP IHTTs for measuring age-related decline, if aging is associated with a shortening of the contralateral peak latency. A quickening of P1 or N1 latencies has not typically been reported for older adults (Curran et al., 2001; Emmerson-Hanover, Shearer, Creel, & Dustman, 1994; Hoptman, Davidson, Gudmundsson, Schreiber, & Ershler, 1996; Onofrj, Thomas, Iacono, D'Andreamatteo, & Paci, 2001). We therefore assume that our finding of such is a result specific to the theta band, since the effect was not present for alpha band peaks. Further research on visual EEG responses in specific frequency bands will be necessary to uncover whether this effect is robust across different samples.

The pattern of results seen in the theta band results was not observed in the alpha band peaks. In fact, there was a trend towards an elongated P1 IHTT in younger adults compared to older adults, which was driven by delayed ipsilateral latencies in the young adults, rather than a reduction in contralateral latencies as observed in the theta band for older adults. Although this effect was weaker than those observed in the theta band, IHTT driven by elongated ipsilateral latencies, rather than shortened contralateral latencies, is a more conceptually valid manifestation of IHTT. Our results therefore suggest that older adults do not experience an elongated transfer in the alpha band, and that they may even be reduced compared to young adults.

4.4.3 Conclusions and future directions

From the results of this study we conclude that interhemispheric transfer as measured by the Poffenberger paradigm is not affected in older adults. Our results largely map on to the many studies that have documented age-related structural change in the CC (Bastin

et al., 2008, 2010; Hou et al., 2012; Madden et al., 2009; Salat et al., 2005), which suggest that only the genu of the CC experiences degeneration with advancing age. We have demonstrated that functions governed by the preserved sections of the aging CC are unaffected in older adulthood. Functional measures of the posterior CC could be an important measure for tracking changes in the aging brain that may deviate from the trajectory of normal development. For example, lower splenium integrity has been linked to increases in hypertension in older adults (Wong et al., 2017), which in turn is associated with increased risk of coronary heart disease and cardiovascular problems later in life (Scott, 2004).

Additionally, structural imaging studies have suggested that the CC splenium may be more specifically targeted than other regions by Alzheimer's dementia (AD) pathology (Fletcher et al., 2016; Genc et al., 2016; Hanyu et al., 1999; Hoy et al., 2017; Madhavan et al., 2016; Sandson et al., 1999; Xiaoying Tang et al., 2017). The CUD may not be an appropriate measure of functional decline of the CC in AD, as equivalent performance in AD and control groups has been demonstrated previously (Reuter-Lorenz & Mikels, 2005). Functions of the splenium, such as ERP-derived IHTT, may be a useful marker for structural decline in AD as they are independent of aging effects. Functional measures of structural integrity that are resistant to age effects are highly desirable for clinical assessment of age-related disorders (Logie et al., 2015). To our knowledge, ERP-IHTT in AD and its preclinical or prodromal stages has not yet been investigated.

From a methodological point of view, we consider the constrained ERP approach extremely useful for measuring IHTT, as it filters out trials in which the P1 and N1 ERPs were not elicited, and therefore avoids conflating the morphology of the single-subject average with noisy trials. The development of this easily replicable approach highlights

the need for synthesis between the ERP and EEG oscillation literatures, in order to avoid the issues associated with traditional ERP methods.

Chapter 5

5. Study 4: Resting state EEG power and connectivity are associated with alpha peak frequency slowing in healthy ageing (Scally et al., 2018a, *Neurobiology of Aging*)

5.1 Introduction

Aging is associated with a host of functional changes in the resting brain. Using the electroencephalography (EEG) neuroimaging method, some of the most commonly documented changes in older age are (i) reductions in oscillatory power, (ii) a weakening of functional connectivity between electrode time series data and (iii) a slowing of the dominant alpha EEG frequency. The relationship between these hallmark changes has rarely been systematically investigated. Of particular interest is how the use of conventional EEG frequency bands, which do not account for age-related frequency shifts, may influence age-group differences in EEG power and connectivity. These relationships may have important implications for the interpretation of previous findings and for progression in the analysis of resting state EEG in aging research.

The EEG frequency spectrum ranges from 0 to ~100 Hz. Most commonly, spectral properties of the EEG are analysed within conventional frequency bands: Delta (0-4 Hz), theta (4-8 Hz), alpha (8-12 Hz), beta (12-30 Hz) and gamma (>30 Hz) bands. Research into the cognitive modulation of EEG frequency power emphasises the inter-individual variation across the spectral boundaries of these conventional frequency bands, and also the boundaries of sub-bands within the alpha range (for a review, see Klimesch, 1999). A suggested marker for determining the individualised frequency boundaries is the

individual alpha peak frequency (IAPF). The IAPF is the average frequency of highest power between 6-13 Hz across the electrodes of the EEG montage (Angelakis, Lubar, & Stathopoulou, 2004). The IAPF is a stable and highly heritable physiological characteristic (Grandy et al., 2013; Posthuma, Neale, Boomsma, & De Geus, 2001; Christine M Smit, Wright, Hansell, Geffen, & Martin, 2006) that typically increases during the first 20 years of development and commences slowing from age 40 (Aurlien et al., 2004; Bazanova, 2008; Chiang, Rennie, Robinson, van Albada, & Kerr, 2011). Reported averages range from 9.8-10.5 Hz in young adults (age 17-30), to 8.5-9.7 in older adults aged 60 and above (Dustman, Shearer, & Emmerson, 1993).

An abundance of research has demonstrated that there are clear age-related modulations of the IAPF. Despite this, very few studies have abandoned the use of conventional frequency bands when investigating oscillatory power and connectivity. Duffy, Albert, McAnulty and Garvey (1984) observed a weak negative correlation between chronological age and alpha (8-11.75 Hz) amplitude in 30-80-year-old males (r = -0.27). Barry & De Blasio (2017) reported reduced delta (0.5-3.5 Hz), theta (4-7.5 Hz) and alpha (8-13 Hz) power, and increased beta (13.5-24 Hz) power in older compared to young adults; age-related alpha reductions were mainly evident in the posterior right hemisphere, with a weaker effect than observed in the other frequency bands. Gaál et al. (2010) observed reductions of delta and alpha power in older adults. Babiloni et al. (2006) also reported reduced power for older adults in the lower and upper alpha bands (8-10.5 Hz, 10.5-13 Hz). However, reduced alpha power may not be specific to the latest decades of development, as Aurlien et al. (2004) described a steady decline of IAPF amplitude from birth to age 30, where amplitude stabilised for the rest of the lifespan.

Functional connectivity in EEG generally refers to the temporal correlations between time series data from two or more independent EEG channels or sources. Connectivity strength between regions of interest may be extracted from the data, or the entire dataset may be summarized in terms of its network properties (Rubinov & Sporns, 2010). Connectivity metrics, which attempt to characterize the strength of connectivity in the presence of noise, are plentiful. Many early investigations of EEG functional connectivity have relied on the EEG coupling metric known as spectral coherence. Coherence is an estimate of the linear correlation between a pair of signals in the time-frequency domain (Bowyer, 2016; French & Beaumont, 1984), and is usually computed within a frequency band of interest. Coherence between EEG channels is prone to overestimation due to volume conduction, whereby neighbouring electrodes may record the signal from the same underlying neural generator, resulting in inflated estimates of connectivity between them. Novel connectivity metrics such as the phase-lag index (Stam, Nolte, & Daffertshofer, 2007) and weighted phase-lag index (Vinck, Oostenveld, Van Wingerden, Battaglia, & Pennartz, 2011) aim to attenuate the effects of volume conduction by disregarding the zero-phase relationships between a pair of EEG signals. In many cases, EEG functional connectivity has been shown to reflect the underlying structural properties of the brain. For example, coherence between electrodes placed on each hemisphere is weakened in individuals with surgically sectioned or underdeveloped commissural white matter fibres (Koeda et al., 1995; Montplaisir et al., 1990; Nagase et al., 1994; Nielsen et al., 1993). Furthermore, studies have noted positive correlations between functional EEG coherence and white matter tract integrity in patients with Alzheimer's disease pathology (Pogarell et al., 2005; Teipel et al., 2009; Vecchio et al., 2015).

While many studies have investigated EEG connectivity in age-related diseases, relatively few have characterised the connectivity changes that occur with typical aging. Duffy, Mcanulty and Albert (1996) examined EEG coherence in a large sample (N = 350) of adults aged 20-79 and reported age-related reductions in theta, alpha and beta frequencies. However, they exclusively considered interhemispheric pairs of electrodes and could not differentiate between eyes-open and eyes-closed conditions in their factor-analytic approach, which are known to generate distinct functional connectivity networks (Miraglia, Vecchio, Bramanti, & Rossini, 2016). Kikuchi and colleagues (2000) also found reductions in delta, theta, upper alpha (11-12.5 Hz) and beta interhemispheric EEG coherence during eyes-closed recordings. In a large sample of 17,722 individuals, an age-related decrease of global theta and alpha (8-12.5 Hz) coherence, along with an increase in beta coherence was reported (Vysata et al., 2014). Few studies have employed connectivity measures that aim to reduce volume conduction. In a sample of 1500 individuals between age 5-71, alpha PLI (6-13 Hz) derived from minimum spanning tree graphs declined in late adulthood from about age 50 (Smit, de Geus, Boersma, Boomsma, & Stam, 2016). Vecchio, Miraglia, Bramanti and Rossini (2014) described a reduction of lagged linear coherence in the upper alpha frequencies (10.5-13 Hz) in early (50-70) and later old aged (>70) adults, which were accompanied by age-related increases in delta and theta connectivity.

A critical issue for the study of EEG power and connectivity in the conventional alpha frequency range is the role of inter-individual IAPF variability. In 1999, Klimesch argued that because the spectral boundaries of the alpha frequency band and sub-bands vary between individuals, the alpha frequency boundaries should be adapted to the IAPF of the individual under study (Klimesch, 1999). Older adults would therefore be at an

artificial disadvantage when compared to young adults within conventional frequency bands, such as the upper alpha (10-12 Hz) frequencies, due to the age-related slowing of the IAPF. While this is certain for EEG power, the relationship between IAPF variability and connectivity is largely unknown. We are unaware of any studies that have investigated age-related changes of EEG connectivity while also considering age-related IAPF slowing. By considering IAPF, we can uncover real age-related modulations of EEG activity and connectivity to inform future studies of aging and age-related neuropathology.

The present study aimed to examine whether the IAPF is associated with EEG power and connectivity in the context of age-related physiological differences. We first replicated the finding of a slowed IAPF in older adults, to demonstrate that our data is coherent with previous findings. We then determined whether global connectivity was modulated by the IAPF, that is, whether the frequency at which connectivity was strongest was correlated with, and different to the IAPF across and within participant groups. We then compared younger and older adults on global power and connectivity at both the IAPF and the conventional upper alpha frequency band. We hypothesised that age differences would be observed in the conventional upper alpha band, as reported in previous studies (Gaál et al., 2010; Kikuchi et al., 2000; Vecchio et al., 2014), while age differences may be absent at the IAPF, outlining the redundancy of conventional frequency boundaries where IAPF is slowed in one group.

5.2 Materials and methods

5.2.1 Participants

Data from 32 older adults (11 male, 21 female, mean age = 69.75, SD = 4.91) and 37 young adults (13 male, 24 female, mean age = 20.31, SD = 2.06) were analysed in this study. Older adults were recruited from the community and young adults were recruited from the undergraduate psychology programme of the School of Psychology, University of Leeds, UK. All participants were self-reportedly right-handed. No participant reported a history of neurological disease or head trauma. Older adults were screened for dementia-related cognitive impairment with the Memory Alteration Test (Ozer et al., 2016; Rami, Molinuevo, Sanchez-Valle, Bosch, & Villar, 2007), and for depression using the depression subscale of the Hospital Anxiety and Depressions Scale (Zigmond & Snaith, 1983). No participant breached the guideline cut-off criteria for memory impairment or depression. Informed consent was obtained from all participants.

5.2.2 EEG recording and pre-processing

Continuous EEG recordings were made on a Neuroscan SynAmps2 system using a 64 channel headcap. Five minutes of eyes-closed resting state EEG was recorded at a sampling rate of 1000 Hz. The ground electrode at the time of recording was at AFZ, with the reference electrode located on the vertex between CZ and CPZ. Data pre-processing was performed offline. The data were filtered between 1-40 Hz and downsampled to 200 Hz. Noisy channels were omitted from the dataset by way of visual inspection (2.78 channels on average were removed, SD = 1.92). The continuous data were segmented into

epochs of 2 seconds with 0% overlap. An iterative amplitude thresholding process was applied to the epochs to eliminate noisy trials from the dataset. The threshold was set at ±100 μV, and reduced by ±1 μV with each iteration. Epochs containing data that breached the adaptive threshold were removed until 80 epochs remained. The remaining epochs were visually inspected for artefacts such as eye-blinks that happened to evade the thresholding process. At least 75 epochs per participant were selected for further analysis. The data were re-referenced to the common average reference.

5.2.3 Dominant alpha frequency estimation

The power spectral density of each EEG channel was estimated using the *spectopo* function from the EEGLAB software (Delorme & Makeig, 2004). The *findpeaks* function in Matlab (version 2015a) was used to locate the frequency of maximum absolute logarithmic power between 6 Hz and 14 Hz. The peak frequency from each channel was averaged to determine the IAPF (see Figure 5-1).

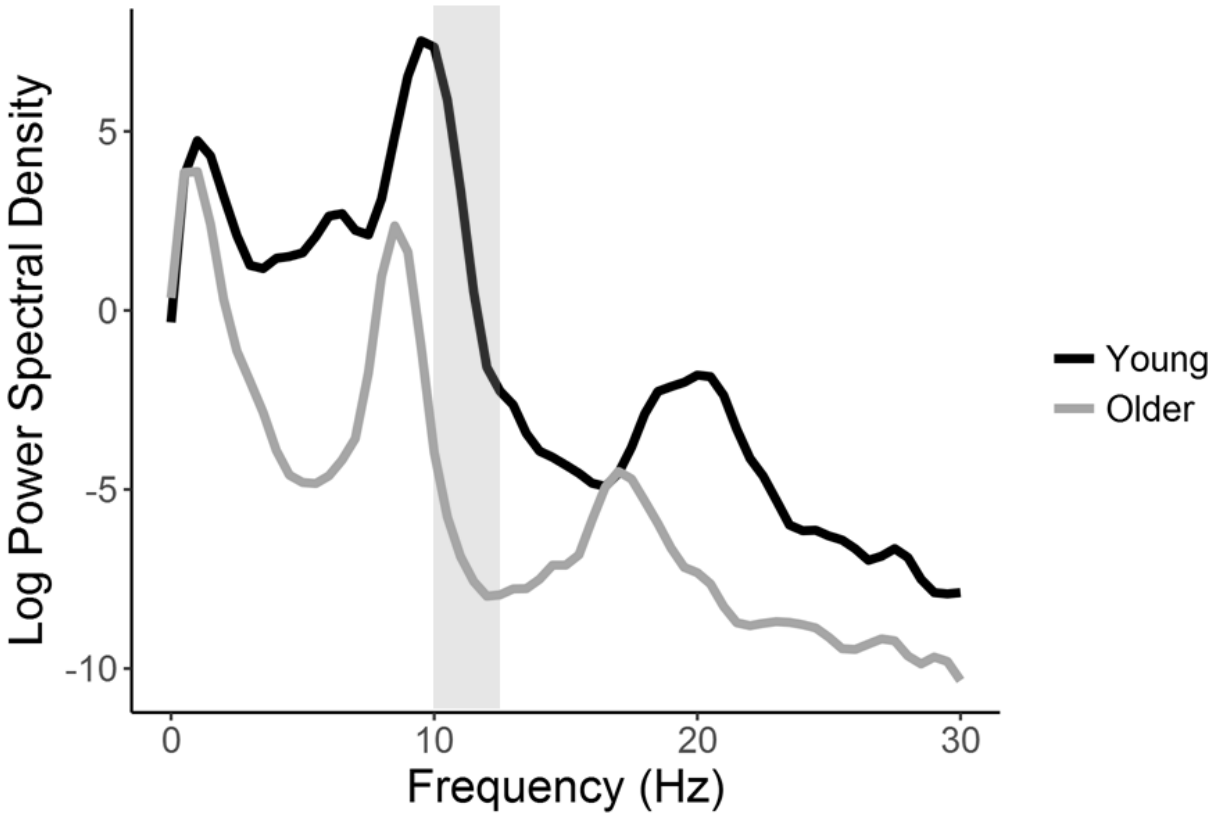

Figure 5-1: Power spectral density of EEG from electrode OZ plotted as a function of frequency (1-30 Hz) for one young adult and one older adult participant. The IAPF values are the frequencies of maximum power between 7-14 Hz. The shaded area outlines the conventional upper alpha frequency limits (see e.g. Fink, Grabner, Neuper, & Neubauer, 2005; Klimesch, Schack, & Sauseng, 2005; Krause, Pörn, Lang, & Laine, 1997).

5.2.4 Power and connectivity analysis

Time-frequency information was extracted from the EEG signals using the Fieldtrip toolbox (Oostenveld, Fries, Maris, & Schoffelen, 2011) within Matlab. Sliding Hanning windows with a fixed length of 2 seconds (offering a 0.5 Hz frequency resolution) were used to extract the power-spectral density for every EEG channel, and cross-spectral

density between every pair of EEG channels, from 6 to 12 Hz in steps of 0.5 Hz. Absolute spectral power at the IAPF and the upper alpha frequency band (10-12 Hz) was extracted and averaged across channels and trials. The array of power values at each frequency were log transformed to normalise their distribution. Power at the IAPF and upper alpha frequencies (10-12 Hz) were recorded for each individual.

The phase lag index (PLI; Stam et al., 2007) and weighted phase-lag index (WPLI; Vinck et al., 2011) were used to measure connectivity between all pairs of electrodes. Both measures stem from a longstanding development of connectivity metrics that attempt to account for the spurious connectivity estimates caused by the volume conduction phenomenon. Nolte et al. (2004) initially proposed that the imaginary part of spectral coherence between two signals was less sensitive to volume conduction than the real part of coherence. However, imaginary coherence was influenced both by the signal amplitude and the magnitude of the phase delay between the signals (Stam et al., 2007), and was prone to Type II errors; real connectivity was sometimes dismissed as volume conduction. This was improved upon with the introduction of the phase-lag index (PLI), which measures connectivity based on the imbalance in the distribution of phase angle differences between a pair of oscillations (Stam et al., 2007). To control for volume conduction, zero-phase relationships are disqualified by the PLI (Stam et al., 2007; Vinck et al., 2011) under the rationale that instantaneous phasic relationships are not representative of inter-regional neural connectivity, which must incorporate some time delay, characteristic of axonal transmission. The PLI is defined by the absolute value of the average sign of the imaginary part of the cross spectrum. The PLI was calculated from the imaginary part of the cross-spectral density using the formula:

$$PLI_{xy} = \left|\langle sign\left(imag\left(S_{xy}\right)\right)\rangle\right|$$

whereby $imag(S_{xy})$ denotes the imaginary component of the cross-spectrum between channels *x* and *y*, and $sign(imag(S_{xy}))$ refers to the sign (-/0/+) of this property. According to Vinck et al. (2011), the signal-to-noise ratio of the PLI is limited, as volume conducted noise components in the data could alter the sign of the imaginary component, leading to spuriously inflated connectivity estimates. The WPLI was developed in response, which weighted the phase leads and lags by the magnitude of the imaginary component of the cross-frequency spectrum (Vinck et al., 2011), thus further removing the contribution of zero-lag phase differences and improving the signal-to-noise ratio. Here, the WPLI was calculated as follows:

$$WPLI_{xy} = \frac{\left|\langle imag(S_{xy})\rangle\right| * \langle sign(imag(S_{xy}))\rangle}{\langle\left|imag(S_{xy})\right|\rangle}$$

Global PLI and WPLI connectivity were calculated by taking the average of connectivity values between every possible pair of channels.

5.2.4 Statistical analysis

IAPF values were compared between younger and older adults using t-tests for independent samples, with Welch's correction for unmatched sample variances. Pearson product-moment correlations were used to measure the relationships between the IAPF and the peak PLI and WPLI frequencies in young adults, older adults, and the entire sample. To investigate whether or not the peak connectivity frequencies differed from the IAPF, we conducted a one-sample t-test on the signed differences between the IAPF and peak connectivity frequency values, to determine if the mean of the difference distribution did not statistically differ from zero. Power and connectivity estimates were

analysed using a Group (young/older) x Frequency (IAPF/upper alpha) ANOVA, to determine whether between-group differences varied according to the choice of frequency implemented in the analysis. As we are interested in age differences, we specify a priori *t*-tests between young and older adults at each level of frequency. The false discovery rate was implemented to control for multiple comparisons in the planned contrasts. For t-tests, effect sizes in the form of Cohen's *D* are reported. For the fixed ANOVA effects, generalized eta squared (n_G^2) effect sizes are reported (Bakeman, 2005; Olejnik & Algina, 2003).

5.3 Results

5.3.1 Age differences in IAPF

IAPF values were compared between young and older adults. Young adults had a mean IAPF of 10.04 Hz (SD = 0.83), while older adults had a mean IAPF of 8.78 Hz (SD = 1.19). On average, older adults had significantly slower IAPFs compared to younger adults, $t(53.92) = 4.96$, $p < .001$, *Cohen's D* = 1.23, consistent with a slowing of EEG frequencies in older age (Aurlien et al., 2004) (Figure 5-2).

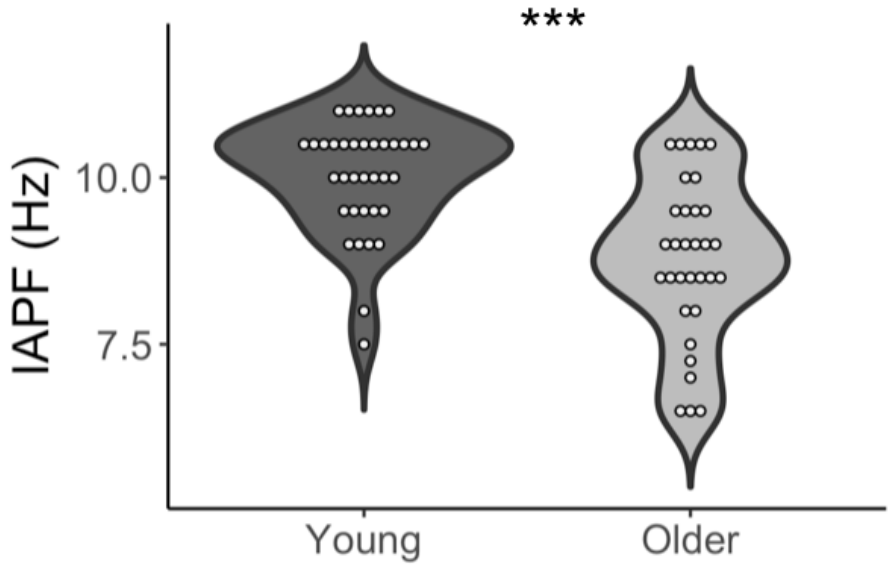

Figure 5-2: Violin plots illustrating the distributions of IAPF values in young (dark grey region) and older adults (light grey region). White dots represent participant data points. Older adults show a significant slowing of IAPF values compared to younger adults. *** $p < .001$.

5.3.2 IAPF and peak connectivity frequencies

IAPF was positively correlated with peak PLI frequency across the entire group ($r = 0.82$, $p < .001$), and within the younger ($r = 0.74$, $p < .001$) and older subgroups ($r = 0.77$, $p < .001$; Figure 5-3). A one-sample t-test demonstrated that the mean of the difference distribution between the IAPF and peak PLI frequency values was not significantly different from 0, $t(68) = 1.16$, $p = .248$, *Cohen's D* = 0.14.

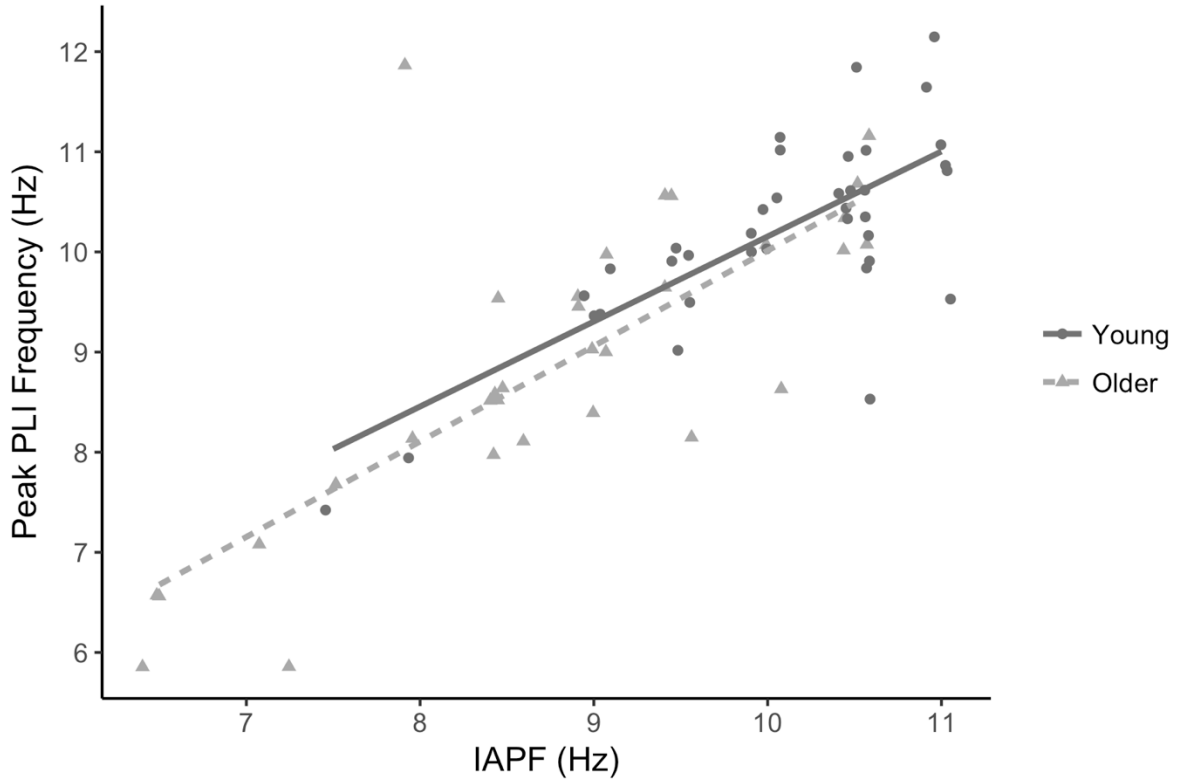

Figure 5-3: Positive correlations are shown between IAPF and peak PLI frequencies in both younger (dark grey dots/line) and older adults (light grey triangles/line).

For WPLI, high positive correlations were observed between IAPF and peak WPLI frequency across the entire sample (r = 0.85, p < .001), in the young adult group (r = 0.72, p < .001) and in the older adult group (r = 0.84, p < .001; Figure 5-4). A one sample t-test showed that the mean difference between the IAPF and WPLI peak connectivity values was not significantly different from 0, $t(68)$ = 0.37, p = .711, *Cohen's D* = 0.04.

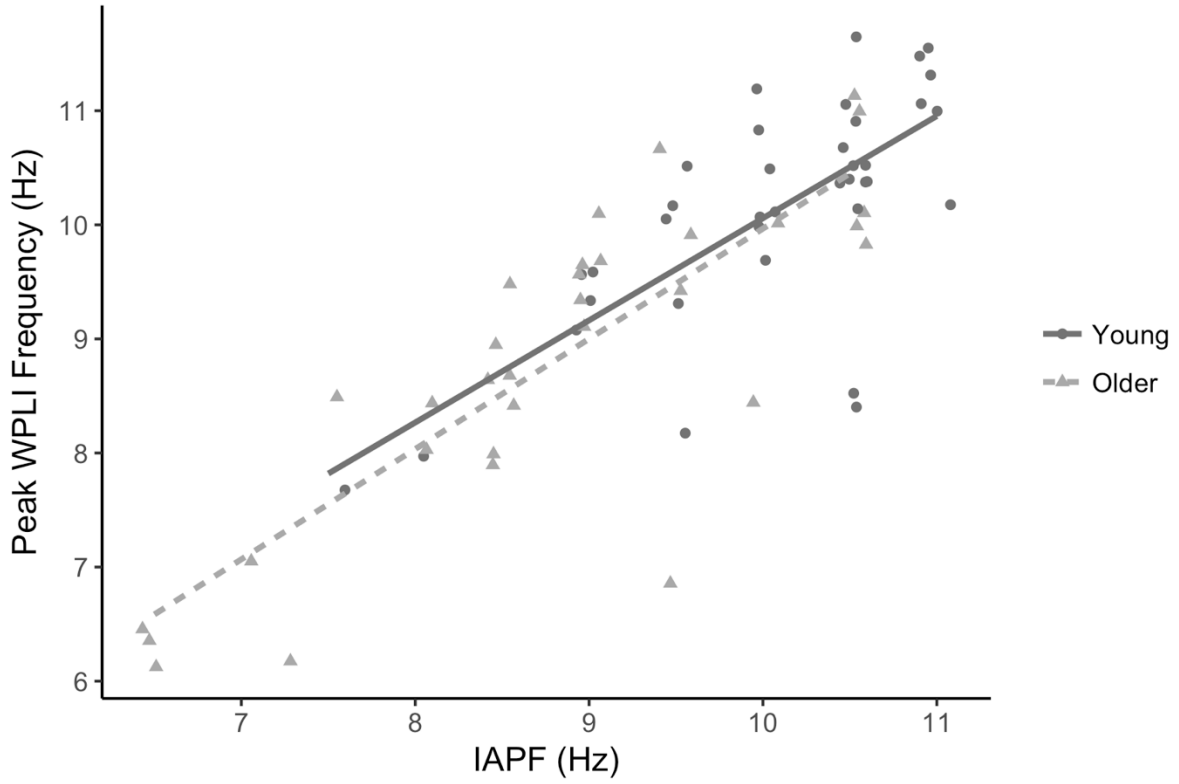

Figure 5-4: Positive correlations are shown between IAPF and peak WPLI frequencies in both younger (dark grey dots/line) and older adults (light grey triangles/line).

5.3.3 EEG power

A Shapiro-Wilks test for normality demonstrated that the log transformed EEG power values were normally distributed (W = 0.99, p = 0.433). The Group (young/older) x Frequency (upper alpha/IAPF) ANOVA yielded a significant Group x Frequency interaction on EEG power estimates, $F(1,67) = 17.2$, $p < .001$, $n_G^2 = 0.02$. Between-group t-tests suggested that young adults had significantly higher upper alpha power than younger adults, $t(66.93) = 3.87$, *adjusted* $p < .001$, *Cohen's D* = 0.93 (Figure 5-5). The difference in IAPF power between young and older adults was not significant, $t(66.98) = 1.48$, *adjusted* $p = .141$, *Cohen's D* = 0.36.

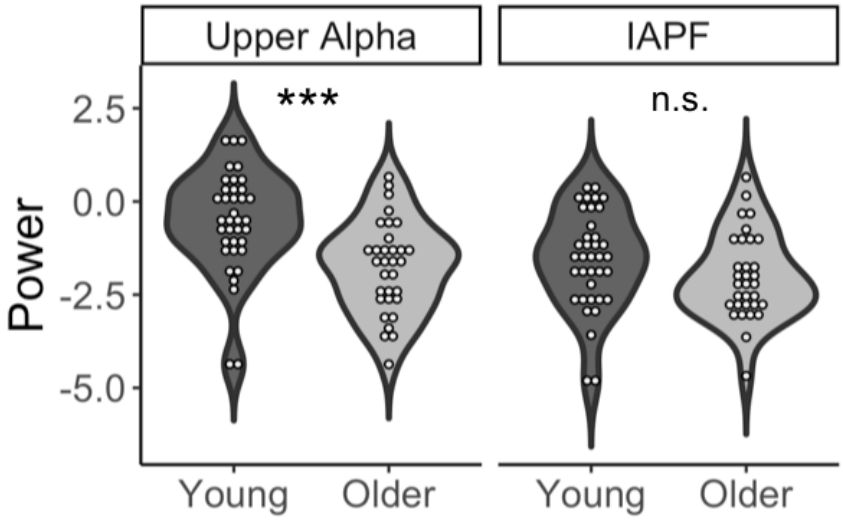

Figure 5-5: Distribution of EEG spectral power in young (dark grey) and older (light grey) adults at the IAPF (right) and upper alpha (left) frequency range. White dots represent participant data points. Young adults had significantly higher upper alpha power than older adults. *** $p < .001$, n.s. not significant.

5.3.4 EEG connectivity

The PLI values were positively skewed and not normally distributed ($W = 0.89$, $p < .001$) and were log transformed to assume a normal distribution ($W = 0.99$, $p = .887$). There was a significant Group x Frequency interaction, $F(1,67) = 9.04$, $p = .003$, $n_G^2 = 0.04$. Between-group t-tests showed that older adults had significantly weaker global PLI connectivity than young adults in the upper alpha frequency band, $t(63.76) = 3.81$, *adjusted* $p = .001$, *Cohen's D* = 0.93, whereas the group difference for PLI in the IAPF frequencies was negligible, $t(59.19) = 0.32$, *adjusted* $p = .75$, *Cohen's D* = 0.08 (Figure 5-6).

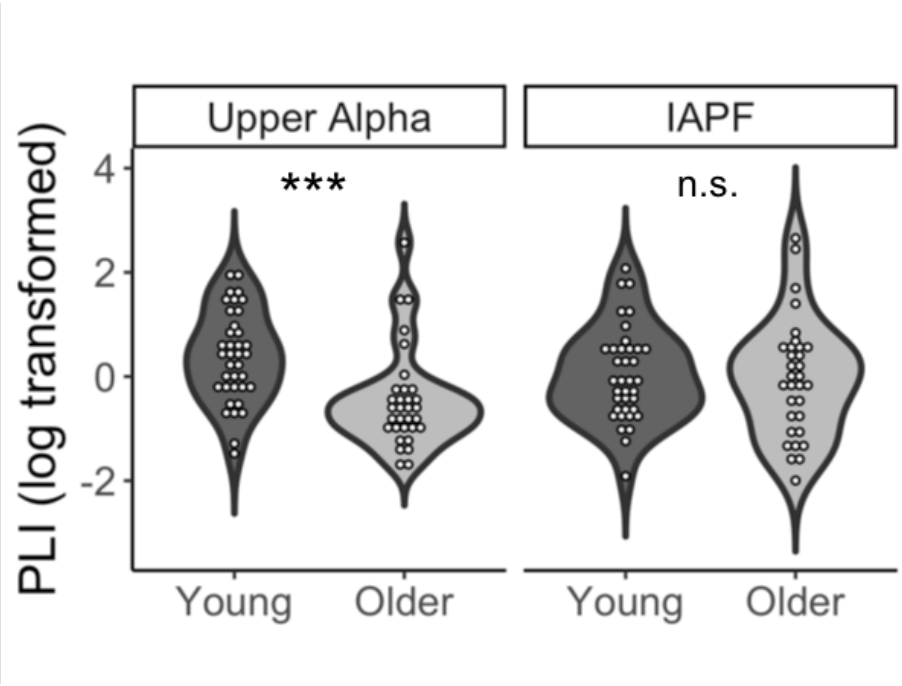

Figure 5-6: Distribution of global PLI values (log normalised) in young and older adults at the IAPF and at the upper alpha frequency range. White dots represent participant data points. Older adults had significantly weaker global PLI connectivity in upper alpha frequencies (but not IAPF) when compared to younger adults. *** $p < .001$, n.s. not significant.

The raw WPLI values were positively skewed ($W = 0.93$, $p < .001$) and were log transformed to satisfy the normality assumptions of ANOVA ($W = 0.98$, $p = .414$). There was a significant Group x Frequency interaction on WPLI, $F(1,67) = 8.17$, $p = .006$, $n_G^2 = 0.04$. Older adults had weaker WPLI connectivity than young adults in the upper alpha band, $t(61.83) = 4.58$, *adjusted* $p < .001$, *Cohen's D* = 1.12. At the IAPF frequencies, WPLI was equivalent across groups, $t(52.53) = 0.89$, $p = .374$, *Cohen's D* = 0.22 (Figure 5-7).

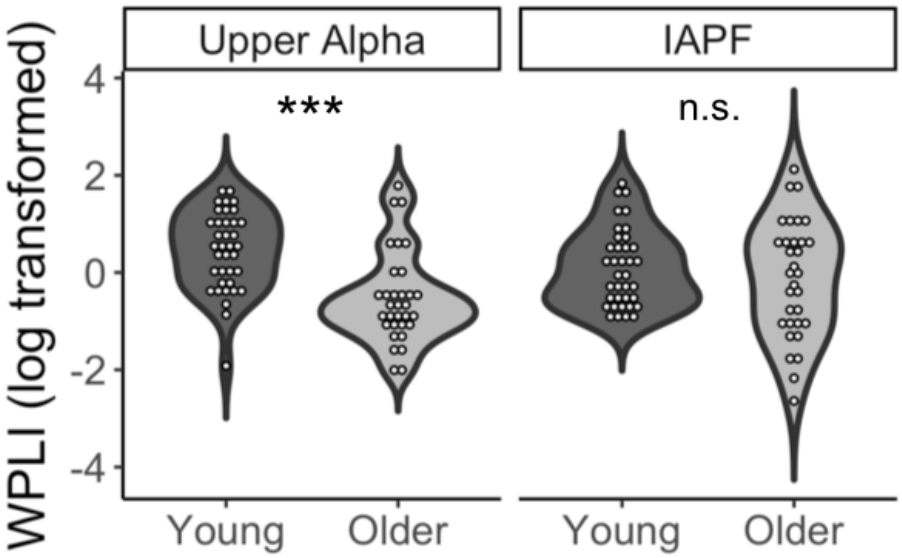

Figure 5-7: Distribution of global WPLI values (log normalised) in young and older adults at the IAPF and at the upper alpha frequency range. White dots represent participant data points. Global WPLI connectivity in the upper alpha range was weaker for older adults than younger adults, whereas there was no effect of age on WPLI at the IAPF. *** $p < .001$, n.s. not significant.

5.4 Discussion

In the present study we sought to evaluate the effect of age-related dominant EEG frequency slowing on EEG power and connectivity differences between young and older adults. We replicated the well-documented finding of a slower IAPF in older adults, detecting an average slowing of 1.26 Hz. Across all participants, there was a strong positive correlation between the IAPF and the peak PLI and WPLI frequencies suggesting that global connectivity strength was generally highest at or around the IAPF. For each

connectivity metric, there was no statistical difference between the mean IAPF and peak connectivity frequencies. This and the replication of slowed IAPF in older adults highlights the key disparity between young and older adults in the context of conventional frequency bands. For example, the majority of the strongest connectivity frequencies for young adults were in the 10-12 Hz (conventional upper alpha) range, whereas age-related IAPF slowing allocated the strongest connectivity frequencies for older adults to the 8-10 Hz (conventional lower alpha) range. Testing for group differences in the conventional upper alpha band therefore leads to ambiguous age effects that may lead to spurious interpretations concerning the underlying brain properties of older adults.

As expected, upper alpha frequency power was significantly reduced in older adults compared to young adults. In contrast, IAPF power was preserved, suggesting that alpha power differences in aging are due to IAPF slowing with advancing age. Consistent with this finding, we demonstrated that older adults had significantly weakened global PLI and WPLI connectivity in the conventional upper alpha band, as has been demonstrated in previous studies (Gaál et al., 2010; Kikuchi et al., 2000; Vecchio et al., 2014). There was no modulation of connectivity by age in the IAPF frequencies, demonstrating that age-related IAPF slowing not only impacts spectral power, but also estimates of brain connectivity. Aging studies should therefore consider individualizing frequency bands to avoid misinterpretations of power and connectivity differences that might be due to age-related changes in the frequency spectrum. Furthermore, there was considerable intra-group variability of IAPF, suggesting that individualized frequency analysis should be implemented regardless of the age group of interest.

Our analysis of global connectivity at the IAPF revealed no effects of age. It is therefore unlikely that these IAPF parameters reflect the underlying microstructural relationships of the older brain, which encompasses degeneration of both gray and white matter (Allen et al., 2005; Lebel et al., 2010; Westlye et al., 2010; Yeatman et al., 2014), and compromised functional connectivity within the default mode network (Ferreira & Busatto, 2013). However, it is yet unknown if local IAPF connectivity is affected by age, rather than global connectivity as studied here. Eyes-closed IAPF oscillations, which dominate the EEG frequency spectrum, are heavily localized to occipital areas (Bazanova & Vernon, 2014; Michel, Lehmann, Henggeler, & Brandeis, 1992) and therefore may not be appropriate for the examination of whole-brain functional connectivity. Indeed, functional magnetic resonance imaging (fMRI) studies have shown that IAPF power is associated with reduced blood-oxygen-level dependent (BOLD) signal power in the visual cortex and other cortical areas, and increased BOLD activity in subcortical regions such as the thalamus (Goldman, Stern, Engel, & Cohen, 2002; Laufs et al., 2003; Zhongming Liu et al., 2012; Scheeringa, Petersson, Kleinschmidt, Jensen, & Bastiaansen, 2012; Tagliazucchi, von Wegner, Morzelewski, Brodbeck, & Laufs, 2012). Additionally, periods of increased alpha oscillatory power have been linked to lapses in attention and sensory suppression (Craddock, Poliakoff, El-deredy, Klepousniotou, & Lloyd, 2017; Jensen & Mazaheri, 2010; Klimesch, Sauseng, & Hanslmayr, 2007), suggesting that alpha activity at rest has a highly inhibitory function. For these reasons, task-related EEG and eyes-open resting state recordings may be more useful when attempting to make inferences about underlying brain connectivity that relates to oscillations in the IAPF domain, instead of focusing on electrophysiological signals that are generated by subcortical structures. Alternatively, eyes-closed resting state EEG during periods of attenuated IAPF power may be more informative of cortical activity (Kanda, Oliveira, & Fraga, 2017).

In our study, older and younger adults had equivalent global power at the IAPF, leading to the conclusion that despite the slowing of IAPF oscillations, the output of the dominant alpha generator was uncompromised. Age-related structural changes to the thalamus have been noted using magnetic resonance imaging (Cherubini, Péran, Caltagirone, Sabatini, & Spalletta, 2009), and may therefore be expressed in the EEG by dominant frequency slowing, rather than by attenuation of activity. Further multimodal imaging work is necessary to tease apart these relationships.

In the present study, we demonstrated that power and connectivity differences between younger and older adults in the alpha range are biased against older adults when adopting fixed spectral boundaries for frequency analysis. Our study was well powered to account for inter-individual variability of IAPF values in both the younger and older adult group. Unlike the majority of previous studies on resting state EEG, we utilised a connectivity metric that is insensitive to the effects of volume conduction, which traditional measures such as coherence are vulnerable to (Stam, Nolte, & Daffertshofer, 2007; Vinck et al., 2011). We supported the finding of slowed IAPF in older adults, in line with previous literature (Aurlien et al., 2004; Bazanova, 2008; Chiang et al., 2011; Dustman et al., 1993). We went on to show that the global EEG power and connectivity of young and older adults dissociate at the conventional upper alpha band, but not when the frequency of interest was adapted to the IAPF.

Our findings have important implications for the interpretation of resting state EEG studies on aging and age-associated neuropathology such as the dementias. Countless spectral analyses of individuals with Alzheimer's disease and its prodromal stages have described neuropathological changes to alpha band connectivity and power (Babiloni et al., 2006; Jelic et al., 2000; Jeong, 2004; Kwak, 2006; Locatelli, Cursi, Liberati,

Franceschi, & Comi, 1998) without considering the slowing of the IAPF, which has been shown to slow even further in neuropathological states (Jelic et al., 2000; Jeong, 2004; Kwak, 2006; Penttilä, Partanen, Soininen, & Riekkinen, 1985). Adapting resting state analysis to the IAPF should compensate for the bias accrued by using conventional frequency bands across groups that may vary in terms of the IAPF. Future analysis of resting state EEG parameters should consider the presence of the IAPF and its underlying neurophysiology (i.e. subcortical generation) when making inferences about cortico-cortical connectivity. Correct classification and interpretation of the electrophysiological features expressed by healthy older adults are critical when making inferences about age-related disease and neuropathology, to determine how sensitive and specific the effects are to the disease of interest.

Chapter 6

6. Study 5: Interhemispheric functional EEG connectivity in healthy ageing

6.1 Introduction

The ageing corpus callosum (CC) has been shown to adhere to a specific pattern of decline in older age, whereby anterior callosal fibres (e.g. in the genu) degenerate while posterior sections are relatively preserved (Bennett & Madden, 2014; Davis et al., 2009; Sullivan, Rohlfing, & Pfefferbaum, 2010). This anterior-posterior gradient has been observed in countless structural imaging studies using DTI (Abe et al., 2002; Barrick, Charlton, Clark, & Markus, 2010; Bennett, Madden, Vaidya, Howard, & Howard, 2010a; Bucur et al., 2008; Davis et al., 2009; Ota et al., 2006; Salat et al., 2005). Age-related degeneration of the anterior commissural fibres is in line with classic age-induced reductions of frontally driven cognitive functions such as processing speed (Bors & Forrin, 1995; Kuznetsova et al., 2016), working memory (De Jager et al., 2002; Zahr et al., 2009), attention and executive functions (Kennedy & Raz, 2009; Pfefferbaum et al., 2005; Wasylyshyn et al., 2011; Wen & Sachdev, 2004). The deterioration of the anterior CC may therefore be considered a useful marker for normal cognitive aging.

Links between the structural integrity of the CC and resting state interhemispheric functional connectivity (IFC) recorded from the scalp EEG have been demonstrated, with a weakening of IFC in individuals with compromised structural CC integrity (Koeda et al., 1995; Montplaisir et al., 1990; Nagase et al., 1994; Nielsen et al., 1993). A case study by Montplaisir et al. (1990) provided causal evidence for this relationship by demonstrating

significant reductions in interhemispheric coherence after the surgical sectioning of the CC (callosotomy) compared to pre-surgery coherence in two patients. Furthermore, spatial patterns of disconnectivity were consistent with the site of callosotomy (anterior or posterior), indicating that EEG-based IFC may be sensitive to major disruption of underlying white matter pathways (Montplaisir et al., 1990).

Very few studies have investigated the relationship between IFC and more subtle alterations of CC white matter integrity assumed to manifest during normal ageing (Lebel, Caverhill-Godkewitsch, & Beaulieu, 2010; Westlye et al., 2010). Duffy, Mcanulty and Albert (1996) examined interhemispheric coherence in 350 individuals aged 20-79, finding a broad decrease across frontal, temporal and parietal sites. Koyama, Hirasawa, Okubo and Karasawa (1997) measured IFC at exclusively central and occipital sites and detected no differences between young and older adults. Kikuchi et al. (2002) observed reduced IFC in older adults, predominantly between frontal channels in high alpha frequencies (11-12.5 Hz), which is in line with the anterior-posterior gradient of CC degeneration. Jorge, Botelho and Melo (2007) found no evidence of age-related interhemispheric disconnectivity between any electrodes in 72 adults aged 20-50 years old.

A number of methodological developments in the field of resting state EEG connectivity have been made since these studies of age-related IFC were conducted. The coupling measure utilised in previous studies of interhemispheric EEG connectivity has exclusively been spectral EEG coherence. Spectral coherence is an estimate of the linear correlation between a pair of signals in the frequency domain (Bowyer, 2016; French & Beaumont, 1984). Coherence between EEG channels is prone to the effects of volume conduction, whereby the activity recorded by two independent EEG channels may be

confounded by a mutual signal generator, resulting in a conflated estimate of connectivity. Novel connectivity metrics (Brookes et al., 2011; Hipp, Hawellek, Corbetta, Siegel, & Engel, 2012; Stam et al., 2007; Vinck et al., 2011) aim to reduce the effects of volume conduction by disregarding zero-phase relationships between a pair of signals. In terms of age-related IFC, these measures remain untested and may be more sensitive to underlying microstructural degeneration than spectral coherence.

In addition to methodological developments, novel theoretical developments have been proposed. Scally, Burke, Bunce and Delvenne (2018a; see also Chapter 5) advised that the use of fixed frequency band limits in comparisons of young and older adult groups leads to group differences that are biased against older adults due to the age-related slowing of dominant EEG alpha frequencies. It was therefore recommended that frequency band limits should be adapted to each individual, relative to that individual's dominant alpha frequency (Klimesch, 1999; Moretti et al., 2004), to avoid inducing bias against older adults.

In the present study, we investigated IFC in young and older adults. Two connectivity metrics were considered: Spectral coherence and the weighted phase lag index. We used adapted frequency bands to account for the influence of slowed dominant alpha frequencies in older adults (Aurlien et al., 2004; Scally et al., 2018a). It was hypothesised that IFC would reflect the anterior-posterior gradient of CC disconnectivity that is typical of older adults, by demonstrating specific reductions of frontal IFC in older as opposed to younger adults. Additionally, we anticipated that parietal IFC would be reduced in older adults, based on results from Study 1 of this thesis, which demonstrated that the commissural parietal tracts of the CC experience reduced integrity in older age.

6.2 Method

6.2.1 Participants

Thirty-seven young adults and 33 healthy older adults participated this study. Young adults consisted of undergraduate psychology students from the University of Leeds who received course credits for participation. Older adults were recruited from communities in and around the city of Leeds, UK. All older adults performed above cut-off on the Memory Alteration Test (Ozer et al., 2016; Rami, Bosch, Sanchez-Valle, & Molinuevo, 2010) to rule out memory impairment related to Alzheimer's dementia. Participant demographics are presented in Table 6-1.

Table 6-1: Participant demographics

	Young (n = 24)	**Older (n = 32)**
Age	20.3 (2.06)	69.75 (4.91)
Years of Education	14.9 (1.94)	17.0 (4.67)*
Sex (M/F)	(13/24)	$(11/21)^{ns}$
M@T	-	45.21 (37-50; cut-off = 37)

*$p < .05$, ns = non-significant

6.2.2 EEG recording and preprocessing

Five minutes of eyes-closed resting state EEG was recorded from each participant. The data was recorded at 1000 Hz using a Neuroscan Synamps2 amplifier (Compudemics) via an electrode cap comprising of 57 electrodes. Electrode impedances were kept below 10 kOhms when possible. During recording, participants were asked to sit in a dimly lit room with their eyes closed and to remain still for five minutes. EEG data was pre-processed

using EEGLAB software for Matlab. The EEG data was visually inspected to identify noisy channels that were poorly connected, which were removed from the data. The data was segregated into a series of 2 second epochs. Zero-phase band-pass butterworth filtering was applied to the data between 1 and 45 Hz. Amplitude thresholding was applied to each epoch, whereby epochs containing activity that breached a threshold of +/- 75uV were removed. Independent component analysis using the *fastica* algorithm was used to remove electrode noise, muscle artefacts, eye blinks and lateral eye movements. Data were re-referenced to the common average reference. Omitted noisy channels were re-estimated using spherical spline interpolation. We acknowledge that interpolating channels may lead to inflated connectivity estimates if connectivity between neighbouring channels is of interest. In the present study, none of the channel pairs of interest were immediately adjacent and therefore interpolation was used to avoid cases of missing data. Fifty epochs per participant were pseudo-randomly selected and submitted to connectivity analysis. Sixteen EEG channels were chosen for connectivity analysis and were grouped into homologous interhemispheric regions of interest (ROIs; Fp1-Fp2, F7-F8, F3-F4, T7-T8, C3-C4, P7-P8, P3-P4, O1-O2).

6.2.3 Connectivity analysis

Time-frequency information was extracted from the EEG signals using the Fieldtrip toolbox (Oostenveld et al., 2011) for Matlab. A sliding Hanning window with a fixed length of 2 seconds (yielding a 0.5 Hz frequency resolution) was used to extract the power spectrum for each channel and cross-spectral density between each channel pair of interest. Frequencies from 1 to 45 Hz in steps of 0.5 Hz were extracted. Frequencies were

averaged into bins that were constructed in reference to the individual alpha peak EEG frequency (IAPF) and theta/alpha transitional frequency (TF; Klimesch, 1999; Moretti et al., 2004). The IAPF was defined as the frequency of maximum power between 6 and 14 Hz. The TF was defined as the first local minimum occurring before the IAPF. The frequency bands were assigned as follows: Delta from 1 Hz to TF-2 Hz; Theta from TF-2 Hz to TF; Alpha1 from TF to the midpoint between TF and IAPF; Alpha2 from the midpoint between TF and IAPF to IAPF; Alpha3 from IAPF to IAPF+2 Hz; Beta from IAPF+2 to 30 Hz; Gamma from 30 Hz to 45 Hz.

Two connectivity metrics were used in the present study: *Spectral coherence* and the *weighted-phase lag index* (WPLI). Spectral coherence estimates connectivity by estimating the frequency-specific correlation between two sets of time-series data. Despite its vulnerability to volume conduction, spectral coherence was included in the present study because of the large inter-electrode distance between the electrode pairings of interest, reducing the likelihood that the interhemispheric channels would record common underlying activity. Additionally, inclusion of coherence enabled comparison with previous research studies that utilised the measure. Various metrics have been developed in an attempt to circumvent the volume conduction phenomenon, such as imaginary coherence (Nolte et al., 2004) and phase-lag measures (Stam et al., 2007; Vinck et al., 2011; see Chapter 6 for a more in depth discussion on connectivity metrics). Here, we also estimate connectivity using the WPLI. The WPLI examines the consistency of phase angle differences between pairs of time-series data to estimate connectivity. It discounts zero-phase relationships that are indicative of volume conduction, thus improving the signal-to-noise ratio of connectivity (Vinck et al., 2011).

The possible values of each connectivity metric ranges from 0 (completely unsynchronised) to 1 (perfect synchronisation between channels).

6.2.4 Statistical analysis

Age group differences in coherence and WPLI were assessed between all electrodes of interest using independent-sample t-tests with false discovery rate adjustments for multiple tests. Effect sizes are reported as Cohen's *D* (Venegas-Barrera & Manjarrez, 2011); general guidelines suggest that an effect is of 0.2 is small, 0.5 is medium and 0.8 is large. We also reported the accuracy of coherence and WPLI IFC for the classification of age group using receiver operating characteristic analysis and reported the area under the curve (AUC) for the IFC parameters that were significantly different between groups. Coherence and WPLI IFC were tested separately and then in combination.

6.3 Results

6.3.1 Spectral coherence

Coherence between electrode pairings at frequencies that significantly differentiated between young and older adults before FDR correction are displayed in Table 6-2. Age group differences in spectral coherence were evident across all frequency bands exclusively between frontal EEG channels, with the exception of temporal (T7-T8) coherence in the gamma band (Figure 6-1).

Table 6-2: Age group differences in resting state interhemispheric spectral coherence

Frequency	Electrode	Young	Older	*t*	*df*	*p*	p_{FDR}	*Cohen's D*
Delta	Fp1-Fp2	0.75	0.65	2.81	61.25	.007	.041*	0.68
Delta	F3-F4	0.53	0.42	2.19	63.60	.032	.120	0.53
Theta	Fp1-Fp2	0.74	0.65	2.23	59.89	.030	.118	0.54
Alpha1	Fp1-Fp2	0.79	0.69	3.06	48.68	.004	.029*	0.76
Alpha1	F7-F8	0.22	0.16	2.43	65.31	.018	.076	0.57
Alpha2	Fp1-Fp2	0.89	0.77	4.10	45.17	.000	.002**	1.02
Alpha2	F7-F8	0.47	0.27	4.65	67.99	.000	.000***	1.10
Alpha2	F3-F4	0.73	0.62	2.65	66.13	.010	.056	0.64
Alpha3	Fp1-Fp2	0.92	0.79	4.80	36.55	.000	.000***	1.21
Alpha3	F7-F8	0.55	0.31	5.79	62.69	.000	.000***	1.40
Alpha3	F3-F4	0.79	0.63	4.61	59.75	.000	.000***	1.12
Beta	F7-F8	0.21	0.16	2.49	67.77	.015	.071	0.59
Gamma	Fp1-Fp2	0.58	0.45	2.88	66.29	.005	.037*	0.69
Gamma	F3-F4	0.37	0.28	2.49	67.93	.015	.071	0.59
Gamma	T7-T8	0.26	0.17	3.32	63.78	.001	.014*	0.78

Note: *$p < .05$, **$p < .01$, ***$p < .001$. p_{FDR} *= p-values adjusted with the false discovery rate.*

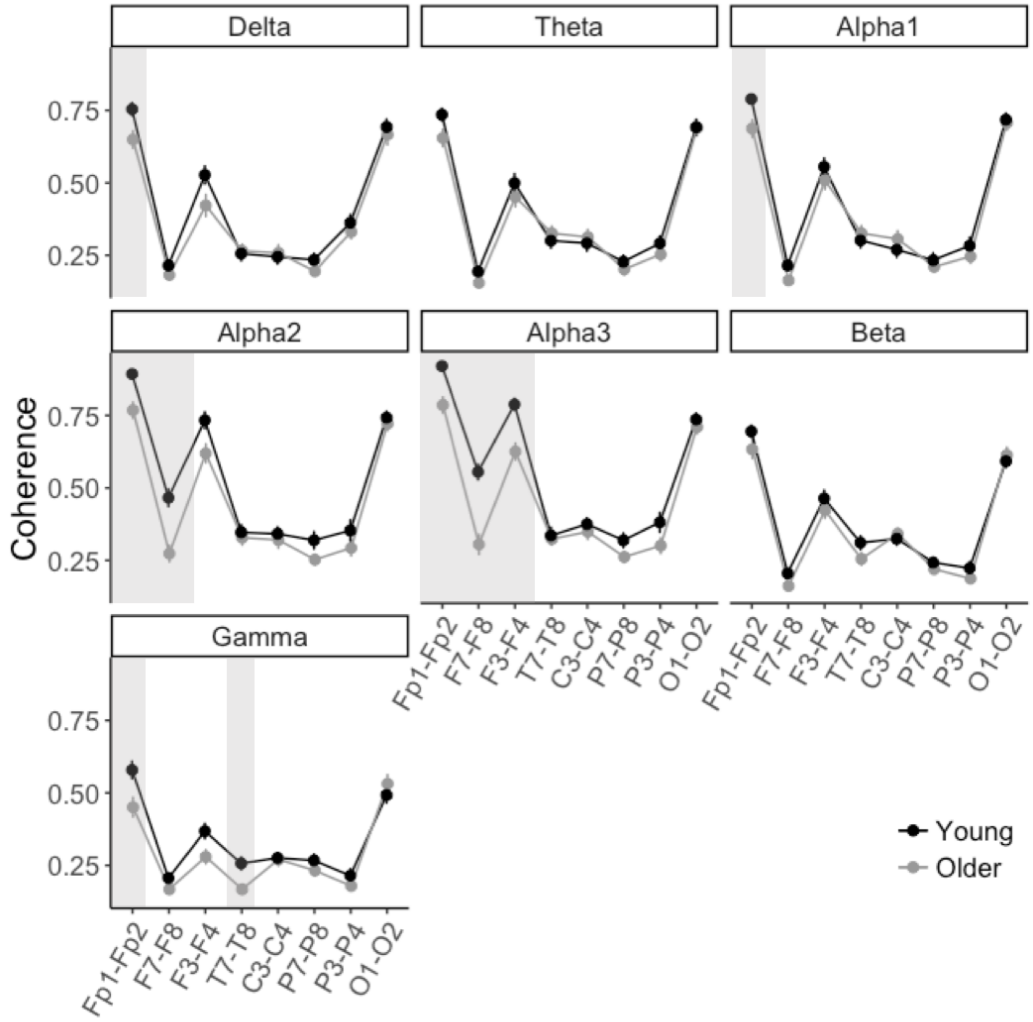

Figure 6-1: Average group differences in interhemispheric coherence at each electrode pair and individualised frequency band. Shaded regions indicate statistically significant t-test differences with a FDR-corrected significance threshold of at most p = .049. Error bars represent standard error of the group mean.

6.3.2 Weighted phase-lag index

WPLI between electrode pairings at frequencies that significantly differentiated between young and older adults are displayed in **Table 3**. WPLI revealed widespread differences both in terms of electrodes and frequency bands before *p*-value adjustments. After FDR correction, connectivity differences were observed in the frontal and temporal alpha2 frequencies, temporal and parietal gamma frequencies, and frontal, central and parietal beta frequencies (Figure 6-3).

Table 6-3: Age group differences in resting state interhemispheric WPLI connectivity

Frequency	Electrode	Young	Older	*t*	*df*	*p*	p_{FDR}	*Cohen's D*
Delta	C3-C4	0.17	0.13	2.57	40.77	.014	.057	0.58
Theta	Fp1-Fp2	0.15	0.13	2.37	67.93	.021	.058	0.56
Alpha1	Fp1-Fp2	0.15	0.13	2.60	67.23	.011	.053	0.62
Alpha1	F7-F8	0.15	0.13	2.51	57.48	.015	.057	0.61
Alpha1	T7-T8	0.15	0.13	2.08	67.84	.041	.090	0.49
Alpha2	Fp1-Fp2	0.21	0.14	3.55	50.21	.001	.007**	0.82
Alpha2	F7-F8	0.21	0.17	2.47	65.03	.016	.057	0.58
Alpha2	F3-F4	0.21	0.16	2.60	64.77	.011	.053	0.61
Alpha2	T7-T8	0.22	0.17	2.80	65.83	.007	.037*	0.66
Alpha2	C3-C4	0.21	0.17	2.44	67.39	.017	.057	0.58
Alpha3	Fp1-Fp2	0.21	0.16	2.25	55.40	.029	.073	0.52
Alpha3	P7-P8	0.22	0.17	2.42	67.90	.018	.057	0.57
Beta	Fp1-Fp2	0.15	0.12	4.23	54.78	.000	.002**	0.98
Beta	F7-F8	0.15	0.13	3.06	53.62	.003	.021*	0.71
Beta	F3-F4	0.15	0.13	4.11	57.52	.000	.002**	0.95
Beta	T7-T8	0.15	0.13	2.43	67.73	.018	.057	0.58
Beta	C3-C4	0.15	0.13	3.67	57.57	.001	.006**	0.85
Beta	P7-P8	0.16	0.13	4.72	47.33	.000	.001**	1.08
Beta	P3-P4	0.15	0.13	3.56	55.06	.001	.007**	0.82
Beta	O1-O2	0.16	0.14	2.15	67.95	.035	.082	0.51
Gamma	F7-F8	0.17	0.14	2.40	67.82	.019	.057	0.57
Gamma	T7-T8	0.17	0.13	3.70	64.61	.000	.006**	0.87
Gamma	P7-P8	0.15	0.13	2.33	61.04	.023	.062	0.54
Gamma	P3-P4	0.15	0.12	3.48	57.52	.001	.007**	0.81

Note: *$p < .05$, **$p < .01$, ***$p < .001$. p_{FDR} = *p-values adjusted with the false discovery rate.*

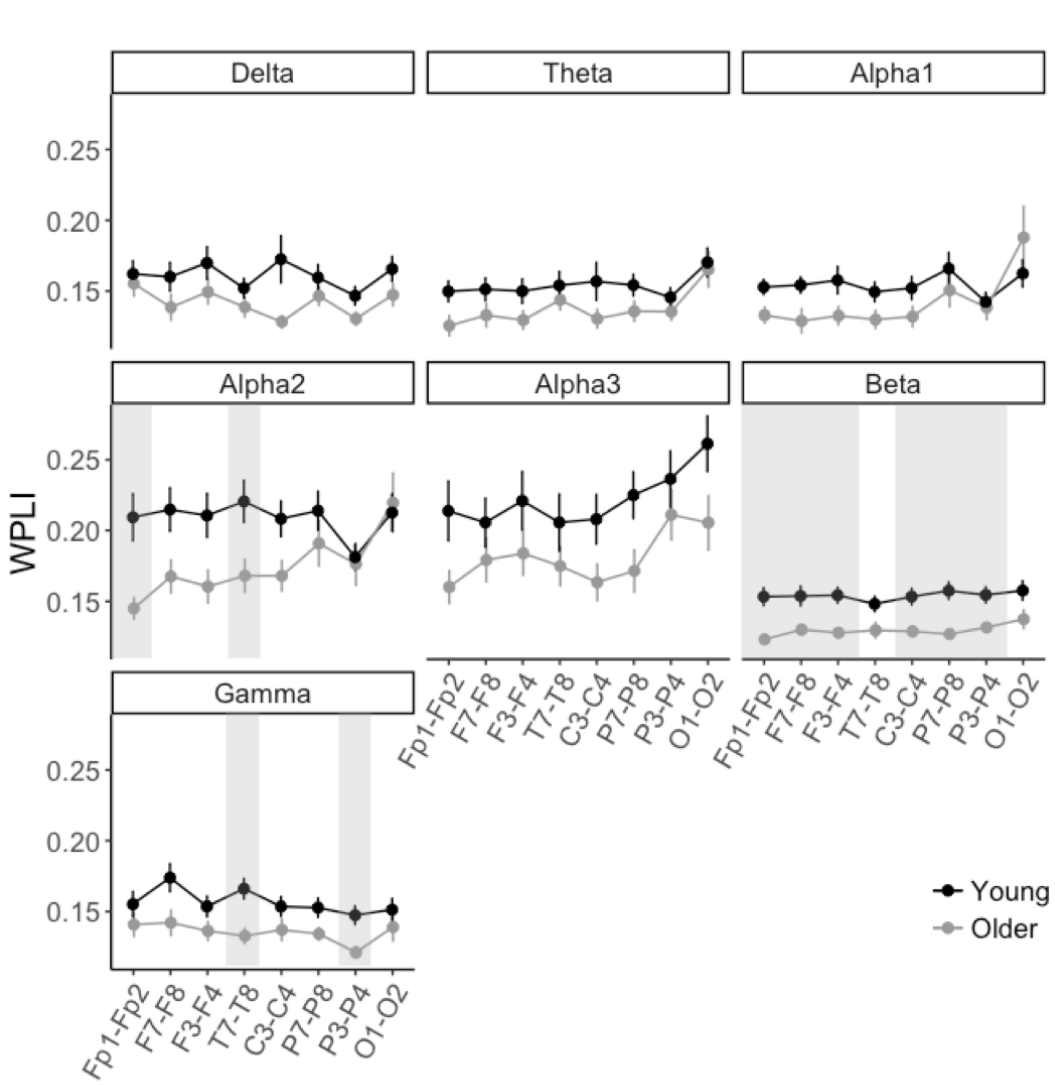

Figure 6-2: Average group differences in interhemispheric WPLI at each electrode pair and individualised frequency band. Shaded regions indicate statistically significant t-test differences with a FDR-corrected significance threshold of at most p = .049. Error bars represent standard error of the group mean.

6.3.3 Classification of older adults

Electrode and frequency combinations that significantly differentiated between young and older adults after FDR correction were submitted to ROC analysis. Coherence and WPLI were analysed separately, then together. Coherence parameters dissociated young and older groups with a classification accuracy (AUC) of 88.78% (sensitivity = 81.81%, specificity = 86.48%; Figure 6-3A). WPLI parameters successfully dissociated between age groups with an AUC of 86.65% (sensitivity = 78.78%, specificity = 81.1%; Figure 6-3B). The combination of coherence and WPLI parameters dissociated between young and older adults with an AUC of 95.17% (sensitivity = 84.84%, specificity = 94.59%; Figure 6-3C).

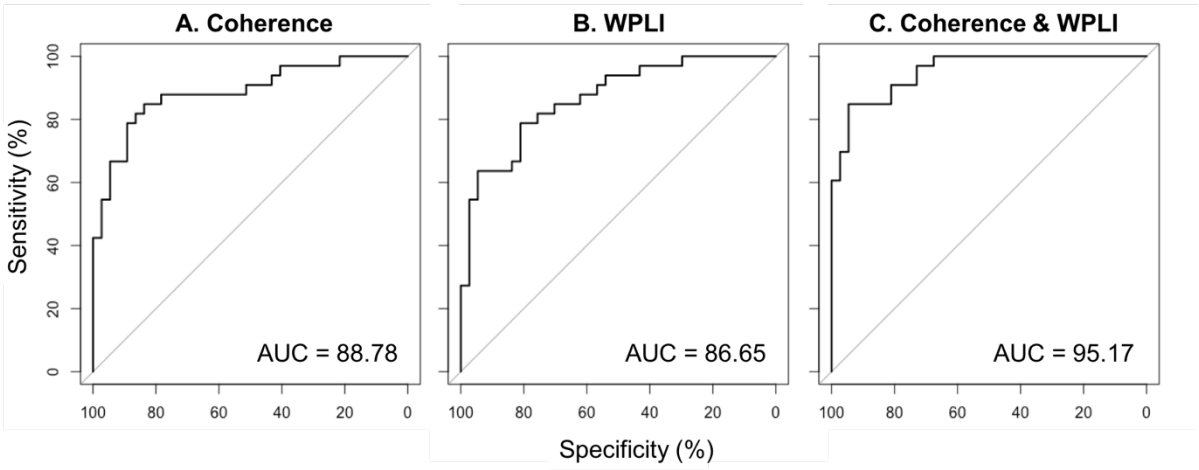

Figure 6-3: Receiver operator characteristic (ROC) curves for the classification of older adults against younger adults. (A) ROC using interhemispheric coherence parameters. (B) ROC using interhemispheric WPLI parameters. (C) ROC using both coherence and WPLI parameters.

6.4 Discussion

We set out to determine whether age-related patterns of CC atrophy were evident in EEG-derived IFC. Specifically, we hypothesised that older adults would exhibit reduced IFC in frontal and parietal channels. We recorded eyes-closed resting state EEG in a group of younger and older adults and used classic and updated connectivity metrics to measure IFC. Indeed, older adults displayed significantly reduced spectral coherence in frontal channels (Fp1-Fp2, F3-F4, F7-F8) in the delta, alpha and gamma frequency bands compared to the young adult group. The WPLI yielded widespread beta disconnectivity in older adults, and additional reductions in IFC at frontal, temporal and parietal sites in the alpha2 and gamma frequency bands.

Analysis of interhemispheric spectral coherence revealed spatial patterns consistent with CC disconnectivity observed in structural imaging studies of normal ageing, with strong reductions evident in the anterior channels. Significantly lower frontal connectivity in older adults was also reported by Duffy et al. (1996) using spectral coherence, though they neglected to adjust their significance threshold for multiple comparisons. Consistent with the present results, Kikuchi, Wada, Koshino, Nanbu and Hashimoto (2000) reported reduced anterior interhemispheric coherence for older adults in alpha frequencies between 11-12.5 Hz. They also reported a reduction in O1-O2 coherence in the theta band, and a C3-C4 coherence reduction across all frequencies, which were not detected by the measures in this study. Again, these effects may be conflated as the authors did not adjust the *p*-value threshold to correct for multiple testing, although such patterns weren't evident in our uncorrected results. Alternatively, neglecting to adjust frequency band borders to the individual peak alpha frequency may have led to a comparison of young adult theta frequencies with older adult alpha

frequencies (Scally et al., 2018a), thus biasing differences in favour of younger adults. While it is not yet known if frontal IFC is associated with age-related declines in cognition, our results suggest that frontal interhemispheric coherence may be a useful feature for classifying adults over the age of 65 with decent accuracy (88.78%).

The WPLI metric did not express the same pattern of interhemispheric frontal disconnectivity as seen with coherence in older adults, but was instead sensitive to group differences in interhemispheric beta synchronisation across the majority of electrode sites. Beta WPLI disconnectivity had a high classification accuracy (AUC) for older participants of 86.65%. To our knowledge, no other studies have reported specific reductions of interhemispheric beta-band connectivity in older adults with phase-lag metrics. Knyazev, Volf and Belousova (2015) examined whole-brain network connectivity between young and older adults using lagged phase synchronisation (Pascual-Marqui et al., 2011), a phase-based connectivity measure with adjustments for zero-phase relationships. Compared to young adults, they found reduced modularity (the extent to which a network can be segregated into distinct subnetworks) in beta networks of older adults, indicating altered topology and reduced specialisation of beta networks in older participants. Additionally, they reported that the difference between eyes-open and eyes-closed beta connectivity strength was reduced in older adults, and that this difference correlated with performance on attentional tasks (Knyazev et al., 2015). However, unlike the present study, only marginal group differences in beta connectivity strength were reported. In task-related EEG, Wang et al. (2017) described increased phase-lag index connectivity in older adult beta frequencies compared to young adults during audio-visual integration, which was interpreted as compensatory neural recruitment to manage increased task demands (Roberto Cabeza, Anderson, Locantore,

& McIntosh, 2002; Reuter-Lorenz & Park, 2014). Beta frequency power has been linked to fMRI resting state networks, such as the default mode, frontal, somatosensory and attentional networks, which exhibit reduced connectivity in older adults (Balsters et al., 2013). However, high alpha power was also correlated with many of the same networks (Balsters et al., 2013), which showed no modulation by age in the present study. Further investigations of beta phase disorganisation are warranted to determine if age group differences are functionally relevant.

One interpretation of the discrepancy between coherence and WPLI is that the interhemispheric coupling evident in spectral coherence was largely influenced by volume conduction components that were ignored by the WPLI metric. Indeed, spectral coherence tended to increase somewhat with reduced inter-electrode distance (see Figure 6-1), indicating the presence of volume conduction. However, this argument suggests that the group differences in spectral coherence reflect group differences in volume conduction at frontal sites. Furthermore, high interhemispheric connectivity between electrodes close to the midline is consistent with the organisation of the commissural fibre tracts, which project to bilateral superior areas of each hemisphere (Hofer & Frahm, 2006). The consistency of between-group coherence differences with the well acknowledged anterior-posterior gradient of CC degeneration in older adults (Bennett et al., 2010; Lebel et al., 2010), as well as the documented modulation of interhemispheric coherence by trauma to the CC (Brázdil et al., 1997; Corsi-Cabrera, Trías, Guevara, Haro, & Hernández, 1995; Montplaisir et al., 1990; Nagase et al., 1994; Nielsen et al., 1993), suggests that frontal interhemispheric coherence may be indicative of genuine differences in IFC between young and older adults.

In terms of limitations, this study would benefit from direct measures of the CC to correlate with EEG derived IFC, considering that the few studies that have explicitly explored this link were conducted on clinical samples with lesions to the CC (Montplaisir et al., 1990; Nagase et al., 1994; Nielsen et al., 1993; Pogarell et al., 2005; Teipel, Pogarell, et al., 2009). Pogarell et al. (2005) found positive correlations between interhemispheric coherence and CC size in a group of patients with Alzheimer's disease. Similarly, Teipel et al. (2009) demonstrated that temporal and posterior EEG alpha coherence was correlated with posterior white matter structures, including the posterior CC fibres, in a sample of healthy older adults and older adults with Mild Cognitive Impairment. The inclusion of DTI measures in the present study would have allowed us to directly test the relationship between interhemispheric connectivity and specific tracts of the CC. As discussed in Scally et al. (2018a), localisation studies have determined that the source of alpha oscillations in the eyes-closed EEG is the thalamus (Goldman et al., 2002; Zhongming Liu et al., 2012; Scheeringa et al., 2012), activity from which is negatively correlated with visual areas and the majority of the cerebral cortex in fMRI studies (Zhongming Liu et al., 2012). Activity measured during eyes-closed resting state EEG may therefore not represent cortico-cortical activity. However, the present findings of reduced coherence between frontal interhemispheric channels for older adults, in addition to prior findings of IFC reductions in split brain patients (e.g. Montplaisir et al., 1990), suggest that IFC may indeed map onto underlying white matter architecture. With respect to this issue, the study could have taken advantage of an eyes-open resting state condition, which are increasingly omitted from investigations of resting state EEG connectivity. Eyes-open conditions may be less sensitive to thalamic sources of alpha oscillations and more sensitive to cortico-cortical connectivity.

To summarise, we demonstrated that older adults exhibited reductions in interhemispheric EEG connectivity that are predominantly restricted to anterior EEG channels. This pattern was evident using spectral coherence, while WPLI detected age group differences predominantly in beta frequencies. The finding of reduced frontal interhemispheric coherence in older adults is consistent with a large body of literature suggesting that the anterior genu of the CC is targeted by older age (Bennett et al., 2010b; Davis et al., 2009; Lebel et al., 2012; Lebel et al., 2010), and that older age leads to disruption of frontally localised cognitive functions (Kennedy & Raz, 2009; Wasylyshyn et al., 2011). The combination of spectral coherence and WPLI IFC enabled a classification accuracy of 95.17% for differentiating the older from the younger adult group, suggesting that IFC could be an useful marker of normal ageing. Future investigations of interhemispheric connectivity in ageing or age-related pathology should continue to adapt frequency band limits to the individual, and include an eyes-open resting state condition to avoid the influence of thalamic alpha oscillations on cortico-cortical connectivity.

Chapter 7

7. General Discussion

A considerable amount of research has examined the effects of age and AD-related pathology on the commissural white matter tracts of the CC. The studies presented in this thesis were designed to further examine structural and functional properties of the brain's commissural white matter fibres in healthy ageing and AD, in order to extend this body of work. Our primary goal was to characterise age and disease effects on the occipital, parietal and temporal tract bundles of the posterior CC splenium (Chapters 2 and 3), which have rarely been directly explored in previous research studies. Subsequent studies were designed to examine differences in functions of the CC between young and older adults, including interhemispheric transfer of visual information (Chapter 4) and resting state functional EEG connectivity (Chapters 5 and 6). Additionally, attempts were made to offer methodological developments for the study of interhemispheric transfer functions (Chapter 4) and EEG-derived functional connectivity (Chapter 5).

7.1 Novel insights into the CC splenium in older age and AD pathology

In Study 1 (Chapter 2) we used DTI tractography to examine differences between young and older adults in the occipital, parietal and temporal tracts of the CC splenium, both in a sample of locally recruited participants (Study 1A) and a slightly older sample obtained from a publicly available cohort dataset (CamCAN; Study 1B). Across both studies, robust spatial patterns of age-group differences were evident in midsagittal segments of the CC.

MD and RD diffusion parameters from parietal and temporal tract segments were significantly increased in older adults compared to young adults, while occipital segment MD and RD were equivalent between groups. In the analysis of full unsegmented tract bundles, Study A revealed reduced FA, increased MD and increased RD in parietal tracts of older adults, whereas Study B observed differences across all metrics and tract bundles (except temporal FA). The discrepancy between Study 1A and Study 1B was attributed to the small sample size of Study 1A and age differences between the two samples. According to previous studies that have documented the cross-sectional lifespan trajectory of CC tract diffusion parameters (e.g. Lebel et al., 2010), tracts of the more mature young adults in Study 1B (mean age = 30.75 years) would be more developed than those of young adults in Study 1A (mean age = 22.41 years). Similarly, older adults in Study 1B were of older age (mean age = 80.21 years) than those in Study 1A (mean age = 68.33 years), and were therefore likely to exhibit weaker white matter integrity due to more advanced age-related degeneration (Lebel et al., 2012). Lifespan trajectories of the distinct splenium bundles have been investigated in previous work, but not in participants beyond age 60. Both Lebel et al. (2010) and Hasan et al. (2009) examined the splenium tract bundle parameters as a function of age in 5-59 year olds, samples not mature enough to observe patterns of decline in older age. To our knowledge, Study 1 (Chapter 2) identified for the first time that parietal and temporal, but not occipital segments of the midsagittal CC are affected by older age.

Older adults exhibited increased temporal tract density compared to young adults in two independent samples and MRI scanning facilities (Study 1; Chapter 2), which may indicate a continued growth or accumulation of interhemispheric temporal fibres throughout the lifespan. Age-related increases in tract density coincided with increases

in temporal tract RD, indicating reduced white matter integrity in older age. This pattern was evident for both the full and segmented tract analysis. This robust finding may have implications for network (or 'connectome') models of DTI tractography data that use measures of tract quantification to indicate the degree of connectivity between regions of interest in the brain (Hagmann et al., 2008), as increased tract density may not indicate improved diffusivity in older adults for particular tracts. As discussed by Jones et al. (2013), quantification metrics like tract density should not be directly interpreted as a 'fibre count', due to the probabilistic nature of DTI tract reconstruction. Further work should explore whether age-related increases in temporal tract density are observable using other neuroimaging methods, and correlate with functions in older adults.

Study 2 (Chapter 3) investigated whether the same occipital, parietal or temporal splenium tract bundles were differentially affected by MCI and AD, in comparison to healthy older adults. The study benefitted greatly from patient data obtained from the NACC initiative, categorised into groups using diagnostic clinical criteria. The participants were also accurately age and sex matched. Study 1 (Chapter 2) had previously described the effects of normal ageing on these tracts, making it possible to infer whether particular tracts were sensitive or specific to AD pathology over normal ageing. Segmented parietal tracts were significantly affected in AD patients, and both MD and DA parameters classified AD patients against controls with an accuracy of > 95%. MCI patients also had significantly higher parietal tract MD and RD than controls, which demonstrated low to moderate accuracy for classifying MCI patients against controls. Previously, Preti et al. (2012) found that AD patients had lower FA than healthy controls across all sections of the CC, while MCI patients exhibited significant FA reductions in only the full occipital, parietal and temporal tracts of the splenium. Interestingly, we did not observe such FA

reductions in Study 2, while our analysis of the segmented tracts revealed specific reductions in parietal MD and RD, rather than FA for MCI patients. Also in contrast to Preti et al. (2012), AD patients in our study did not exhibit reduced FA in any of the unsegmented tracts bundles, but reduced parietal tract MD and RD. At the CC midline, AD patients did not exhibit FA reductions in the parietal tracts, but increases in all other diffusion parameters (MD, RD and DA). Similar effects on parietal tracts were seen in both the ageing (Study 1B) and AD studies (Study 2): increased MD/RD and increased DA. It is possible to conclude that, in the context of AD, changes to parietal tract integrity is a sensitive rather than specific feature of disease, and may represent an acceleration of the white matter changes that occur in normal ageing.

A mutual finding of Study 1 and Study 2 was increased parietal tract DA in the groups expected to be associated with reduced white matter integrity. In Study 1B, older adults had significantly elevated DA in parietal CC segments compared to young adults. Similarly, AD patients exhibited significantly increased parietal segment DA compared to controls in Study 2, while MCI patients showed a trend towards elevated parietal DA. Each observation of increased DA was accompanied by an increase in MD and/or RD, which were interpreted as reductions in the myelin content of the underlying fibres (Wei et al., 2013). This simultaneous increase in DA and reduction in RD has been observed in ageing studies that examined diffusivity of the CC genu (Bennett et al., 2010; Zahr et al., 2009). Furthermore, age trends illustrated by Lebel et al. (2010) demonstrate an upwards trend of DA in occipital, temporal and parietal CC tract bundles from ~30 years of age. Bennett et al. (2012) suggested that a reduction of axonal packing density in thinly myelinated, small-diameter white matter structures like the genu may be responsible for this phenomenon:

> For example, age differences in microstructural level variables contributing to decreased axonal packing density may be mild enough in Radial Increase Only and Radial Increase/Axial Decrease clusters to only increase RD. However, more severe decreases in axonal packing density from, for example, a greater loss of myelin or axons in aging, would lead to a global increase in extracellular water, resulting in larger RD increases and subsequent [axial diffusivity] increases in Radial/Axial Increase clusters. (Bennett et al., 2010, p. 8)

Our data provides some support for this interpretation. Like the CC genu, the midsagittal parietal CC segment contains small-diameter fibres that are thinly myelinated (Aboitiz et al., 2003, 1992; Caminiti et al., 2013). In fact, Caminiti et al. (2013) demonstrated that the human parietal CC area contained fibres identical in diameter to the CC genu. Therefore, both ageing and AD may target CC regions of small axonal diameter.

The axonal diameter hypothesis is in opposition to the retrogenesis hypothesis of CC degeneration in AD. Retrogenesis proposes a "last in, first out" process, whereby white matter connections that mature latest in development are the first to degrade with the onset of AD symptomology. Lebel et al. (2010) used curve fitting to estimate the age of peak maturation for FA and MD parameters of tract bundles within the CC. They reported that the occipital and orbitofrontal tracts were the first to mature, while the superior parietal and superior frontal sections of the CC midbody were latest to mature. In support of the retrogenesis model, Stricker et al. (2016) divided the CC into regions of early, middle and late myelination and found that regions of later development (CC midbody; in accordance with Lebel et al., 2010) were associated with reduced FA in MCI patients compared to controls. The late-maturing CC midbody consists mainly of large-diameter fibres that project to motor and somatosensory areas, whereas the earlier-maturing

orbitofrontal, temporal and posterior parietal tracts contain small diameter fibres (Aboitiz et al., 2003, 1992; Caminiti et al., 2013). In contrast to the findings in support of retrogenesis, the axonal diameter hypothesis would conceive that small-diameter, early maturing tracts would be the first to experience degeneration in AD. A direct comparison of these models would be beneficial to further our understanding of how commissural white matter is targeted by ageing and AD neuropathology.

7.2 Differences in functions of the CC in older age

The results from Study 1 (Chapter 2) suggested that the occipital segments of the CC were unaffected by ageing, relative to parietal and temporal tracts. However, older adults in Study 1B exhibited significantly reduced white matter integrity in the full unsegmented occipital tract bundles. This creates ambiguity as to whether functions that rely on the occipital commissural tracts are impaired in older age. Several studies had reported that the speed of transferring visual information between the hemispheres (a function heavily reliant on interhemispheric occipital tracts) was compromised in older adults (Bellis & Wilber, 2001; Davis, Kragel, Madden, & Cabeza, 2012; Jeeves & Moes, 1996; Reuter-Lorenz & Stanczak, 2000), while others studies found no differences (Boyson, 2013; Hoptman et al., 1996; Linnet & Roser, 2012; Schulte et al., 2013). Study 3 (Chapter 4) was designed to examine age group differences in IHTT between young and older adults. No age-group differences were found in the classic reaction time measure of IHTT, using either mean or median measures of response time. In response to methodological shortcomings of previous studies, we proposed a constrained ERP methodology for the detection of cleaner stimulus-evoked visual potentials from which to calculate visual

IHTT, and analysed the results within the alpha and theta frequency bands separately. In the theta band, older adults had elongated IHTT for P1 and N1 components, which was entirely driven by earlier activations in the hemisphere contralateral to the stimulus, rather than delayed activations in the ipsilateral hemisphere. In the alpha band, no age group effects were evident. Thus, it was concluded that IHTT was not impaired in older adults, in line with preserved integrity of the midsagittal segments of occipital tracts in older adults (Study 1A, 1B).

In Studies 4 and 5 (Chapters 5 and 6) we examined EEG functional connectivity in young and older adults. We acknowledged that although a number of studies had reported about disparities in functional connectivity between younger and older adults, none had considered the influence of age-induced dominant EEG frequency slowing on inter-group connectivity differences. We firstly replicated the finding that older age is associated with a significant slowing of the IAPF (Aurlien et al., 2004; Duffy et al., 1984; Klimesch, 1999), and noted considerable variability of the IAPF within age groups (Klimesch, 1999). We demonstrated that the frequencies at which connectivity was highest were strongly and positively correlated with the IAPF, such that global connectivity strength was highest at the IAPF. Thus it was argued that frequency band limits should be adapted to the IAPF of the individual participant when conducting connectivity analyses in the time-frequency domain. Taking the upper alpha band (conventionally 10-12 Hz) as an example, we showed that older adults had significantly reduced global upper alpha connectivity compared to young adults when the conventional frequency limits were applied. In contrast, there were no group differences in global connectivity at the IAPF. This suggested that significant age group differences observed in connectivity analyses of conventional frequency bands likely arise due to the

slowing of the frequency spectrum in older adults. We therefore suggested that studies of time-frequency domain EEG connectivity should adapt frequency limits to the individual IAPF, to account for inter- and intra-group variability in the frequency spectrum.

Study 5 (Chapter 6) examined IFC differences between young and older adults. An abundance of previous studies have shown that physiology of the CC modulates IFC, in individuals with a severed CC (Brázdil et al., 1997; Corsi-Cabrera et al., 1995; Montplaisir et al., 1990), individuals with agenesis of the CC (Knyazeva et al., 1997; Koeda et al., 1995; Kuks, Vos, & O'Brien, 1987; Nagase et al., 1994; Nielsen et al., 1993) and in individuals with AD (Pogarell et al., 2005; Teipel et al., 2009). However, investigations of IFC in normal ageing have not considered (a) the effects of age-related IAPF slowing on age group differences in IFC and (b) updated connectivity metrics that are insensitive to volume conduction (as emphasised in Study 4). In Study 5 we calculated IFC in frequency bands that were adapted to the individual participant IAPF. Additionally, we used both classic (spectral coherence) and more novel (WPLI) connectivity metrics to examine group differences when zero-phase connectivity was disregarded. We found that interhemispheric spectral coherence expressed spatial patterns of disconnectivity in older adults that were in line with well-documented patterns of age-related CC degeneration from studies utilising *in vivo* imaging (Bennett, Madden, Vaidya, Howard, & Howard, 2010; Lebel et al., 2012; Lebel, Caverhill-Godkewitsch, & Beaulieu, 2010; Sullivan & Pfefferbaum, 2006; Sullivan et al., 2010). Specifically, older adults had significantly reduced interhemispheric coherence between anterior electrodes of the left and right hemisphere in several frequency bands, which aligns with the anterior-posterior gradient of CC atrophy in DTI studies (Bennett et al., 2010; Davis et al., 2012).

Interhemispheric WPLI connectivity revealed a more frequency- than spatially-specific pattern of differences, with age reductions evident at high frequencies, predominantly in the beta band. Beta frequencies have been linked to the default mode, and other networks using co-registered fMRI/EEG methods (Balsters et al., 2013) and our findings may therefore reflect disconnected properties of these networks in ageing. However, further research using simultaneous fMRI and EEG connectivity measures is necessary to fully understand the functional significance of age-related disconnectivity in beta WPLI.

Both IHTT and IFC studies suggested that functional connectivity between the bilateral occipital lobes, presumably governed by the large-diameter fibres of the occipital splenium projections, is preserved in older age. This is consistent with the majority of results from Study 1, which suggested that diffusion parameters of the interhemispheric occipital tracts were equivalent in young and older adults. Notably, the results are inconsistent with Study 1B, which reported that the full unsegmented occipital tracts experienced reduced integrity in older age. This could be attributed to age differences between the older adult samples in each study. Older adults in Studies 4 and 5 had a mean age of 69.75, whereas older adults in Study 1B had a mean age of 80.21. Future research should assess whether IHTT and occipital IFC are affected in older adults later in the lifespan, and whether these functional measures correlate with DTI metrics. Coherent with the reductions of temporal CC tract integrity in older adults in Study 1, there was some evidence of reduced temporal IFC in the older adult group within the gamma and alpha2 bands. Additionally, reduced parietal IFC in beta and gamma WPLI was evident in older adults, which maps on to the finding of reduced parietal CC tract integrity in Study 1. Multimodal imaging studies are necessary to determine whether these relationships between structural and functional connectivity are tangible.

Further work is required to investigate how IHTT and IFC are affected in MCI and AD patients. Given that IHTT was not detrimentally affected in normal older adults (Study 3, Chapter 4), an elongated IHTT in MCI/AD patients may be a specific effect of disease over ageing. Indeed, Study 2 (Chapter 3) suggested that AD patients (but not MCI patients) experience a degree of degeneration in the midsagittal occipital CC segments, which are assumed to govern visual interhemispheric transfer functions (Westerhausen et al., 2006). Although there is variability across studies in the coupling measures employed and the patient samples used, previous studies have noted reduced IFC in AD patients across both anterior and posterior regions (Hata et al., 2016; Pogarell et al., 2005; Sankari, Adeli, & Adeli, 2011; Wada, Nanbu, Koshino, Yamaguchi, & Hashimoto, 1998). Like the ageing literature, no AD/MCI functional connectivity studies have systematically accounted for the effects of disease on the IAPF, which has been shown to slow further in AD than in older age (Jelic et al., 2000; Jeong, 2004; Kwak, 2006; Penttilä et al., 1985). Reduced interhemispheric coherence in MCI/AD at posterior sites may be a specific predictor of disease, as posterior coherence was unaffected in our sample of normal older adults compared to young adults (Study 5, Chapter 6). However, future studies should control for group differences in IAPF that may be responsible for differences in IFC.

7.3 Future directions and limitations

There is scope for the development and follow-up of the findings presented in this thesis. A major open question concerns the functional significance of the parietal and temporal tracts of the splenium, which is largely unknown. Interhemispheric temporal tracts have

been associated with binaural processing (Westerhausen et al., 2009), although a number of caveats of this study, including uncontrolled family-wise error rate and small sample size, render the finding disputable. Dougherty et al. (2007) found that temporal CC tract FA, MD and RD were significantly correlated with phonological awareness in children. Thus, commissural tracts that project to temporal areas, in particular the auditory cortices, may govern the interhemispheric processing of auditory information. This is consistent with studies that have found elongated IHTT for auditory stimuli and impaired orientation to the left ear during dichotic listening in older adults (Gootjes, Van Strien, & Bouma, 2004; Jerger, Alford, Lew, Rivera, & Chmiel, 1995) and AD patients (Bouma & Gootjes, 2011; Duchek & Balota, 2005; Gootjes et al., 2006). Multimodal imaging is necessary to confirm that interhemispheric processing of auditory information maps onto temporal tract parameters.

Relatively little is known about parietal CC functions. Yin et al. (2012) found that the timing of orienting attention during a flanker task was correlated with FA, MD and RD of the interhemispheric parietal white matter that connected the bilateral inferior parietal lobules. Davis & Cabeza (2015) found that the BFA in a split-field word matching task, but not face matching, was unexpectedly correlated with the midsagittal segment of the parietal CC tracts. However, CC tracts were not partitioned using tractography localisation, so the accuracy of the ROIs in this study is dubious as they may contain tracts from other bundles. Further probing is necessary to determine the functional specifications of these tracts. Candidate functions include the interhemispheric processing of visuospatial information during episodic memory tasks (Delvenne et al., 2011; Delvenne & Holt, 2012; Holt & Delvenne, 2014, 2015; Kraft et al., 2015), which is heavily reliant on the posterior parietal cortex (Corbetta, Kincade, Ollinger, McAvoy, &

Shulman, 2000). As older adults exhibited significantly impaired parietal tract diffusivity and tract density compared to young adults, it should be tested whether older adults exhibit comparable differences in the BFA of visuospatial working memory.

Additional attention should be placed on identifying the patterns of CC degeneration in normal ageing and AD, particularly whether degeneration adheres to a retrogenetic process or whether fibres of a particular diameter are targeted. Although we did not examine CC integrity at middling or anterior sections, our analysis of the parietal, temporal and occipital commissural tracts was in support of a fibre diameter model, which has not been fully tested in the context of either ageing or AD. By ascertaining the exact patterns of structural decline in ageing and AD, interventions can be better targeted at brain structures that experience degeneration at the earliest stages of AD and their associated functions, which may alleviate symptom severity and the burden of care on relatives and at a larger scale, the economy.

A major caveat of this body of work was that we were unable to recruit the same groups of participants to each study, and therefore there was no access to both structural and functional imaging for a single sample of participants. Structural imaging of the CC is required to ensure that any functional measures of interest are correlated with the integrity of the CC region under scrutiny. For example, it would be optimal to correlate the age-related anterior interhemispheric disconnectivity in Study 5 (Chapter 6) with diffusion parameters extracted from the anterior commissural tracts of the same participants, to show that IFC is indeed indexing the microstructural degeneration associated with normal ageing. Similarly, in Study 3 (Chapter 4) visual interhemispheric transfer was assumed to materialise in the occipital tracts of the CC, whereas the CUD was hypothesised to occur through more anterior callosal channels. While a select few studies

have attempted to assess these relationships directly (Omura et al., 2004; Weber et al., 2005; Westerhausen et al., 2006), it would have been useful to extend these endeavours with more novel and updated methods.

Aside from academic advancements, a notable real-world application of this research is for aiding the classification of normal and abnormal ageing using neuroimaging methods. Home-based neuroimaging devices are becoming increasingly available and relevant, especially portable devices based on EEG measurements (Cassani et al., 2017; Cecchi et al., 2015; Scally, Calderon, Anghinah, & Parra, 2016). Metrics from Study 5 (Chapter 6) that had high accuracy for classifying normal older adults may be incredibly useful as features for automatically classifying normal ageing, and deviation from normal ageing, using these portable devices in concurrence with machine learning algorithms. The ability to track deviation from normal ageing quickly may have significant health and economic implications, by identifying abnormalities at early stages, and making GP referrals more efficient.

7.4 Conclusions

The present thesis provides some novel insight into how normal ageing and AD affects structural and functional aspects of the CC. What remains apparent is that particular white matter pathways of the brain that we have demonstrated to degenerate in older age and AD still elude a functional interpretation. Progress in uncovering these functions may be of great benefit to the cognitive neuroscience of age and disease. Further examination of how the CC is spatially targeted by AD is also of interest, and may generalise to other white matter structures.

References

Abe, O., Aoki, S., Hayashi, N., Yamada, H., Kunimatsu, A., Mori, H., … Ohtomo, K. (2002). Normal aging in the central nervous system: Quantitative MR diffusion-tensor analysis. *Neurobiology of Aging*, *23*(3), 433–441. http://doi.org/10.1016/S0197-4580(01)00318-9

Aboitiz, F., López, J., & Montiel, J. (2003). Long distance communication in the human brain: Timing constraints for inter-hemispheric synchrony and the origin of brain lateralization. *Biological Research*, *36*(1), 89-99. http://doi.org/10.4067/S0716-97602003000100007

Aboitiz, F., & Montiel, J. (2003). One hundred million years of interhemispheric communication: The history of the corpus callosum. *Brazilian Journal of Medical and Biological Research*, *36*(4), 409-420. http://doi.org/10.1590/S0100-879X2003000400002

Aboitiz, F., Rodriguez, E., Olivares, R., & Zaidel, E. (1996). Age-related changes in fibre composition of the human corpus callosum: sex differences. *Neuroreport*, *7*(11), 1761–1764. https://doi.org/10.1097/00001756-199607290-00013

Aboitiz, F., Scheibel, A. B., Fisher, R. S., & Zaidel, E. (1992). Fiber composition of the human corpus callosum. *Brain Research*, *598*(1–2), 143–153. http://doi.org/10.1016/0006-8993(92)90178-C

Acosta-Cabronero, J., Alley, S., Williams, G. B., Pengas, G., & Nestor, P. J. (2012). Diffusion Tensor Metrics as Biomarkers in Alzheimer's Disease. *PLoS ONE*, *7*(11). http://doi.org/10.1371/journal.pone.0049072

Acosta-Cabronero, J., Williams, G. B., Pengas, G., & Nestor, P. J. (2010). Absolute diffusivities define the landscape of white matter degeneration in Alzheimer's disease. *Brain*, *133*(2), 529–539. http://doi.org/10.1093/brain/awp257

Agosta, F., Pievani, M., Sala, S., & Geroldi, C. (2011). White matter damage in Alzheimer disease and its relationship to gray matter atrophy. *Radiology*, *258*(3), 853–863. http://doi.org/10.1148/radiol.10101284/-/DC1

Albert, M. S., DeKosky, S. T., Dickson, D., Dubois, B., Feldman, H. H., Fox, N. C., … Phelps, C. H. (2011). The diagnosis of mild cognitive impairment due to Alzheimer's disease: Recommendations from the National Institute on Aging-Alzheimer's Association workgroups on diagnostic guidelines for Alzheimer's disease. *Alzheimer's and Dementia*, *7*(3), 270–279. http://doi.org/10.1016/j.jalz.2011.03.008

Allen, J. S., Bruss, J., Brown, C. K., & Damasio, H. (2005). Normal neuroanatomical variation due to age: The major lobes and a parcellation of the temporal region. *Neurobiology of Aging*, *26*(9), 1245–1260. http://doi.org/10.1016/j.neurobiolaging.2005.05.023

Alves, G. S., O'Dwyer, L., Jurcoane, A., Oertel-Knöchel, V., Knöchel, C., Prvulovic, D., … Laks, J. (2012). Different Patterns of White Matter Degeneration Using Multiple Diffusion Indices and Volumetric Data in Mild Cognitive Impairment and Alzheimer Patients. *PLoS ONE*, *7*(12). http://doi.org/10.1371/journal.pone.0052859

Alves, G. S., Oertel Knöchel, V., Knöchel, C., Carvalho, A. F., Pantel, J., Engelhardt, E., & Laks, J. (2015). Integrating retrogenesis theory to alzheimer's disease pathology: Insight from DTI-TBSS investigation of the white matter microstructural integrity. *BioMed Research International, 2015*. http://doi.org/10.1155/2015/291658

Amlien, I. K., & Fjell, A. M. (2014). Diffusion tensor imaging of white matter degeneration in Alzheimer's disease and mild cognitive impairment. *Neuroscience*, *276*, 206-215. http://doi.org/10.1016/j.neuroscience.2014.02.017

Angelakis, E., Lubar, J. F., & Stathopoulou, S. (2004). Electroencephalographic peak alpha frequency correlates of cognitive traits. *Neuroscience Letters*, *371*(1), 60–63. http://doi.org/10.1016/j.neulet.2004.08.041

Anstey, K. J., Mack, H. A., Christensen, H., Li, S. C., Reglade-Meslin, C., Maller, J., … Sachdev, P. (2007). Corpus callosum size, reaction time speed and variability in mild cognitive disorders and in a normative sample. *Neuropsychologia*, *45*(8), 1911–1920. http://doi.org/10.1016/j.neuropsychologia.2006.11.020

Association, A. (2015). 2015 Alzheimer's disease facts and figures. *Alzheimer's and Dementia*, *11*(3), 332–384. http://doi.org/10.1016/j.jalz.2015.02.003

Aung, W. Y., Mar, S., & Benzinger, T. L. (2013). Diffusion tensor MRI as a biomarker in axonal and myelin damage. *Imaging in Medicine*. *5*(5), 427. http://doi.org/10.2217/iim.13.49

Aurlien, H., Gjerde, I. O., Aarseth, J. H., Eldøen, G., Karlsen, B., Skeidsvoll, H., & Gilhus, N. E. (2004). EEG background activity described by a large computerized database. *Clinical Neurophysiology*, *115*(3), 665–673. http://doi.org/10.1016/j.clinph.2003.10.019

Babiloni, C., Binetti, G., Cassarino, A., Dal Forno, G., Del Percio, C., Ferreri, F., … Rossini, P. M. (2006). Sources of cortical rhythms in adults during physiological aging: A multicentric EEG study. *Human Brain Mapping*, *27*(2), 162–172.

http://doi.org/10.1002/hbm.20175

Bakeman, R. (2005). Recommended effect size statistics for repeated measures designs. *Behavior Research Methods*, *37*(3), 379–384. http://doi.org/10.3758/BF03192707

Ball, M. J., Hachinski, V., Fox, A., Kirshen, A. J., Fisman, M., Blume, W., … Merskey, H. (1985). A New Definition of Alzheimer's Disease: A Hippocampal Dementia. *The Lancet*, *325*(8419), 14–16. http://doi.org/10.1016/S0140-6736(85)90965-1

Balsters, J. H., O'Connell, R. G., Galli, A., Nolan, H., Greco, E., Kilcullen, S. M., … Robertson, I. H. (2013). Changes in resting connectivity with age: A simultaneous electroencephalogram and functional magnetic resonance imaging investigation. *Neurobiology of Aging*, *34*(9), 2194–2207. http://doi.org/10.1016/j.neurobiolaging.2013.03.004

Banich, M. (2003). The Divided Visual Field Technique in Laterality and Interhemispheric Integration. In K. Hugdahl (Ed.), *Experimental Methods in Neuropsychology* (pp. 47–63). Springer US. http://doi.org/10.1007/978-1-4615-1163-2_3

Barrick, T. R., Charlton, R. A., Clark, C. A., & Markus, H. S. (2010). White matter structural decline in normal ageing: A prospective longitudinal study using tract-based spatial statistics. *NeuroImage*, *51*(2), 565–577. http://doi.org/10.1016/j.neuroimage.2010.02.033

Barry, R. J., & De Blasio, F. M. (2017). EEG differences between eyes-closed and eyes-open resting remain in healthy ageing. *Biological Psychology*, *129*, 293–304. http://doi.org/10.1016/j.biopsycho.2017.09.010

Bastin, M. E., Maniega, S. M., Ferguson, K. J., Brown, L. J., Wardlaw, J. M., MacLullich, A. M. J., & Clayden, J. D. (2010). Quantifying the effects of normal ageing on white matter structure using unsupervised tract shape modelling. *NeuroImage*, *51*(1), 1–10. http://doi.org/10.1016/j.neuroimage.2010.02.036

Bastin, M. E., Piatkowski, J. P., Storkey, A. J., Brown, L. J., MacLullich, A. M. J., & Clayden, J. D. (2008). Tract shape modelling provides evidence of topological change in corpus callosum genu during normal ageing. *NeuroImage*, *43*(1), 20–28. http://doi.org/10.1016/j.neuroimage.2008.06.047

Bazanova, O. M. (2008). Age Related Alpha Activity Change Differs for Males and Females and for Low and High Al- pha Frequency EEG Pattern. *Revista Espanola de Neurop- Sicologia*, *10*(1), 82–83. https://doi.org/10.1016/0094-730x(80)90012-1

Bazanova, O. M., & Vernon, D. (2014). Interpreting EEG alpha activity. *Neuroscience and Biobehavioral Reviews*, *44*, 94–110. http://doi.org/10.1016/j.neubiorev.2013.05.007

Beekly, D. L., Ramos, E. M., Lee, W. W., Deitrich, W. D., Jacka, M. E., Wu, J., … Raskind, M. (2007). The National Alzheimer's Coordinating Center (NACC) database: The uniform data set. *Alzheimer Disease and Associated Disorders*, *21*(3), 249-258. http://doi.org/10.1097/WAD.0b013e318142774e

Behrens, T. E. J., Berg, H. J., Jbabdi, S., Rushworth, M. F. S., & Woolrich, M. W. (2007). Probabilistic diffusion tractography with multiple fibre orientations: What can we gain? *NeuroImage*, *34*(1), 144–155. http://doi.org/10.1016/j.neuroimage.2006.09.018

Belger, A., & Banich, M. T. (1992). Interhemispheric interaction affected by computational complexity. *Neuropsychologia*, *30*(10), 923–929. http://doi.org/10.1016/0028-3932(92)90036-L

Bellis, T. J., & Wilber, L. A. (2001). Effects of Aging and Gender on Interhemispheric Function. *Journal of Speech Language and Hearing Research*, *44*(2), 246. http://doi.org/10.1044/1092-4388(2001/021)

Bennett, I. J., & Madden, D. J. (2014). Disconnected aging: Cerebral white matter integrity and age-related differences in cognition. *Neuroscience*, *276*, 187–205. http://doi.org/10.1016/j.neuroscience.2013.11.026

Bennett, I. J., Madden, D. J., Vaidya, C. J., Howard, D. V., & Howard, J. H. (2010). Age-related differences in multiple measures of white matter integrity: A diffusion tensor imaging study of healthy aging. *Human Brain Mapping*, *31*(3), 378–390. http://doi.org/10.1002/hbm.20872

Biegon, A., Eberling, J. L., Richardson, B. C., Roos, M. S., Wong, S. T. S., Reed, B. R., & Jagust, W. J. (1994). Human corpus callosum in aging and alzheimer's disease: a magnetic resonance imaging study. *Neurobiology of Aging*, *15*(4), 393–397. http://doi.org/10.1016/0197-4580(94)90070-1

Birba, A., Hesse, E., Sedeño, L., Mikulan, E. P., García, M. del C., ávalos, J., … Ibáñez, A. (2017). Enhanced working memory binding by direct electrical stimulation of the parietal cortex. *Frontiers in Aging Neuroscience*, *9,* 178. http://doi.org/10.3389/fnagi.2017.00178

Black, S. E., Moffat, S. D., Yu, D. C., Parker, J., Stanchev, P., & Bronskill, M. (2000). Callosal

atrophy correlates with temporal lobe volume and mental status in Alzheimer's disease. *Canadian Journal of Neurological Sciences*, *27*(3), 204–209. http://doi.org/10.1017/S0317167100000846

Bloom, J. S., & Hynd, G. W. (2005). The role of the corpus callosum in interhemispheric transfer of information: Excitation or inhibition? *Neuropsychology Review*, *15*(2), 59–71. http://doi.org/10.1007/s11065-005-6252-y

Bors, D. A., & Forrin, B. (1995). Age, speed of information processing, recall, and fluid intelligence. *Intelligence*, *20*(3), 229–248. http://doi.org/10.1016/0160-2896(95)90009-8

Bosch, B., Arenaza-Urquijo, E. M., Rami, L., Sala-Llonch, R., Junqué, C., Solé-Padullés, C., … Bartrés-Faz, D. (2012). Multiple DTI index analysis in normal aging, amnestic MCI and AD. Relationship with neuropsychological performance. *Neurobiology of Aging*, *33*(1), 61–74. http://doi.org/10.1016/j.neurobiolaging.2010.02.004

Bouma, A., & Gootjes, L. (2011). Effects of attention on dichotic listening in elderly and patients with dementia of the Alzheimer type. *Brain and Cognition*, *76*(2), 286-293. http://doi.org/10.1016/j.bandc.2011.02.008

Bowley, M. P., Cabral, H., Rosene, D. L., & Peters, A. (2010). Age changes in myelinated nerve fibers of the cingulate bundle and corpus callosum in the rhesus monkey. *Journal of Comparative Neurology*, *518*(15), 3046–3064. http://doi.org/10.1002/cne.22379

Bowyer, S. M. (2016). Coherence a measure of the brain networks: past and present. *Neuropsychiatric Electrophysiology*, *2*(1), 1. http://doi.org/10.1186/s40810-015-

0015-7

Boyson, A. (2013). The effect of age on interhemispheric transfer time: an event related potential study. *The Plymouth Student Scientist*, *6*(2), 78-97.

Bozoki, A. C., Korolev, I. O., Davis, N. C., Hoisington, L. A., & Berger, K. L. (2012). Disruption of limbic white matter pathways in mild cognitive impairment and Alzheimer's disease: A DTI/FDG-PET Study. *Human Brain Mapping*, *33*(8), 1792–1802. http://doi.org/10.1002/hbm.21320

Bozzali, M., Falini, A., Franceschi, M., Cercignani, M., Zuffi, M., Scotti, G., … Filippi, M. (2002). White matter damage in Alzheimer's disease assessed in vivo using diffusion tensor magnetic resonance imaging. *Journal of Neurology Neurosurgery and Psychiatry*, *72*(6), 742–746. http://doi.org/10.1136/jnnp.72.6.742

Braun, C. M. J., Villeneuve, L., & Achim, A. (1996). Balance of cost and interhemispheric relay: Evidence from omission errors in the Poffenberger paradigm. *Neuropsychology*, *10*(4), 565–572. http://doi.org/10.1037/0894-4105.10.4.565

Brázdil, M., Brichta, J., Krajča, V., Kuba, R., & Daniel, P. (1997). Interhemispheric EEG coherence after corpus callosotomy. *European Journal of Neurology*, *4*(4), 419–425. http://doi.org/10.1111/j.1468-1331.1997.tb00373.x

Brickman, A. M., Meier, I. B., Korgaonkar, M. S., Provenzano, F. A., Grieve, S. M., Siedlecki, K. L., … Zimmerman, M. E. (2012). Testing the white matter retrogenesis hypothesis of cognitive aging. *Neurobiology of Aging*, *33*(8), 1699–1715. http://doi.org/10.1016/j.neurobiolaging.2011.06.001

Brier, M. R., Thomas, J. B., & Ances, B. M. (2014). Network Dysfunction in Alzheimer's

Disease: Refining the Disconnection Hypothesis. *Brain Connectivity*, *4*(5), 299–311. http://doi.org/10.1089/brain.2014.0236

Bronge, L., Bogdanovic, N., & Wahlund, L. O. (2002). Postmortem MRI and histopathology of white matter changes in Alzheimer brains: A quantitative, comparative study. *Dementia and Geriatric Cognitive Disorders*, *13*(4), 205–212. http://doi.org/10.1159/000057698

Brookes, M. J., Hale, J. R., Zumer, J. M., Stevenson, C. M., Francis, S. T., Barnes, G. R., … Nagarajan, S. S. (2011). Measuring functional connectivity using MEG: Methodology and comparison with fcMRI. *NeuroImage*, *56*(3), 1082–1104. http://doi.org/10.1016/j.neuroimage.2011.02.054

Brown, W. S., Bjerke, M. D., & Galbraith, G. C. (1998). Interhemispheric transfer in normals and acallosals: Latency adjusted evoked potential averaging. *Cortex*, *34*(5), 677–692. http://doi.org/10.1016/S0010-9452(08)70772-X

Brun, A., & Englund, E. (1986). A white matter disorder in dementia of the Alzheimer type: A pathoanatomical study. *Annals of Neurology*, *19*(3), 253-262. http://doi.org/10.1002/ana.410190306

Bucur, B., Madden, D. J., Spaniol, J., Provenzale, J. M., Cabeza, R., White, L. E., & Huettel, S. A. (2008). Age-related slowing of memory retrieval: Contributions of perceptual speed and cerebral white matter integrity. *Neurobiology of Aging*, *29*(7), 1070–1079. http://doi.org/10.1016/j.neurobiolaging.2007.02.008

Budde, M. D., Xie, M., Cross, A. H., & Song, S.-K. (2009). Axial Diffusivity Is the Primary Correlate of Axonal Injury in the Experimental Autoimmune Encephalomyelitis

Spinal Cord: A Quantitative Pixelwise Analysis. *Journal of Neuroscience*, *29*(9), 2805–2813. http://doi.org/10.1523/JNEUROSCI.4605-08.2009

Cabeza, R., Anderson, N. D., Locantore, J. K., & McIntosh, A. R. (2002). Aging gracefully: Compensatory brain activity in high-performing older adults. *NeuroImage*, *17*(3), 1394–1402. http://doi.org/10.1006/nimg.2002.1280

Caminiti, R., Carducci, F., Piervincenzi, C., Battaglia-Mayer, A., Confalone, G., Visco-Comandini, F., … Innocenti, G. M. (2013). Diameter, Length, Speed, and Conduction Delay of Callosal Axons in Macaque Monkeys and Humans: Comparing Data from Histology and Magnetic Resonance Imaging Diffusion Tractography. *Journal of Neuroscience*, *33*(36), 14501–14511. http://doi.org/10.1523/JNEUROSCI.0761-13.2013

Cassani, R., Falk, T. H., Fraga, F. J., Cecchi, M., Moore, D. K., & Anghinah, R. (2017). Towards automated electroencephalography-based Alzheimer's disease diagnosis using portable low-density devices. *Biomedical Signal Processing and Control*, , *33*, 261-271. http://doi.org/10.1016/j.bspc.2016.12.009

Catani, M., & Ffytche, D. H. (2005). The rises and falls of disconnection syndromes. *Brain*, *128*(10), 2224–2239. http://doi.org/10.1093/brain/awh622

Cecchi, M., Moore, D. K., Sadowsky, C. H., Solomon, P. R., Doraiswamy, P. M., Smith, C. D., … Fadem, K. C. (2015). A clinical trial to validate event-related potential markers of Alzheimer's disease in outpatient settings. *Alzheimer's and Dementia: Diagnosis, Assessment and Disease Monitoring*, *1*(4), 387–394. http://doi.org/10.1016/j.dadm.2015.08.004

Chaim, T. M., Duran, F. L. S., Uchida, R. R., Périco, C. A. M., de Castro, C. C., & Busatto, G. F. (2007). Volumetric reduction of the corpus callosum in Alzheimer's disease in vivo as assessed with voxel-based morphometry. *Psychiatry Research - Neuroimaging*, *154*(1), 59–68. http://doi.org/10.1016/j.pscychresns.2006.04.003

Chaumillon, R., Blouin, J., & Guillaume, A. (2014). Eye dominance influences triggering action: The Poffenberger paradigm revisited. *Cortex*, *58*, 86–98. http://doi.org/10.1016/j.cortex.2014.05.009

Cherubini, A., Péran, P., Caltagirone, C., Sabatini, U., & Spalletta, G. (2009). Aging of subcortical nuclei: Microstructural, mineralization and atrophy modifications measured in vivo using MRI. *NeuroImage*, *48*(1), 29–36. http://doi.org/10.1016/j.neuroimage.2009.06.035

Chiang, A. K. I., Rennie, C. J., Robinson, P. A., van Albada, S. J., & Kerr, C. C. (2011). Age trends and sex differences of alpha rhythms including split alpha peaks. *Clinical Neurophysiology*, *122*(8), 1505–1517. http://doi.org/10.1016/j.clinph.2011.01.040

Choi, S. J., Lim, K. O., Monteiro, I., & Reisberg, B. (2005). Diffusion tensor imaging of frontal white matter microstructure in early Alzheimer's disease: A preliminary study. *Journal of Geriatric Psychiatry and Neurology*, *18*(1), 12–19. http://doi.org/10.1177/0891988704271763

Chua, T. C., Wen, W., Slavin, M. J., & Sachdev, P. S. (2008). Diffusion tensor imaging in mild cognitive impairment and Alzheimer's disease: A review. *Current Opinion in Neurology*, *21*(1), 83–92. http://doi.org/10.1097/WCO.0b013e3282f4594b

Clerx, L., Visser, P. J., Verhey, F., & Aalten, P. (2012). New MRI markers for alzheimer's

disease: A meta-analysis of diffusion tensor imaging and a comparison with medial temporal lobe measurements. *Journal of Alzheimer's Disease*, *29*(2), 405–429. http://doi.org/10.3233/JAD-2011-110797

Concha, L., Gross, D. W., Wheatley, B. M., & Beaulieu, C. (2006). Diffusion tensor imaging of time-dependent axonal and myelin degradation after corpus callosotomy in epilepsy patients. *NeuroImage*, *32*(3), 1090-1099. http://doi.org/10.1016/j.neuroimage.2006.04.187

Corbetta, M., Kincade, J. M., Ollinger, J. M., McAvoy, M. P., & Shulman, G. L. (2000). Voluntary orienting is dissociated from target detection in human posterior parietal cortex. *Nature Neuroscience*, *3*(3), 292. http://doi.org/10.1038/73009

Corsi-Cabrera, M., Trías, G., Guevara, M. A., Haro, R., & Hernández, A. (1995). EEG Interhemispheric Correlation after Callosotomy: One Case Study. *Perceptual and Motor Skills*, *80*(2), 504–506. http://doi.org/10.2466/pms.1995.80.2.504

Craddock, M., Poliakoff, E., El-deredy, W., Klepousniotou, E., & Lloyd, D. M. (2017). Pre-stimulus alpha oscillations over somatosensory cortex predict tactile misperceptions. *Neuropsychologia*, *96*, 9–18. http://doi.org/10.1016/j.neuropsychologia.2016.12.030

Crawford, T. (2013). Alzheimer's disease: is the clue in the eyes?. *Neurodegenerative Disease Management*, *3*(1), 5-7. https://doi.org/10.2217/nmt.12.73

Cummings, J. L., Doody, R., & Clark, C. (2007). Disease-modifying therapies for Alzheimer disease: Challenges to early intervention. *Neurology*, *69*(16), 1622-1634. http://doi.org/10.1212/01.wnl.0000295996.54210.69

Curran, T., Hills, A., Patterson, M. B., & Strauss, M. E. (2001). Effects of aging on visuospatial attention: An ERP study. *Neuropsychologia*, *39*(3), 288–301. http://doi.org/10.1016/S0028-3932(00)00112-3

Daselaar, S. M., & Cabeza, R. (2005). Age-Related Changes in Hemispheric Organization. In R. Cabeza, L. Nyberg, & D. C. Park (Eds.), *Cognitive neuroscience of aging: Linking cognitive and cerebral aging* (pp. 325–353). New York: Oxford University Press. https://doi.org/10.1093/acprof:oso/9780195156744.003.0014

Daselaar, S. M., Iyengar, V., Davis, S. W., Eklund, K., Hayes, S. M., & Cabeza, R. E. (2015). Less wiring, more firing: Low-performing older adults compensate for impaired white matter with greater neural activity. *Cerebral Cortex*, *25*(4), 983–990. http://doi.org/10.1093/cercor/bht289

Davis, S. W., & Cabeza, R. (2015). Cross-Hemispheric Collaboration and Segregation Associated with Task Difficulty as Revealed by Structural and Functional Connectivity. *Journal of Neuroscience*, *35*(21), 8191–8200. http://doi.org/10.1523/JNEUROSCI.0464-15.2015

Davis, S. W., Dennis, N. A., Buchler, N. G., White, L. E., Madden, D. J., & Cabeza, R. (2009). Assessing the effects of age on long white matter tracts using diffusion tensor tractography. *NeuroImage*, *46*(2), 530–541. http://doi.org/10.1016/j.neuroimage.2009.01.068

Davis, S. W., Kragel, J. E., Madden, D. J., & Cabeza, R. (2012). The architecture of cross-hemispheric communication in the aging brain: Linking behavior to functional and structural connectivity. *Cerebral Cortex*, *22*(1), 232–242. http://doi.org/10.1093/cercor/bhr123

De Jager, C. A., Blackwell, A. D., Budge, M. M., & Sahakian, B. J. (2005). Predicting cognitive decline in healthy older adults. *American Journal of Geriatric Psychiatry*, *13*(8), 735–740. http://doi.org/10.1097/00019442-200508000-00014

De Jager, C. A., Milwain, E., & Budge, M. (2002). Early detection of isolated memory deficits in the elderly: The need for more sensitive neuropsychological tests. *Psychological Medicine*, *32*(3), 483–491. http://doi.org/10.1017/S003329170200524X

De Oliveira, M. S., Balthazar, M. L. F., D'Abreu, A., Yasuda, C. L., Damasceno, B. P., Cendes, F., & Castellano, G. (2011). MR imaging texture analysis of the corpus callosum and thalamus in amnestic mild cognitive impairment and mild alzheimer disease. *American Journal of Neuroradiology*, *32*(1), 60–66. http://doi.org/10.3174/ajnr.A2232

Deary, I. J., Pattie, A., & Starr, J. M. (2013). The Stability of Intelligence From Age 11 to Age 90 Years: The Lothian Birth Cohort of 1921. *Psychological Science*, *24*(12), 2361–2368. http://doi.org/10.1177/0956797613486487

Delbeuck, X., Van der Linden, M., Collette, F., & Linden, M. Van Der. (2003). Alzheimer's Disease as a Disconnection Syndrome? *Neuropsychology Review*, *13*(2), 79–92. http://doi.org/10.1023/A:1023832305702

Della Sala, S., Parra, M. A., Fabi, K., Luzzi, S., & Abrahams, S. (2012). Short-term memory binding is impaired in AD but not in non-AD dementias. *Neuropsychologia*, *50*(5), 833–840. http://doi.org/10.1016/j.neuropsychologia.2012.01.018

Delorme, A., & Makeig, S. (2004). EEGLAB: An open source toolbox for analysis of single-

trial EEG dynamics including independent component analysis. *Journal of Neuroscience Methods*, *134*(1), 9–21. http://doi.org/10.1016/j.jneumeth.2003.10.009

Delvenne, J. F., Castronovo, J., Demeyere, N., & Humphreys, G. W. (2011). Bilateral field advantage in visual enumeration. *PLoS ONE*, *6*(3), e17743. http://doi.org/10.1371/journal.pone.0017743

Delvenne, J. F., & Holt, J. L. (2012). Splitting attention across the two visual fields in visual short-term memory. *Cognition*, *122*(2), 258–263. http://doi.org/10.1016/j.cognition.2011.10.015

Derakhshan, I. (2006). Crossed-uncrossed difference (CUD) in a new light: Anatomy of the negative CUD in Poffenberger's paradigm. *Acta Neurologica Scandinavica*, *113*(3), 203–208. http://doi.org/10.1111/j.1600-0404.2005.00563.x

Di Paola, M., Di Iulio, F., Cherubini, A., Blundo, C., Casini, A. R., Sancesario, G., … Spalletta, G. (2010). When, where, and how the corpus callosum changes in MCI and AD: A multimodal MRI study. *Neurology*, *74*(14), 1136–1142. http://doi.org/10.1212/WNL.0b013e3181d7d8cb

Di Paola, M., Luders, E., Di Iulio, F., Cherubini, A., Passafiume, D., Thompson, P. M., … Spalletta, G. (2010). Callosal atrophy in mild cognitive impairment and Alzheimer's disease: Different effects in different stages. *NeuroImage*, *49*(1), 141–149. http://doi.org/10.1016/j.neuroimage.2009.07.050

Di Paola, M., Spalletta, G., & Caltagirone, C. (2010). In vivo structural neuroanatomy of corpus callosum in Alzheimer's disease and mild cognitive impairment using

different MRI techniques: A review. *Journal of Alzheimer's Disease*, *20*(1), 67–95. http://doi.org/10.3233/JAD-2010-1370

Di Stefano, M. R., Sauerwein, H. C., & Lassonde, M. (1992). Influence of anatomical factors and spatial compatibility on the stimulus-response relationship in the absence of the corpus callosum. *Neuropsychologia*, *30*(2), 177–185. http://doi.org/10.1016/0028-3932(92)90026-I

Dolcos, F., Rice, H. J., & Cabeza, R. (2002). Hemispheric asymmetry and aging: Right hemisphere decline or asymmetry reduction. *Neuroscience and Biobehavioral Reviews*, *26*(7), 819–825. http://doi.org/10.1016/S0149-7634(02)00068-4

Dorion, A. A., Chantome, M., Hasboun, D., Zouaoui, A., Marsault, C., Capron, C., & Duyme, M. (2000). Hemispheric asymmetry and corpus callosum morphometry: a magnetic resonance imaging study, *Journal of Neuroscience Research*, *36*(1), 9–13. https://doi.org/10.1016/s0168-0102(99)00102-9

Dougherty, R. F., Ben-Shachar, M., Deutsch, G. K., Hernandez, A., Fox, G. R., & Wandell, B. A. (2007). Temporal-callosal pathway diffusivity predicts phonological skills in children. *Proceedings of the National Academy of Sciences*, *104*(20), 8556–8561. http://doi.org/10.1073/pnas.0608961104

Duan, J.-H., Wang, H.-Q., Xu, J., Lin, X., Chen, S.-Q., Kang, Z., & Yao, Z.-B. (2006). White matter damage of patients with Alzheimer's disease correlated with the decreased cognitive function. *Surgical and Radiologic Anatomy*, *28*(2), 150–156. http://doi.org/10.1007/s00276-006-0111-2

Dubois, B., Hampel, H., Feldman, H. H., Scheltens, P., Aisen, P., Andrieu, S., … Jack, C. R.

(2016). Preclinical Alzheimer's disease: Definition, natural history, and diagnostic criteria. *Alzheimer's and Dementia*, *12*(3), 292–323. http://doi.org/10.1016/j.jalz.2016.02.002

Duchek, J. M., & Balota, D. A. (2005). Failure to control prepotent pathways in early stage dementia of the Alzheimer's type: Evidence from dichotic listening. *Neuropsychology*, *19*(5), 687. http://doi.org/10.1037/0894-4105.19.5.687

Duffy, F. H., Albert, M. S., McAnulty, G., & Garvey, A. J. (1984). Age-related differences in brain electrical activity of healthy subjects. *Annals of Neurology*, *16*(4), 430–438. http://doi.org/10.1002/ana.410160403

Duffy, F. H., Mcanulty, G. B., & Albert, M. S. (1996). Effects of age upon interhemispheric EEG coherence in normal adults. *Neurobiology of Aging*, *17*(4), 587–599. http://doi.org/10.1016/0197-4580(96)00007-3

Dustman, R. E., Shearer, D. E., & Emmerson, R. Y. (1993). EEG and event-related potentials in normal aging. *Progress in Neurobiology*, *41*(3), 369-401. http://doi.org/10.1016/0301-0082(93)90005-D

Elahi, S., Bachman, A. H., Lee, S. H., Sidtis, J. J., & Ardekani, B. A. (2015). Corpus Callosum Atrophy Rate in Mild Cognitive Impairment and Prodromal Alzheimer's Disease. *Journal of Alzheimer's Disease*, *45*(3), 921–931. http://doi.org/10.3233/JAD-142631

Ellendt, S., Voβ, B., Kohn, N., Wagels, L., S Goerlich, K., Drexler, E., … Habel, U. (2017). Predicting stability of mild cognitive impairment (MCI): findings of a community based sample. *Current Alzheimer Research*, *14*(6), 608–619.

https://doi.org/10.2174/1567205014666161213120807

Emmerson-Hanover, R., Shearer, D. E., Creel, D. J., & Dustman, R. E. (1994). Pattern reversal evoked potentials: gender differences and age-related changes in amplitude and latency. *Electroencephalography and Clinical Neurophysiology/ Evoked Potentials*, *92*(2), 93–101. http://doi.org/10.1016/0168-5597(94)90049-3

Englund, E., & Brun, A. (1990). White matter changes in dementia of Alzheimer's type: the difference in vulnerability between cell compartments. *Histopathology*, *16*(5), 433–439. http://doi.org/10.1111/j.1365-2559.1990.tb01542.x

Ferreira, L. K., & Busatto, G. F. (2013). Resting-state functional connectivity in normal brain aging. *Neuroscience and Biobehavioral Reviews*, *37*(3), 384–400. http://doi.org/10.1016/j.neubiorev.2013.01.017

Fieremans, E., Benitez, A., Jensen, J. H., Falangola, M. F., Tabesh, A., Deardorff, R. L., … Helpern, J. A. (2013). Novel white matter tract integrity metrics sensitive to Alzheimer disease progression. *American Journal of Neuroradiology*, *34*(11), 2105–2112. http://doi.org/10.3174/ajnr.A3553

Fink, A., Grabner, R. H., Neuper, C., & Neubauer, A. C. (2005). EEG alpha band dissociation with increasing task demands. *Cognitive Brain Research*, *24*(2), 252–259. http://doi.org/10.1016/j.cogbrainres.2005.02.002

Fletcher, E., Villeneuve, S., Maillard, P., Harvey, D., Reed, B., Jagust, W., & DeCarli, C. (2016). B-Amyloid, Hippocampal Atrophy and Their Relation To Longitudinal Brain Change in Cognitively Normal Individuals. *Neurobiology of Aging*, *40*, 173–180. http://doi.org/10.1016/j.neurobiolaging.2016.01.133

Fowler, K. S., Saling, M. M., Conway, E. L., Semple, J. M., & Louis, W. J. (2002). Paired associate performance in the early detection of DAT. *Journal of the International Neuropsychological Society*, *8*(1), 58–71. http://doi.org/10.1017/S1355617702811067

Frederiksen, K. S., Garde, E., Skimminge, A., Barkhof, F., Scheltens, P., Van Straaten, E. C. W., … Waldemar, G. (2012). Corpus callosum tissue loss and development of motor and global cognitive impairment: The LADIS study. *Dementia and Geriatric Cognitive Disorders*, *32*(4), 279–286. http://doi.org/10.1159/000334949

French, C. C., & Beaumont, J. G. (1984). A critical review of EEG coherence studies of hemisphere function. *International Journal of Psychophysiology*, *1*(3), 241–254. http://doi.org/10.1016/0167-8760(84)90044-8

Freunberger, R., Höller, Y., Griesmayr, B., Gruber, W., Sauseng, P., & Klimesch, W. (2008). Functional similarities between the P1 component and alpha oscillations. *European Journal of Neuroscience*, *27*(9), 2330–2340. http://doi.org/10.1111/j.1460-9568.2008.06190.x

Frye, R. E., Hasan, K., Xue, L., Strickland, D., Malmberg, B., Liederman, J., & Papanicolaou, A. (2008). Splenium microstructure is related to two dimensions of reading skill. *NeuroReport*, *19*(16), 1627–1631. http://doi.org/10.1097/WNR.0b013e328314b8ee

Gaál, Z. A., Boha, R., Stam, C. J., & Molnár, M. (2010). Age-dependent features of EEG-reactivity-Spectral, complexity, and network characteristics. *Neuroscience Letters*, *479*(1), 79–84. http://doi.org/10.1016/j.neulet.2010.05.037

Gall, F., & Spurzheim, J. (1809). *Recherches sur Ie Systeme Nerveux*. Paris: Schoell.

Gawryluk, J. R., D'Arcy, R. C. N., Mazerolle, E. L., Brewer, K. D., & Beyea, S. D. (2011). Functional mapping in the corpus callosum: A 4T fMRI study of white matter. *NeuroImage*, *54*(1), 10–15. http://doi.org/10.1016/j.neuroimage.2010.07.028

Genc, S., Steward, C. E., Malpas, C. B., Velakoulis, D., O'Brien, T. J., & Desmond, P. M. (2016). Short-term white matter alterations in Alzheimer's disease characterized by diffusion tensor imaging. *Journal of Magnetic Resonance Imaging*, *43*(3), 627–634. http://doi.org/10.1002/jmri.25017

Goldman, R. I., Stern, J. M., Engel, J., & Cohen, M. S. (2002). Simultaneous EEG and fMRI of the alpha rhythm. *NeuroReport*, *13*(18), 2487–2492. http://doi.org/10.1097/00001756-200212200-00022

Gooijers, J., & Swinnen, S. P. (2014). Interactions between brain structure and behavior: The corpus callosum and bimanual coordination. *Neuroscience and Biobehavioral Reviews*, *43*, 1–19. http://doi.org/10.1016/j.neubiorev.2014.03.008

Gootjes, L., Bouma, A., Van Strien, J. W., Schijndel, R. Van, Barkhof, F., & Scheltens, P. (2006). Corpus callosum size correlates with asymmetric performance on a dichotic listening task in healthy aging but not in Alzheimer's disease. *Neuropsychologia*, *44*(2), 208-217. http://doi.org/10.1016/j.neuropsychologia.2005.05.002

Gootjes, L., Van Strien, J. W., & Bouma, A. (2004). Age effects in identifying and localising dichotic stimuli: A corpus callosum deficit? *Journal of Clinical and Experimental Neuropsychology*, *26*(6), 826-837. http://doi.org/10.1080/13803390490509448

Gow, A. J., Johnson, W., Pattie, A., Brett, C. E., Roberts, B., Starr, J. M., & Deary, I. J. (2011). Stability and Change in Intelligence From Age 11 to Ages 70, 79, and 87: The Lothian Birth Cohorts of 1921 and 1936. *Psychology and Aging*, *26*(1), 232–240. http://doi.org/10.1037/a0021072

Grady, C. L., McIntosh, A. R., Horwitz, B., & Rapoport, S. I. (2000). Age-related changes in the neural correlates of degraded and nondegraded face processing. *Cognitive Neuropsychology*, *17*(1–3), 165–186. http://doi.org/10.1080/026432900380553

Grandy, T. H., Werkle-Bergner, M., Chicherio, C., Schmiedek, F., Lövdén, M., & Lindenberger, U. (2013). Peak individual alpha frequency qualifies as a stable neurophysiological trait marker in healthy younger and older adults. *Psychophysiology*, *50*(6), 570–582. http://doi.org/10.1111/psyp.12043

Gruber, W. R., Klimesch, W., Sauseng, P., & Doppelmayr, M. (2005). Alpha phase synchronization predicts P1 end N1 latency and amplitude size. *Cerebral Cortex*, *15*(4), 371–377. http://doi.org/10.1093/cercor/bhh139

Gruber, W. R., Zauner, A., Lechinger, J., Schabus, M., Kutil, R., & Klimesch, W. (2014). Alpha phase, temporal attention, and the generation of early event related potentials. *NeuroImage*, *103*, 119–129. http://doi.org/10.1016/j.neuroimage.2014.08.055

Gunning-Dixon, F. M., Brickman, A. M., Cheng, J. C., & Alexopoulos, G. S. (2009). Aging of cerebral white matter: A review of MRI findings. *International Journal of Geriatric Psychiatry*, *24*(2), 109–117. http://doi.org/10.1002/gps.2087

Hagmann, P., Cammoun, L., Gigandet, X., Meuli, R., Honey, C. J., Van Wedeen, J., & Sporns,

O. (2008). Mapping the structural core of human cerebral cortex. *PLoS Biology*, *6*(7), e159. http://doi.org/10.1371/journal.pbio.0060159

Hampel, H., Teipel, S. J., Alexander, G. E., Horwitz, B., Teichberg, D., Schapiro, M. B., & Rapoport, S. I. (1998). Corpus callosum atrophy is a possible indicator of region- and cell type-specific neuronal degeneration in Alzheimer disease: A magnetic resonance imaging analysis. *Archives of Neurology*, *55*(2), 193–198. http://doi.org/10.1001/archneur.55.2.193

Hanyu, H., Asano, T., Sakurai, H., Imon, Y., Iwamoto, T., Takasaki, M., … Abe, K. (1999). Diffusion-weighted and magnetization transfer imaging of the corpus callosum in Alzheimer's disease. *Journal of the Neurological Sciences*, *167*(1), 37–44. http://doi.org/10.1016/S0022-510X(99)00135-5

Hasan, K. M., Ewing-Cobbs, L., Kramer, L. A., Fletcher, J. M., & Narayana, P. A. (2008). Diffusion tensor quantification of the macrostructure and microstructure of human midsagittal corpus callosum across the lifespan. *NMR in Biomedicine*, *21*(10), 1094–1101. http://doi.org/10.1002/nbm.1286

Hasan, K. M., Iftikhar, A., Kamali, A., Kramer, L. A., Ashtari, M., Cirino, P. T., … Ewing-Cobbs, L. (2009). Development and aging of the healthy human brain uncinate fasciculus across the lifespan using diffusion tensor tractography. *Brain Research*, *1276*, 67–76. http://doi.org/10.1016/j.brainres.2009.04.025

Hasan, K. M., Kamali, A., Abid, H., Kramer, L. A., Fletcher, J. M., & Ewing-Cobbs, L. (2010). Quantification of the spatiotemporal microstructural organization of the human brain association, projection and commissural pathways across the lifespan using diffusion tensor tractography. *Brain Structure and Function*, *214*(4), 361–373.

http://doi.org/10.1007/s00429-009-0238-0

Hasan, K. M., Kamali, A., Iftikhar, A., Kramer, L. A., Papanicolaou, A. C., Fletcher, J. M., & Ewing-Cobbs, L. (2009). Diffusion tensor tractography quantification of the human corpus callosum fiber pathways across the lifespan. *Brain Research*, *1249*, 91–100. http://doi.org/10.1016/j.brainres.2008.10.026

Hasan, K. M., Kamali, A., Kramer, L. A., Papnicolaou, A. C., Fletcher, J. M., & Ewing-Cobbs, L. (2008). Diffusion tensor quantification of the human midsagittal corpus callosum subdivisions across the lifespan. *Brain Research*, *1227*, 52–67. http://doi.org/10.1016/j.brainres.2008.06.030

Hata, M., Kazui, H., Tanaka, T., Ishii, R., Canuet, L., Pascual-Marqui, R. D., … Takeda, M. (2016). Functional connectivity assessed by resting state EEG correlates with cognitive decline of Alzheimer's disease - An eLORETA study. *Clinical Neurophysiology*, *127*(2), 1269–1278. http://doi.org/10.1016/j.clinph.2015.10.030

He, W., Goodkind, D., & Kowal, P. (2016). An Aging World : 2015 International Population Reports. *Aging*, P95/16-1. http://doi.org/P95/09-1

Head, D. (2004). Differential Vulnerability of Anterior White Matter in Nondemented Aging with Minimal Acceleration in Dementia of the Alzheimer Type: Evidence from Diffusion Tensor Imaging. *Cerebral Cortex*, *14*(4), 410–423. http://doi.org/10.1093/cercor/bhh003

Heinzel, S., Lorenz, R. C., Duong, Q. L., Rapp, M. A., & Deserno, L. (2017). Prefrontal-parietal effective connectivity during working memory in older adults. *Neurobiology of Aging*, *57*, 18–27.

http://doi.org/10.1016/j.neurobiolaging.2017.05.005

Heise, V., Filippini, N., Ebmeier, K. P., & MacKay, C. E. (2011). The APOE 4 allele modulates brain white matter integrity in healthy adults. *Molecular Psychiatry*, *16*(9), 908–916. http://doi.org/10.1038/mp.2010.90

Heller, K. B., DeCarli, C., Beekly, D., Besser, L. M., Bollenbeck, M., Wu, J., … Kukull, W. (2014). The National Alzheimer's Coordinating Center MRI database. *Alzheimer's and Dementia*, *10*, P833–P834. http://doi.org/10.1016/j.jalz.2014.05.1645

Hipp, J. F., Hawellek, D. J., Corbetta, M., Siegel, M., & Engel, A. K. (2012). Large-scale cortical correlation structure of spontaneous oscillatory activity. *Nature Neuroscience*, *15*(6), 884–890. http://doi.org/10.1038/nn.3101

Hofer, S., & Frahm, J. (2006). Topography of the human corpus callosum revisited-Comprehensive fiber tractography using diffusion tensor magnetic resonance imaging. *NeuroImage*, *32*(3), 989–994. http://doi.org/10.1016/j.neuroimage.2006.05.044

Holt, J. L., & Delvenne, J. F. (2014). A bilateral advantage in controlling access to visual short-term memory. *Experimental Psychology*, *61*(2), 127–133. http://doi.org/10.1027/1618-3169/a000232

Holt, J. L., & Delvenne, J. F. (2015). A bilateral advantage for maintaining objects in visual short term memory. *Acta Psychologica*, *154*, 54–61. http://doi.org/10.1016/j.actpsy.2014.11.007

Hommet, C., Mondon, K., Berrut, G., Gouyer, Y., Isingrini, M., Constans, T., & Belzung, C. (2010). Central auditory processing in aging: The dichotic listening paradigm.

Journal of Nutrition, Health and Aging, *14*(9), 751–756. http://doi.org/10.1007/s12603-010-0097-7

Hoptman, M. J., Davidson, R. J., Gudmundsson, A., Schreiber, R. T., & Ershler, W. B. (1996). Age differences in visual evoked potential estimates on interhemishperic transfer. *Neuropsychology*, *10*(2), 263–271. http://doi.org/10.1037/0894-4105.10.2.263

Hou, J., & Pakkenberg, B. (2012). Age-related degeneration of corpus callosum in the 90+ years measured with stereology. *Neurobiology of Aging*, *33*(5), 1009.e1-1009.e9. http://doi.org/10.1016/j.neurobiolaging.2011.10.017

Hoy, A. R., Ly, M., Carlsson, C. M., Okonkwo, O. C., Zetterberg, H., Blennow, K., … Bendlin, B. B. (2017). Microstructural white matter alterations in preclinical Alzheimer's disease detected using free water elimination diffusion tensor imaging. *PLoS ONE*, *12*(3), e0173982. http://doi.org/10.1371/journal.pone.0173982

Huang, H., Fan, X., Weiner, M., Martin-Cook, K., Xiao, G., Davis, J., … Diaz-Arrastia, R. (2012). Distinctive disruption patterns of white matter tracts in Alzheimer's disease with full diffusion tensor characterization. *Neurobiology of Aging*, *33*(9), 2029–2045. http://doi.org/10.1016/j.neurobiolaging.2011.06.027

Iacoboni, M., & Zaidel, E. (2000). Crossed-uncrossed difference in simple reaction times to lateralized flashes: Between- and within-subjects variability. *Neuropsychologia*, *38*(5), 535–541. http://doi.org/10.1016/S0028-3932(99)00121-9

Iacoboni, M., & Zaidel, E. (2004). Interhemispheric visuo-motor integration in humans: The role of the superior parietal cortex. *Neuropsychologia*, *42*(4), 419–425.

http://doi.org/10.1016/j.neuropsychologia.2003.10.007

Ibanez, A., & Parra, M. A. (2014). Mapping memory binding onto the connectome's temporal dynamics: toward a combined biomarker for Alzheimer's disease. *Frontiers in Human Neuroscience*, *8*, 237. http://doi.org/10.3389/fnhum.2014.00237

Ishizaki, J., Meguro, K., Nara, N., Kasai, M., & Yamadori, A. (2013). Impaired shifting of visuospatial attention in Alzheimer's disease as shown by the covert orienting paradigm: Implications for visual construction disability. *Behavioural Neurology*, *26*(1–2), 121–129. http://doi.org/10.3233/BEN-2012-110208

Jack, C. R., Albert, M. S., Knopman, D. S., McKhann, G. M., Sperling, R. A., Carrillo, M. C., … Phelps, C. H. (2011). Introduction to the recommendations from the National Institute on Aging-Alzheimer's Association workgroups on diagnostic guidelines for Alzheimer's disease. *Alzheimer's and Dementia*, *7*(3), 257–262. http://doi.org/10.1016/j.jalz.2011.03.004

Jain, P., Kumar Wadhwa, P., & Ramanlal Jadhav, H. (2015). Reactive astrogliosis: Role in Alzheimer's disease. *CNS & Neurological Disorders-Drug Targets (Formerly Current Drug Targets-CNS & Neurological Disorders)*, *14*(7), 872–879. https://doi.org/10.2174/1871527314666150713104738

Janowsky, J. S., Kaye, J. A., & Carper, R. A. (1996). Atrophy of the corpus callosum in Alzheimer's disease versus healthy aging. *Journal of the American Geriatrics Society*, *44*(7), 798–803. http://doi.org/10.1111/j.1532-5415.1996.tb03736.x

Janve, V. A., Zu, Z., Yao, S. Y., Li, K., Zhang, F. L., Wilson, K. J., … Gochberg, D. F. (2013). The

radial diffusivity and magnetization transfer pool size ratio are sensitive markers for demyelination in a rat model of type III multiple sclerosis (MS) lesions. *NeuroImage*, *74*, 298–305. http://doi.org/10.1016/j.neuroimage.2013.02.034

Jeeves, M. A., & Moes, P. (1996). Interhemispheric transfer time differences related to aging and gender. *Neuropsychologia*, *34*(7), 627–636. http://doi.org/10.1016/0028-3932(95)00157-3

Jelic, V., Johansson, S. E., Almkvist, O., Shigeta, M., Julin, P., Nordberg, A., … Wahlund, L. O. (2000). Quantitative electroencephalography in mild cognitive impairment: Longitudinal changes and possible prediction of Alzheimer's disease. *Neurobiology of Aging*, *21*(4), 533–540. http://doi.org/10.1016/S0197-4580(00)00153-6

Jensen, O., & Mazaheri, A. (2010). Shaping Functional Architecture by Oscillatory Alpha Activity: Gating by Inhibition. *Frontiers in Human Neuroscience*, *4*. http://doi.org/10.3389/fnhum.2010.00186

Jeong, J. (2004). EEG dynamics in patients with Alzheimer's disease. *Clinical Neurophysiology*, *115*(7), 1490-1505. http://doi.org/10.1016/j.clinph.2004.01.001

Jerger, J., Alford, B., Lew, H., Rivera, V., & Chmiel, R. (1995). Dichotic listening, event-related potentials, and interhemispheric transfer in the elderly. *Ear and Hearing*, *16*(5), 482–498. http://doi.org/10.1097/00003446-199510000-00005

Jeurissen, B., Leemans, A., Jones, D. K., Tournier, J. D., & Sijbers, J. (2011). Probabilistic fiber tracking using the residual bootstrap with constrained spherical deconvolution. *Human Brain Mapping*, *32*(3), 461–479. http://doi.org/10.1002/hbm.21032

Jeurissen, B., Leemans, A., Tournier, J. D., Jones, D. K., & Sijbers, J. (2013). Investigating the prevalence of complex fiber configurations in white matter tissue with diffusion magnetic resonance imaging. *Human Brain Mapping*, *34*(11), 2747–2766. http://doi.org/10.1002/hbm.22099

Johansen-Berg, H., & Behrens, T. E. J. (2006). Just pretty pictures? What diffusion tractography can add in clinical neuroscience. *Current Opinion in Neurology*, *19*(4), 379. http://doi.org/10.1097/01.wco.0000236618.82086.01

Johnston, J. M., Vaishnavi, S. N., Smyth, M. D., Zhang, D., He, B. J., Zempel, J. M., … Raichle, M. E. (2008). Loss of Resting Interhemispheric Functional Connectivity after Complete Section of the Corpus Callosum. *Journal of Neuroscience*, *28*(25), 6453–6458. http://doi.org/10.1523/JNEUROSCI.0573-08.2008

Jokinen, H., Ryberg, C., Kalska, H., Ylikoski, R., Rostrup, E., Stegmann, M. B., … Erkinjuntti, T. (2007). Corpus callosum atrophy is associated with mental slowing and executive deficits in subjects with age-related white matter hyperintensities: The LADIS Study. *Journal of Neurology, Neurosurgery and Psychiatry*, *78*(5), 491–496. http://doi.org/10.1136/jnnp.2006.096792

Jones, D. K. (2010). Challenges and limitations of quantifying brain connectivity in vivo with diffusion MRI. *Imaging in Medicine*, *2*(3), 341–355. http://doi.org/10.2217/iim.10.21

Jones, D. K., Knösche, T. R., & Turner, R. (2013). White matter integrity, fiber count, and other fallacies: The do's and don'ts of diffusion MRI. *NeuroImage*. http://doi.org/10.1016/j.neuroimage.2012.06.081

Jorge, M. S., Botelho, R. V., & Melo, A. C. D. P. (2007). Study of interhemispheric coherence on healthy adults. *Arquivos de Neuro-Psiquiatria*, *65*(2 B), 377–380. http://doi.org/10.1590/S0004-282X2007000300002

Kanda, P. A. M., Oliveira, E. F., & Fraga, F. J. (2017). EEG epochs with less alpha rhythm improve discrimination of mild Alzheimer's. *Computer Methods and Programs in Biomedicine*, *138*, 13–22. http://doi.org/10.1016/j.cmpb.2016.09.023

Kennedy, K. M., & Raz, N. (2009). Aging white matter and cognition: Differential effects of regional variations in diffusion properties on memory, executive functions, and speed. *Neuropsychologia*, *47*(3), 916–927. http://doi.org/10.1016/j.neuropsychologia.2009.01.001

Kikuchi, M., Wada, Y., Koshino, Y., Nanbu, Y., & Hashimoto, T. (2000). Effect of Normal Aging upon Interhemispheric EEG Coherence: Analysis during Rest and Photic Stimulation. *Clinical EEG and Neuroscience*, *31*(4), 170–174. http://doi.org/10.1177/155005940003100404

Kikuchi, M., Wada, Y., Takeda, T., Oe, H., Hashimoto, T., & Koshino, Y. (2002). EEG harmonic responses to photic stimulation in normal aging and Alzheimer's disease: Differences in interhemispheric coherence. *Clinical Neurophysiology*, *113*(7), 1045–1051. http://doi.org/10.1016/S1388-2457(02)00129-3

Klawiter, E. C., Schmidt, R. E., Trinkaus, K., Liang, H. F., Budde, M. D., Naismith, R. T., … Benzinger, T. L. (2011). Radial diffusivity predicts demyelination in ex vivo multiple sclerosis spinal cords. *NeuroImage*, *55*(4), 1454–1460. http://doi.org/10.1016/j.neuroimage.2011.01.007

Klimesch, W. (1999). EEG alpha and theta oscillations reflect cognitive and memory performance: A review and analysis. *Brain Research Reviews*, *29*(2-3), 169-195. http://doi.org/10.1016/S0165-0173(98)00056-3

Klimesch, W., Sauseng, P., & Hanslmayr, S. (2007). EEG alpha oscillations: The inhibition-timing hypothesis. *Brain Research Reviews*, *53*(1), 63-88. http://doi.org/10.1016/j.brainresrev.2006.06.003

Klimesch, W., Schack, B., & Sauseng, P. (2005). The functional significance of theta and upper alpha oscillations. *Experimental Psychology*, *52*(2), 99–108. http://doi.org/10.1027/1618-3169.52.2.99

Klimesch, W., Schack, B., Schabus, M., Doppelmayr, M., Gruber, W., & Sauseng, P. (2004). Phase locked alpha and theta oscillations generate the P1 - N1 complex and are related to memory performance. *Cognitive Brain Research, 19(3), 302-316. https://doi.org/10.1016/j.cogbrainres.2003.11.016*

Knyazev, G. G., Volf, N. V., & Belousova, L. V. (2015). Age-related differences in electroencephalogram connectivity and network topology. *Neurobiology of Aging*, *36*(5), 1849–1859. http://doi.org/10.1016/j.neurobiolaging.2015.02.007

Knyazeva, M. G. (2013). Splenium of corpus callosum: Patterns of interhemispheric interaction in children and adults. *Neural Plasticity*, *2013*. http://doi.org/10.1155/2013/639430

Knyazeva, M. G., Koeda, T., Njiokiktjien, C., Jonkman, E. J., Kurganskaya, M., De Sonneville, L., & Vildavsky, V. (1997). EEG coherence changes during finger tapping in acallosal and normal children: A study of inter- and intrahemispheric

connectivity. *Behavioural Brain Research*, *89*(1–2), 243–258. http://doi.org/10.1016/S0166-4328(97)00070-3

Koeda, T., Knyazeva, M., Njiokiktjien, C., Jonkman, E. J., De Sonneville, L., & Vildavsky, V. (1995). The EEG in acallosal children. Coherence values in the resting state: left hemisphere compensatory mechanism? *Electroencephalography and Clinical Neurophysiology*, *95*(6), 397–407. http://doi.org/10.1016/0013-4694(95)00171-9

Koepsell, T. D., & Monsell, S. E. (2012). Reversion from mild cognitive impairment to normal or near-Normal cognition; Risk factors and prognosis. *Neurology*, *79*(15), 1591–1598. http://doi.org/10.1212/WNL.0b013e31826e26b7

Koyama, K., Hirasawa, H., Okubo, Y., & Karasawa, A. (1997). Quantitative EEG correlates of normal aging in the elderly. *Clinical EEG (Electroencephalography)*, *28*(3), 160–165. https://doi.org/10.1177/155005949702800308

Kraft, A., Dyrholm, M., Kehrer, S., Kaufmann, C., Bruening, J., Kathmann, N., … Brandt, S. A. (2015). TMS over the right precuneus reduces the bilateral field advantage in visual short term memory capacity. *Brain Stimulation*, *8*(2), 216–223. http://doi.org/10.1016/j.brs.2014.11.004

Krause, C. M., Pörn, B., Lang, A. H., & Laine, M. (1997). Relative alpha desynchronization and synchronization during speech perception. *Cognitive Brain Research*, *5*(4), 295–299. http://doi.org/10.1016/S0926-6410(97)00009-8

Kuks, J. B. M., Vos, J. E., & O'Brien, M. J. (1987). Coherence patterns of the infant sleep EEG in absence of the corpus callosum. *Electroencephalography and Clinical Neurophysiology*, *66*(1), 8–14. http://doi.org/10.1016/0013-4694(87)90132-5

Kuznetsova, K. A., Maniega, S. M., Ritchie, S. J., Cox, S. R., Storkey, A. J., Starr, J. M., … Bastin, M. E. (2016). Brain white matter structure and information processing speed in healthy older age. *Brain Structure & Function*, *221*(6), 3223–3235. http://doi.org/10.1007/s00429-015-1097-5

Kwak, Y. T. (2006). Quantitative EEG findings in different stages of Alzheimer's disease. *Journal of Clinical Neurophysiology*, *23*(5), 457–462. http://doi.org/10.1097/01.wnp.0000223453.47663.63

Laufs, H., Kleinschmidt, A., Beyerle, A., Eger, E., Salek-Haddadi, A., Preibisch, C., & Krakow, K. (2003). EEG-correlated fMRI of human alpha activity. *NeuroImage*, *19*(4), 1463–1476. http://doi.org/10.1016/S1053-8119(03)00286-6

Le Bihan, D., Breton, E., Lallemand, D., Grenier, P., Cabanis, E., & Laval-Jeantet, M. (1986). MR imaging of intravoxel incoherent motions: application to diffusion and perfusion in neurologic disorders. *Radiology*, *161*(2), 401–407. http://doi.org/10.1148/radiology.161.2.3763909

Lebel, C., Caverhill-Godkewitsch, S., & Beaulieu, C. (2010). Age-related regional variations of the corpus callosum identified by diffusion tensor tractography. *NeuroImage*, *52*(1), 20–31. http://doi.org/10.1016/j.neuroimage.2010.03.072

Lebel, C., Gee, M., Camicioli, R., Wieler, M., Martin, W., & Beaulieu, C. (2012). Diffusion tensor imaging of white matter tract evolution over the lifespan. *NeuroImage*, *60*(1), 340–352. http://doi.org/10.1016/j.neuroimage.2011.11.094

Lebel, C., Walker, L., Leemans, A., Phillips, L., & Beaulieu, C. (2008). Microstructural maturation of the human brain from childhood to adulthood. *NeuroImage*, *40*(3),

1044–1055. http://doi.org/10.1016/j.neuroimage.2007.12.053

Lee, D. H., Park, J. W., Park, S. H., & Hong, C. (2015). Have you ever seen the impact of crossing fiber in DTI?: Demonstration of the corticospinal tract pathway. *PLoS ONE*, *10*(7), e0112045. http://doi.org/10.1371/journal.pone.0112045

Leemans, A., Sijbers, J., & Jones, D. K. (2009). ExploreDTI: a graphical tool- box for processing, analyzing, and visualizing diffusion MR data. *Proceedings 17th Scientific Meeting, International Society for Magnetic Resonance in Medicine*, *17*(2), 3537.

Li, S., Pu, F., Shi, F., Xie, S., Wang, Y., & Jiang, T. (2008). Regional white matter decreases in Alzheimer's disease using optimized voxel-based morphometry. *Acta Radiologica*, *49*(1), 84–90. http://doi.org/10.1080/02841850701627181

Li, Y., Bin, G., Hong, B., & Gao, X. (2010). A coded VEP method to measure interhemispheric transfer time (IHTT). *Neuroscience Letters*, *472*(2), 123–127. http://doi.org/10.1016/j.neulet.2010.01.069

Linnet, E., & Roser, M. E. (2012). Age-related differences in interhemispheric visuomotor integration measured by the redundant target effect. *Psychology and Aging*, *27*(2), 399–409. http://doi.org/10.1037/a0024905

Liu, Y., Spulber, G., Lehtimäki, K. K., Könönen, M., Hallikainen, I., Gröhn, H., … Soininen, H. (2011). Diffusion tensor imaging and Tract-Based Spatial Statistics in Alzheimer's disease and mild cognitive impairment. *Neurobiology of Aging*, *32*(9), 1558–1571. http://doi.org/10.1016/j.neurobiolaging.2009.10.006

Liu, Z., de Zwart, J. A., Yao, B., van Gelderen, P., Kuo, L. W., & Duyn, J. H. (2012). Finding thalamic BOLD correlates to posterior alpha EEG. *NeuroImage*, *63*(3), 1060–1069.

http://doi.org/10.1016/j.neuroimage.2012.08.025

Locatelli, T., Cursi, M., Liberati, D., Franceschi, M., & Comi, G. (1998). EEG coherence in Alzheimer's disease. *Electroencephalography and Clinical Neurophysiology*, *106*(3), 229–237. http://doi.org/10.1016/S0013-4694(97)00129-6

Logie, R. H., Parra, M. A., & Della Sala, S. (2015). From Cognitive Science to Dementia Assessment. *Policy Insights from the Behavioral and Brain Sciences*, *2*(1), 81–91. http://doi.org/10.1177/2372732215601370

Lu, P. H., Lee, G. J., Tishler, T. A., Meghpara, M., Thompson, P. M., & Bartzokis, G. (2013). Myelin breakdown mediates age-related slowing in cognitive processing speed in healthy elderly men. *Brain and Cognition*, *81*(1), 131–138. http://doi.org/10.1016/j.bandc.2012.09.006

Luders, E., Narr, K. L., Bilder, R. M., Thompson, P. M., Szeszko, P. R., Hamilton, L., & Toga, A. W. (2007). Positive correlations between corpus callosum thickness and intelligence. *NeuroImage*, *37*(4), 1457–1464. http://doi.org/10.1016/j.neuroimage.2007.06.028

Luders, E., Narr, K. L., Zaidel, E., Thompson, P. M., Jancke, L., & Toga, A. W. (2006). Parasagittal asymmetries of the corpus callosum. *Cerebral Cortex*, *16*(3), 346–354. http://doi.org/10.1093/cercor/bhi112

Madden, D. J., Spaniol, J., Costello, M. C., Bucur, B., White, L. E., Cabeza, R., … Huettel, S. A. (2009). Cerebral white matter integrity mediates adult age differences in cognitive performance. *Journal of Cognitive Neuroscience*, *21*(2), 289–302. http://doi.org/10.1162/jocn.2009.21047

Madden, D. J., Whiting, W. L., Huettel, S. A., White, L. E., MacFall, J. R., & Provenzale, J. M. (2004). Diffusion tensor imaging of adult age differences in cerebral white matter: Relation to response time. *NeuroImage*, *21*(3), 1174–1181. http://doi.org/10.1016/j.neuroimage.2003.11.004

Madhavan, A., Schwarz, C. G., Duffy, J. R., Strand, E. A., Machulda, M. M., Drubach, D. A., … Whitwell, J. L. (2016). Characterizing white matter tract degeneration in syndromic variants of Alzheimer's disease: A diffusion tensor imaging study. *Journal of Alzheimer's Disease*, *49*(3), 633–643. http://doi.org/10.3233/JAD-150502

Magnuson, M. E., Thompson, G. J., Pan, W.-J., & Keilholz, S. D. (2013). Effects of severing the corpus callosum on electrical and BOLD functional connectivity and spontaneous dynamic activity in the rat brain. *Brain Connectivity*, *4*(1). http://doi.org/10.1089/brain.2013.0167

Maguire, E. A. (2003). Aging affects the engagement of the hippocampus during autobiographical memory retrieval. *Brain*, *126*(7), 1511–1523. http://doi.org/10.1093/brain/awg157

Marzi, C. A., Bisiacchi, P., & Nicoletti, R. (1991). Is interhemispheric transfer of visuomotor information asymmetric? Evidence from a meta-analysis. *Neuropsychologia*, *29*(12), 1163–1177. http://doi.org/10.1016/0028-3932(91)90031-3

McLaughlin, N. C. R., Paul, R. H., Grieve, S. M., Williams, L. M., Laidlaw, D., DiCarlo, M., … Gordon, E. (2007). Diffusion tensor imaging of the corpus callosum: a cross-sectional study across the lifespan. *International Journal of Developmental Neuroscience*, *25*(4), 215–221. http://doi.org/10.1016/j.ijdevneu.2007.03.008

Medina, D., deToledo-Morrell, L., Urresta, F., Gabrieli, J. D. E., Moseley, M., Fleischman, D., … Stebbins, G. T. (2006). White matter changes in mild cognitive impairment and AD: A diffusion tensor imaging study. *Neurobiology of Aging*, *27*(5), 663–672. http://doi.org/10.1016/j.neurobiolaging.2005.03.026

Meng, X., & D'Arcy, C. (2012). Education and dementia in the context of the cognitive reserve hypothesis: A systematic review with meta-analyses and qualitative analyses. *PLoS ONE*. http://doi.org/10.1371/journal.pone.0038268

Michel, C. M., Lehmann, D., Henggeler, B., & Brandeis, D. (1992). Localization of the sources of EEG delta, theta, alpha and beta frequency bands using the FFT dipole approximation. *Electroencephalography and Clinical Neurophysiology*, *82*(1), 38–44. http://doi.org/10.1016/0013-4694(92)90180-P

Miraglia, F., Vecchio, F., Bramanti, P., & Rossini, P. M. (2016). EEG characteristics in "eyes-open" versus "eyes-closed" conditions: Small-world network architecture in healthy aging and age-related brain degeneration. *Clinical Neurophysiology*, *127*(2), 1261–1268. http://doi.org/10.1016/j.clinph.2015.07.040

Mitew, S., Kirkcaldie, M. T. K., Halliday, G. M., Shepherd, C. E., Vickers, J. C., & Dickson, T. C. (2010). Focal demyelination in Alzheimer's disease and transgenic mouse models. *Acta Neuropathologica*, *119*(5), 567–577. http://doi.org/10.1007/s00401-010-0657-2

Montplaisir, J., Nielsen, T., Côté, J., Boivin, D., Rouleau, I., & Lapierre, G. (1990). Interhemispheric EEG Coherence before and after Partial Callosotomy. *Clinical EEG and Neuroscience*, *21*(1), 42–47. http://doi.org/10.1177/155005949002100114

Moretti, D. V., Babiloni, C., Binetti, G., Cassetta, E., Dal Forno, G., Ferreric, F., … Rossini, P. M. (2004). Individual analysis of EEG frequency and band power in mild Alzheimer's disease. *Clinical Neurophysiology*, *115*(2), 299–308. http://doi.org/10.1016/S1388-2457(03)00345-6

Mori, S., Oishi, K., Jiang, H., Jiang, L., Li, X., Akhter, K., … Mazziotta, J. (2008). Stereotaxic white matter atlas based on diffusion tensor imaging in an ICBM template. *NeuroImage*, *40*(2), 570–582. http://doi.org/10.1016/j.neuroimage.2007.12.035

Nagase, Y., Terasaki, O., Okubo, Y., Matsuura, M., & Toru, M. (1994). Lower Interhemispheric Coherence in a Case of Agenesis of the Corpus Callosum. *Clinical EEG and Neuroscience*, *25*(1), 36–39. http://doi.org/10.1177/155005949402500110

Naggara, O., Oppenheim, C., Rieu, D., Raoux, N., Rodrigo, S., Dalla Barba, G., & Meder, J. F. (2006). Diffusion tensor imaging in early Alzheimer's disease. *Psychiatry Research - Neuroimaging*, *146*(3), 243–249. http://doi.org/10.1016/j.pscychresns.2006.01.005

Nielsen, T., Montplaisir, J., & Lassonde, M. (1993). Decreased interhemispheric EEG coherence during sleep in agenesis of the corpus callosum. *European Neurology*, *33*(2), 173–176. http://doi.org/10.1159/000116928

Nielsen, T., & Peters, A. (2000). The effects of aging on the frequency of nerve fibers in rhesus monkey striate cortex. *Neurobiology of Aging*, *21*(5), 621–8. https://doi.org/10.1016/s0197-4580(00)00169-x

Nielson, K. A., Langenecker, S. A., & Garavan, H. (2002). Differences in the functional

neuroanatomy of inhibitory control across the adult life span. *Psychol Aging*, *17*(1), 56–71. http://doi.org/10.1037//0882-7974.17.1.56

Nolte, G., Bai, O., Wheaton, L., Mari, Z., Vorbach, S., & Hallett, M. (2004). Identifying true brain interaction from EEG data using the imaginary part of coherency. *Clinical Neurophysiology*, *115*(10), 2292–2307. http://doi.org/10.1016/j.clinph.2004.04.029

Nowrangi, M. A., Lyketsos, C. G., Leoutsakos, J. M. S., Oishi, K., Albert, M., Mori, S., & Mielke, M. M. (2013). Longitudinal, region-specific course of diffusion tensor imaging measures in mild cognitive impairment and Alzheimer's disease. *Alzheimer's and Dementia*, *9*(5), 519–528. http://doi.org/10.1016/j.jalz.2012.05.2186

O'Donnell, L. J., & Westin, C. F. (2011). An introduction to diffusion tensor image analysis. *Neurosurgery Clinics of North America*. http://doi.org/10.1016/j.nec.2010.12.004

O'Dwyer, L., Lamberton, F., Bokde, A. L. W., Ewers, M., Faluyi, Y. O., Tanner, C., … Hampel, H. (2011). Multiple Indices of Diffusion Identifies White Matter Damage in Mild Cognitive Impairment and Alzheimer's Disease. *PLoS ONE*, *6*(6), e21745. http://doi.org/10.1371/journal.pone.0021745

Oishi, K., Mielke, M. M., Albert, M., Lyketsos, C. G., & Mori, S. (2012). The fornix sign: a potential sign for Alzheimer's disease based on diffusion tensor imaging. *Journal of Neuroimaging : Official Journal of the American Society of Neuroimaging*, *22*(4), 365–74. http://doi.org/10.1111/j.1552-6569.2011.00633.x

Oldfield, R. C. (1971). The assessment and analysis of handedness: the Edinburgh inventory. *Neuropsychologia*, *9*(1), 97-113. https://doi.org/10.1016/0028-3932(71)90067-4

Olejnik, S., & Algina, J. (2003). Generalized Eta and Omega Squared Statistics: Measures of Effect Size for Some Common Research Designs. *Psychological Methods*, *8*(4), 434–447. http://doi.org/10.1037/1082-989X.8.4.434

Omura, K., Tsukamoto, T., Kotani, Y., Ohgami, Y., Minami, M., & Inoue, Y. (2004). Different mechanisms involved in interhemispheric transfer of visuomotor information. *Neuroreport*, *15*(18), 2707–11. http://doi.org/00001756-200412220-00004 [pii]

Onofrj, M., Thomas, A., Iacono, D., D'Andreamatteo, G., & Paci, C. (2001). Age-related changes of evoked potentials. *Neurophysiologie Clinique*, *31*(2), 83–103. http://doi.org/10.1016/S0987-7053(01)00248-9

Oostenveld, R., Fries, P., Maris, E., & Schoffelen, J. M. (2011). FieldTrip: Open source software for advanced analysis of MEG, EEG, and invasive electrophysiological data. *Computational Intelligence and Neuroscience*, *2011*. http://doi.org/10.1155/2011/156869

Ota, M., Obata, T., Akine, Y., Ito, H., Ikehira, H., Asada, T., & Suhara, T. (2006). Age-related degeneration of corpus callosum measured with diffusion tensor imaging. *NeuroImage*, *31*(4), 1445–1452. http://doi.org/10.1016/j.neuroimage.2006.02.008

Ozer, S., Noonan, K., Burke, M., Young, J., Barber, S., Forster, A., & Jones, R. (2016). The validity of the Memory Alteration Test and the Test Your Memory test for community-based identification of amnestic mild cognitive impairment. *Alzheimer's*

and Dementia, *12*(9), 987–995. http://doi.org/10.1016/j.jalz.2016.03.014

Pantel, J., Schröder, J., Essig, M., Minakaran, R., Schad, L. R., Friedlinger, M., … Knopp, M. V. (1998). Corpus callosum in Alzheimer's disease and vascular dementia - a quantitative magnetic resonance study. *Journal of Neural Transmission. Supplementum*, *54*, 129–36. https://doi.org/10.1007/978-3-7091-7508-8_12

Pantel, J., Schröder, J., Jauss, M., Essig, M., Minakaran, R., Schönknecht, P., … Knopp, M. V. (1999). Topography of callosal atrophy reflects distribution of regional cerebral volume reduction in Alzheimer's disease. *Psychiatry Research - Neuroimaging*, *90*(3), 181–192. http://doi.org/10.1016/S0925-4927(99)00018-9

Parente, D. B., Gasparetto, E. L., Da Cruz, L. C. H., Domingues, R. C., Baptista, A. C., Carvalho, A. C. P., & Domingues, R. C. (2008). Potential role of diffusion tensor MRI in the differential diagnosis of mild cognitive impairment and Alzheimer's disease. *American Journal of Roentgenology*, *190*(5), 1369–1374. http://doi.org/10.2214/AJR.07.2617

Parra, M. A., Abrahams, S., Logie, R. H., Méndez, L. G., Lopera, F., & Della Sala, S. (2010). Visual short-term memory binding deficits in familial Alzheimer's disease. *Brain*, *133*(9), 2702–2713. http://doi.org/10.1093/brain/awq148

Parra, M. A., Abrahams, S., Logie, R. H., & Sala, S. Della. (2009). Age and binding within-dimension features in visual short-term memory. *Neuroscience Letters*, *449*(1), 1–5. http://doi.org/10.1016/j.neulet.2008.10.069

Parra, M. A., Della Sala, S., Logie, R. H., & Morcom, A. M. (2014). Neural correlates of shape-color binding in visual working memory. *Neuropsychologia*, *52*(1), 27–36.

http://doi.org/10.1016/j.neuropsychologia.2013.09.036

Parra, M. A., Saarimäki, H., Bastin, M. E., Londoño, A. C., Pettit, L., Lopera, F., … Abrahams, S. (2015). Memory binding and white matter integrity in familial Alzheimer's disease. *Brain*, *138*(5), 1355–1369. http://doi.org/10.1093/brain/awv048

Pascual-Marqui, R. D., Lehmann, D., Koukkou, M., Kochi, K., Anderer, P., Saletu, B., … Kinoshita, T. (2011). Assessing interactions in the brain with exact low-resolution electromagnetic tomography. *Philosophical Transactions of the Royal Society A: Mathematical, Physical and Engineering Sciences*, *369*(1952), 3768–3784. http://doi.org/10.1098/rsta.2011.0081

Pedro, T., Weiler, M., Yasuda, C. L., D'Abreu, A., Damasceno, B. P., Cendes, F., & Balthazar, M. L. F. (2012). Volumetric brain changes in thalamus, corpus callosum and medial temporal structures: Mild alzheimer's disease compared with amnestic mild cognitive impairment. *Dementia and Geriatric Cognitive Disorders*, *34*(3–4), 149–155. http://doi.org/10.1159/000342118

Penke, L., Maniega, S. M., Houlihan, L. M., Murray, C., Gow, A. J., Clayden, J. D., … Deary, I. J. (2010). White matter integrity in the splenium of the corpus callosum is related to successful cognitive aging and partly mediates the protective effect of an ancestral polymorphism in ADRB2. *Behavior Genetics*, *40*(2), 146–156. http://doi.org/10.1007/s10519-009-9318-4

Penttilä, M., Partanen, J. V., Soininen, H., & Riekkinen, P. J. (1985). Quantitative analysis of occipital EEG in different stages of Alzheimer's disease. *Electroencephalography and Clinical Neurophysiology*, *60*(1), 1–6. http://doi.org/10.1016/0013-4694(85)90942-3

Peters, a, Moss, M. B., & Sethares, C. (2000). Effects of aging on myelinated nerve fibers in monkey primary visual cortex. *The Journal of Comparative Neurology*, *419*(3), 364–76. http://doi.org/10.1002/(SICI)1096-9861(20000410)419:3<364::AID-CNE8>3.0.CO;2-R

Peters, A. (2002). The effects of normal aging on myelin and nerve fibers: A review. *Journal of Neurocytology*, *31*(8-9), 581-593. http://doi.org/10.1023/A:1025731309829

Peters, A., & Sethares, C. (2002). Aging and the myelinated fibers in prefrontal cortex and corpus callosum of the monkey. *Journal of Comparative Neurology*, *442*(3), 277–291. http://doi.org/10.1002/cne.10099

Petersen, R. C. (2004). Mild cognitive impairment as a diagnostic entity. In *Journal of Internal Medicine* (Vol. 256, pp. 183–194). http://doi.org/10.1111/j.1365-2796.2004.01388.x

Pfefferbaum, A., Adalsteinsson, E., & Sullivan, E. V. (2005). Frontal circuitry degradation marks healthy adult aging: Evidence from diffusion tensor imaging. *NeuroImage*, *26*(3), 891–899. http://doi.org/10.1016/j.neuroimage.2005.02.034

Poffenberger, A. T. (1912). *Reaction time to retinal stimulation with special reference to the time lost in conduction through nerve centers. Archives of Psychology*. New York: Science Press.

Pogarell, O., Teipel, S. J., Juckel, G., Gootjes, L., Möller, T., Bürger, K., … Hampel, H. (2005). EEG coherence reflects regional corpus callosum area in Alzheimer's disease. *Journal of Neurology, Neurosurgery and Psychiatry*, *76*(1), 109–111.

http://doi.org/10.1136/jnnp.2004.036566

Posthuma, D., Neale, M. C., Boomsma, D. I., & De Geus, E. J. C. (2001). Are smarter brains running faster? Heritability of alpha peak frequency, IQ, and their interrelation. *Behavior Genetics*, *31*(6), 567–579. http://doi.org/10.1023/A:1013345411774

Pozzilli, C., Bastianello, S., Bozzao, A., Pierallini, A., Giubilei, F., Argentino, C., & Bozzao, L. (1994). No differences in corpus callosum size by sex and aging. A quantitative study using magnetic resonance imaging. *Journal of Neuroimaging : Official Journal of the American Society of Neuroimaging*, *4*(4), 218–21. http://doi.org/S0149-7634(96)00049-8 [pii]

Preti, M. G., Baglio, F., Laganà, M. M., Griffanti, L., Nemni, R., Clerici, M., … Baselli, G. (2012). Assessing corpus callosum changes in Alzheimer's disease: Comparison between tract-based spatial statistics and atlas-based tractography. *PLoS ONE*, *7*(4), e35856. http://doi.org/10.1371/journal.pone.0035856

Rabbitt, P., & Goward, L. (1994). Age, information processing speed, and intelligence. *Quarterly Journal of Experimental Psychology*, *47*(3), 741–760. https://doi.org/10.1080/14640749408401135

Rami, L., Bosch, B., Sanchez-Valle, R., & Molinuevo, J. L. (2010). The memory alteration test (M@T) discriminates between subjective memory complaints, mild cognitive impairment and Alzheimer's disease. *Archives of Gerontology and Geriatrics*, *50*(2), 171–174. http://doi.org/10.1016/j.archger.2009.03.005

Rami, L., Molinuevo, J. L., Sanchez-Valle, R., Bosch, B., & Villar, A. (2007). Screening for amnestic mild cognitive impairment and early Alzheimer's disease with M??

(Memory Alteration Test) in the primary care population. *International Journal of Geriatric Psychiatry*, *22*(4), 294–304. http://doi.org/10.1002/gps.1672

Randall, M. (2017). *Overview of the UK population: July 2017*. *Office for National Statistics*.

Reuter-Lorenz, P. A., & Cappell, K. A. (2008). Neurocognitive aging and the compensation hypothesis. *Current Directions in Psychological Science*, *17*(3), 177–182. http://doi.org/10.1111/j.1467-8721.2008.00570.x

Reuter-Lorenz, P. A., & Mikels, J. A. (2005). A split-brain model of Alzheimer's disease? Behavioral evidence for comparable intra and interhemispheric decline. *Neuropsychologia*, *43*(9), 1307–1317. http://doi.org/10.1016/j.neuropsychologia.2004.12.007

Reuter-Lorenz, P. A., & Park, D. C. (2014). How Does it STAC Up? Revisiting the Scaffolding Theory of Aging and Cognition. *Neuropsychology Review*, *24*(3), 355–370. http://doi.org/10.1007/s11065-014-9270-9

Reuter-Lorenz, P. A., & Stanczak, L. (2000). Differential effects of aging on the functions of the corpus callosum. *Developmental Neuropsychology*, *18*(1), 113–137. http://doi.org/10.1207/S15326942DN1801_7

Rieckmann, A., Van Dijk, K. R. A., Sperling, R. A., Johnson, K. A., Buckner, R. L., & Hedden, T. (2016). Accelerated decline in white matter integrity in clinically normal individuals at risk for Alzheimer's disease. *Neurobiology of Aging*, *42*, 177–188. http://doi.org/10.1016/j.neurobiolaging.2016.03.016

Roher, A. E., Weiss, N., Kokjohn, T. A., Kuo, Y. M., Kalback, W., Anthony, J., … Beach, T.

(2002). Increased Aβ peptides and reduced cholesterol and myelin proteins characterize white matter degeneration in Alzheimer's disease. *Biochemistry*, *41*(37), 11080–11090. http://doi.org/10.1021/bi026173d

Rose, S. E., Chen, F., Chalk, J. B., Zelaya, F. O., Strugnell, W. E., Benson, M., … Doddrell, D. M. (2000). Loss of connectivity in Alzheimer's disease: An evaluation of white matter tract integrity with colour coded MR diffusion tensor imaging. *Journal of Neurology Neurosurgery and Psychiatry*, *69*(4), 528–530. http://doi.org/10.1136/jnnp.69.4.528

Rosen, A. C., Prull, M. W., O'Hara, R., Race, E. A., Desmond, J. E., Glover, G. H., … Gabrieli, J. D. E. (2002). Variable effects of aging on frontal lobe contributions to memory. *NeuroReport*, *13*(18), 2425–2428. http://doi.org/10.1097/00001756-200212200-00010

Rubinov, M., & Sporns, O. (2010). Complex network measures of brain connectivity: Uses and interpretations. *NeuroImage*, *52*(3), 1059–1069. http://doi.org/10.1016/j.neuroimage.2009.10.003

Rugg, M. D., Milner, A. D., & Lines, C. R. (1985). Visual evoked potentials to lateralised stimuli in two cases of callosal agenesis. *Journal of Neurology Neurosurgery and Psychiatry*, *48*(4), 367–373. http://doi.org/10.1136/jnnp.48.4.367

Ryberg, C., Rostrup, E., Paulson, O. B., Barkhof, F., Scheltens, P., Van Straaten, E. C. W., … Waldemar, G. (2011). Corpus callosum atrophy as a predictor of age-related cognitive and motor impairment: A 3-year follow-up of the LADIS study cohort. *Journal of the Neurological Sciences*, *307*(1–2), 100–105. http://doi.org/10.1016/j.jns.2011.05.002

Sachdev, P. S., Zhuang, L., Braidy, N., & Wen, W. (2013). Is Alzheimer's a disease of the white matter? *Current Opinion in Psychiatry*, *26*(3), 244–251. http://doi.org/10.1097/YCO.0b013e32835ed6e8

Salat, D. H., Tuch, D. S., Greve, D. N., Van Der Kouwe, A. J. W., Hevelone, N. D., Zaleta, A. K., … Dale, A. M. (2005). Age-related alterations in white matter microstructure measured by diffusion tensor imaging. *Neurobiology of Aging*, *26*(8), 1215–1227. http://doi.org/10.1016/j.neurobiolaging.2004.09.017

Salat, D. H., Ward, A., Kaye, J. A., & Janowsky, J. S. (1997). Sex differences in the corpus callosum with aging. *Neurobiology of Aging*, *18*(2), 191–197. http://doi.org/10.1016/S0197-4580(97)00014-6

Sandson, T. A., Felician, O., Edelman, R. R., & Warach, S. (1999). Diffusion-weighted magnetic resonance imaging in Alzheimer's disease. *Dementia and Geriatric Cognitive Disorders*, *10*(2), 166–171. http://doi.org/10.1159/000017099

Sankari, Z., Adeli, H., & Adeli, A. (2011). Intrahemispheric, interhemispheric, and distal EEG coherence in Alzheimer's disease. *Clinical Neurophysiology*, *122*(5), 897–906. http://doi.org/10.1016/j.clinph.2010.09.008

Saron, C., & Davidson, R. (1989). Visual evoked potential measures of interhemispheric transfer time in humans. *Behavioral Neuroscience*, *103*(5), 1115–38. https://doi.org/10.1037/0735-7044.103.5.1115

Scally, B., Burke, M. R., Bunce, D., & Delvenne, J. F. (2018a). Resting state EEG power and connectivity are associated with alpha peak frequency slowing in healthy aging. *Neurobiology of Aging*, *71*, 149-155.

https://doi.org/10.1016/j.neurobiolaging.2018.07.004

Scally, B., Burke, M. R., Bunce, D., & Delvenne, J. F. (2018b). Visual and visuomotor interhemispheric transfer time in older adults. *Neurobiology of Aging*, *65*, 69–76. http://doi.org/10.1016/j.neurobiolaging.2018.01.005

Scally, B., Calderon, P. L., Anghinah, R., & Parra, M. A. (2016). Event-related potentials in the continuum of Alzheimers disease: Would they suit recent guidelines for preclinical assessment? *JBR Journal of Clinical Diagnosis and Research*, *04*(1), 1–9. http://doi.org/10.4172/2376-0311.1000127

Scheeringa, R., Petersson, K. M., Kleinschmidt, A., Jensen, O., & Bastiaansen, M. C. M. (2012). EEG Alpha Power Modulation of fMRI Resting-State Connectivity. *Brain Connectivity*, *2*(5), 254–264. http://doi.org/10.1089/brain.2012.0088

Scholz, J., Tomassini, V., & Johansen-Berg, H. (2013). Individual Differences in White Matter Microstructure in the Healthy Brain. In *Diffusion MRI: From Quantitative Measurement to In vivo Neuroanatomy: Second Edition* (pp. 301–316). http://doi.org/10.1016/B978-0-12-396460-1.00014-7

Schulte, T., Maddah, M., Müller-Oehring, E. M., Rohlfing, T., Pfefferbaum, A., & Sullivan, E. V. (2013). Fiber tract-driven topographical mapping (FTTM) reveals microstructural relevance for interhemispheric visuomotor function in the aging brain. *NeuroImage*, *77*, 195–206. http://doi.org/10.1016/j.neuroimage.2013.03.056

Schulte, T., & Müller-Oehring, E. M. (2010). Contribution of callosal connections to the interhemispheric integration of visuomotor and cognitive processes.

Neuropsychology Review, *20*(2), 174-190. http://doi.org/10.1007/s11065-010-9130-1

Schulte, T., Sullivan, E. V., Müller-Oehring, E. M., Adalsteinsson, E., & Pfefferbaum, A. (2005). Corpus callosal microstructural integrity influences interhemispheric processing: A diffusion tensor imaging study. *Cerebral Cortex*, *15*(9), 1384–1392. http://doi.org/10.1093/cercor/bhi020

Scott, A. K. (2004). Hypertension in older adults. *Reviews in Clinical Gerontology*, *14*(3), 189–198. http://doi.org/10.1017/S0959259805001528

Seehaus, A., Roebroeck, A., Bastiani, M., Fonseca, L., Bratzke, H., Lori, N., … Galuske, R. (2015). Histological validation of high-resolution DTI in human post mortem tissue. *Frontiers in Neuroanatomy*, *9*. http://doi.org/10.3389/fnana.2015.00098

Seitelberger, F. (1997). Theodor Meynert (1833-1892), pioneer and visionary of brain research. *Journal of the History of the Neurosciences*, *6*(3), 264–274. http://doi.org/10.1080/09647049709525713

Serra, L., Fadda, L., Perri, R., Spanò, B., Marra, C., Castelli, D., … Bozzali, M. (2014). Constructional apraxia as a distinctive cognitive and structural brain feature of pre-senile Alzheimer's disease. *Journal of Alzheimer's Disease*, *38*(2), 391–402. http://doi.org/10.3233/JAD-130656

Sexton, C. E., Kalu, U. G., Filippini, N., Mackay, C. E., & Ebmeier, K. P. (2011). A meta-analysis of diffusion tensor imaging in mild cognitive impairment and Alzheimer's disease. *Neurobiology of Aging*. http://doi.org/10.1016/j.neurobiolaging.2010.05.019

Shafto, M. A., Tyler, L. K., Dixon, M., Taylor, J. R., Rowe, J. B., Cusack, R., … Matthews, F. E. (2014). The Cambridge Centre for Ageing and Neuroscience (Cam-CAN) study protocol: A cross-sectional, lifespan, multidisciplinary examination of healthy cognitive ageing. *BMC Neurology*, *14*(1), 204. http://doi.org/10.1186/s12883-014-0204-1

Sharp, E. S., & Gatz, M. (2011). Relationship between education and dementia: An updated systematic review. *Alzheimer Disease and Associated Disorders*, *25*(4), 289. http://doi.org/10.1097/WAD.0b013e318211c83c

Sherman, D. S., Mauser, J., Nuno, M., & Sherzai, D. (2017). The efficacy of cognitive intervention in mild cognitive impairment (MCI): A meta-analysis of outcomes on neuropsychological measures. *Neuropsychology Review*, 1–45. https://doi.org/10.1007/s11065-017-9363-3

Shua, N., Wang, Z., Qib, Z., Li, K., & Hea, Y. (2011). Multiple diffusion indices reveals white matter degeneration in Alzheimer's disease and mild cognitive impairment: A tract-based spatial statistics study. *Advances in Alzheimer's Disease*, *2*, 513–523. http://doi.org/10.3233/978-1-60750-793-2-513

Smit, C. M., Wright, M. J., Hansell, N. K., Geffen, G. M., & Martin, N. G. (2006). Genetic variation of individual alpha frequency (IAF) and alpha power in a large adolescent twin sample. *International Journal of Psychophysiology*, *61*(2), 235–243. http://doi.org/10.1016/j.ijpsycho.2005.10.004

Smit, D. J. A., de Geus, E. J. C., Boersma, M., Boomsma, D. I., & Stam, C. J. (2016). Life-Span Development of Brain Network Integration Assessed with Phase Lag Index Connectivity and Minimum Spanning Tree Graphs. *Brain Connectivity*, *6*(4), 312–

325. http://doi.org/10.1089/brain.2015.0359

Snowden, J. S., Stopford, C. L., Julien, C. L., Thompson, J. C., Davidson, Y., Gibbons, L., … Mann, D. M. A. (2007). Cognitive phenotypes in Alzheimer's disease and genetic risk. *Cortex*, *43*(7), 835–845. http://doi.org/10.1016/S0010-9452(08)70683-X

Soares, J. M., Marques, P., Alves, V., & Sousa, N. (2013). A hitchhiker's guide to diffusion tensor imaging. Frontiers in neuroscience, 7, 31. http://doi.org/10.3389/fnins.2013.00031

Song, S. K., Sun, S. W., Ramsbottom, M. J., Chang, C., Russell, J., & Cross, A. H. (2002). Dysmyelination revealed through MRI as increased radial (but unchanged axial) diffusion of water. *NeuroImage*, *17*(3), 1429–1436. http://doi.org/10.1006/nimg.2002.1267

Song, S. K., Yoshino, J., Le, T. Q., Lin, S. J., Sun, S. W., Cross, A. H., & Armstrong, R. C. (2005). Demyelination increases radial diffusivity in corpus callosum of mouse brain. *NeuroImage*, *26*(1), 132–140. http://doi.org/10.1016/j.neuroimage.2005.01.028

Sperling, R. A., Aisen, P. S., Beckett, L. A., Bennett, D. A., Craft, S., Fagan, A. M., … Phelps, C. H. (2011). Toward defining the preclinical stages of Alzheimer's disease: Recommendations from the National Institute on Aging-Alzheimer's Association workgroups on diagnostic guidelines for Alzheimer's disease. *Alzheimer's & dementia, 7*(3), 280-292. http://doi.org/10.1016/j.jalz.2011.03.003

Sperry, R. W. (1961). Cerebral organization and behavior. *Science*, *133*(3466), 1749–1757. http://doi.org/10.1126/science.133.3466.1749

Stam, C. J., Nolte, G., & Daffertshofer, A. (2007). Phase lag index: Assessment of functional connectivity from multi channel EEG and MEG with diminished bias from common sources. *Human Brain Mapping*, *28*(11), 1178–1193. http://doi.org/10.1002/hbm.20346

Stebbins, G., & Murphy, C. (2010). Diffusion tensor imaging in Alzheimer's disease and mild cognitive impairment. *Behav Neurol*, *21*(1), 39–49. http://doi.org/10.3233/BEN-2009-0234.Diffusion

Storandt, M., Cheney, M., Ferraro, F. R., & Duchek, J. M. (1991). Paired Associate Learning in Senile Dementia of the Alzheimer Type. *Archives of Neurology*, *48*(10), 1038–1040. http://doi.org/10.1001/archneur.1991.00530220054019

Stricker, N. H., Salat, D. H., Kuhn, T. P., Foley, J. M., Price, J. S., Westlye, L. T., … Leritz, E. C. (2016). Mild cognitive impairment is associated with white matter integrity changes in late-myelinating regions within the corpus callosum. *American Journal of Alzheimer's Disease and Other Dementias*, *31*(1), 68–75. http://doi.org/10.1177/1533317515578257

Stricker, N. H., Schweinsburg, B. C., Delano-Wood, L., Wierenga, C. E., Bangen, K. J., Haaland, K. Y., … Bondi, M. W. (2009). Decreased white matter integrity in late-myelinating fiber pathways in Alzheimer's disease supports retrogenesis. *NeuroImage*, *45*(1), 10–16. http://doi.org/10.1016/j.neuroimage.2008.11.027

Sullivan, E. V., Adalsteinsson, E., & Pfefferbaum, A. (2006). Selective age-related degradation of anterior callosal fiber bundles quantified In vivo with fiber tracking. *Cerebral Cortex*, *16*(7), 1030-1039. http://doi.org/10.1093/cercor/bhj045

Sullivan, E. V., & Pfefferbaum, A. (2006). Diffusion tensor imaging and aging. *Neuroscience and Biobehavioral Reviews*, *30*(6), 749–761. http://doi.org/10.1016/j.neubiorev.2006.06.002

Sullivan, E. V., Pfefferbaum, A., Adalsteinsson, E., Swan, G. E., & Carmelli, D. (2002). Differential rates of regional brain change in callosal and ventricular size: a 4-year longitudinal MRI study of elderly men. *Cerebral Cortex*, *12*(4), 438–445. http://doi.org/10.1093/cercor/12.4.438

Sullivan, E. V., Rohlfing, T., & Pfefferbaum, A. (2010). Quantitative fiber tracking of lateral and interhemispheric white matter systems in normal aging: Relations to timed performance. *Neurobiology of Aging*, *31*(3), 464–481. http://doi.org/10.1016/j.neurobiolaging.2008.04.007

Sullivan, E. V., Rosenbloom, M. J., Desmond, J. E., & Pfefferbaum, A. (2001). Sex differences in corpus callosum size: Relationship to age and intracranial size. *Neurobiology of Aging*, *22*(4), 603–611. http://doi.org/10.1016/S0197-4580(01)00232-9

Sun, S. W., Liang, H. F., Le, T. Q., Armstrong, R. C., Cross, A. H., & Song, S. K. (2006). Differential sensitivity of in vivo and ex vivo diffusion tensor imaging to evolving optic nerve injury in mice with retinal ischemia. *NeuroImage*, *32*(3), 1195–1204. http://doi.org/10.1016/j.neuroimage.2006.04.212

Tagliazucchi, E., von Wegner, F., Morzelewski, A., Brodbeck, V., & Laufs, H. (2012). Dynamic BOLD functional connectivity in humans and its electrophysiological correlates. *Frontiers in Human Neuroscience*, *6*. http://doi.org/10.3389/fnhum.2012.00339

Takahashi, M., Hackney, D. B., Zhang, G., Wehrli, S. L., Wright, A. C., O'Brien, W. T., … Selzer, M. E. (2002). Magnetic resonance microimaging of intraaxonal water diffusion in live excised lamprey spinal cord. *Proceedings of the National Academy of Sciences*, *99*(25), 16192–16196. http://doi.org/10.1073/pnas.252249999

Takahashi, S., Yonezawa, H., Takahashi, J., Kudo, M., Inoue, T., & Tohgi, H. (2002). Selective reduction of diffusion anisotropy in white matter of Alzheimer disease brains measured by 3.0 Tesla magnetic resonance imaging. *Neurosci Lett*, *332*, 45–48. http://doi.org/S030439400200914X [pii]

Tang, X., Qin, Y., Zhu, W., & Miller, M. I. (2017). Surface-based vertexwise analysis of morphometry and microstructural integrity for white matter tracts in diffusion tensor imaging: With application to the corpus callosum in Alzheimer's disease. *Human Brain Mapping*, *38*(4), 1875–1893. http://doi.org/10.1002/hbm.23491

Tang, Y., Nyengaard, J. R., Pakkenberg, B., & Gundersen, H. J. G. (1997). Age-induced white matter changes in the human brain: A stereological investigation. *Neurobiology of Aging*, *18*(6), 609–615. http://doi.org/10.1016/S0197-4580(97)00155-3

Tassinari, G., Aglioti, S., Pallini, R., Berlucchi, G., & Rossi, G. F. (1994). Interhemispheric integration of simple visuomotor responses in patients with partial callosal defects. *Behavioural Brain Research*, *64*(1–2), 141–149. http://doi.org/10.1016/0166-4328(94)90126-0

Taylor, J. R., Williams, N., Cusack, R., Auer, T., Shafto, M. A., Dixon, M., … Henson, R. N. (2017). The Cambridge Centre for Ageing and Neuroscience (Cam-CAN) data repository: Structural and functional MRI, MEG, and cognitive data from a cross-

sectional adult lifespan sample. *NeuroImage*, *144*, 262–269. http://doi.org/10.1016/j.neuroimage.2015.09.018

Teipel, S. J., Bayer, W., Alexander, G. E., Bokde, A. L. W., Zebuhr, Y., Teichberg, D., … Hampel, H. (2003). Regional pattern of hippocampus and corpus callosum atrophy in Alzheimer's disease in relation to dementia severity: Evidence for early neocortical degeneration. *Neurobiology of Aging*, *24*(1), 85–94. http://doi.org/10.1016/S0197-4580(02)00044-1

Teipel, S. J., Bayer, W., Alexander, G. E., Zebuhr, Y., Teichberg, D., Kulic, L., … Hampel, H. (2002). Progression of corpus callosum atrophy in Alzheimer disease. *Archives of Neurology*, *59*(2), 243–248. http://doi.org/10.1001/archneur.59.2.243

Teipel, S. J., Hampel, H., Alexander, G. E., Schapiro, M. B., Horwitz, B., Teichberg, D., … Rapoport, S. I. (1998). Dissociation between corpus callosum atrophy and white matter pathology in Alzheimer's disease. *Neurology*, *51*(5), 1381–1385. http://doi.org/10.1212/WNL.51.5.1381

Teipel, S. J., Hampel, H., Pietrini, P., Alexander, G. E., Horwitz, B., Daley, E., … Rapoport, S. I. (1999). Region-specific corpus callosum atrophy correlates with the regional pattern of cortical glucose metabolism in Alzheimer disease. *Archives of Neurology*, *56*(4), 467–473. http://doi.org/10.1001/archneur.56.4.467

Teipel, S. J., Meindl, T., Wagner, M., Kohl, T., Bürger, K., Reiser, M. F., … Hampel, H. (2009). White matter microstructure in relation to education in aging and alzheimer's disease. *Journal of Alzheimer's Disease*. http://doi.org/10.3233/JAD-2009-1077

Teipel, S. J., Pogarell, O., Meindl, T., Dietrich, O., Sydykova, D., Hunklinger, U., … Hampel, H. (2009). Regional networks underlying interhemispheric connectivity: An EEG and DTI study in healthy ageing and amnestic mild cognitive impairment. *Human Brain Mapping*, *30*(7), 2098–2119. http://doi.org/10.1002/hbm.20652

Teipel, S. J., Stahl, R., Dietrich, O., Schoenberg, S. O., Perneczky, R., Bokde, A. L. W., … Hampel, H. (2007). Multivariate network analysis of fiber tract integrity in Alzheimer's disease. *NeuroImage*, *34*(3), 985–995. http://doi.org/10.1016/j.neuroimage.2006.07.047

Tettamanti, M., Paulesu, E., Scifo, P., Maravita, A., Fazio, F., Perani, D., & Marzi, C. A. (2002). Interhemispheric Transmission of Visuomotor Information in Humans: fMRI Evidence. *Journal of Neurophysiology*, *88*(2), 1051–1058. http://doi.org/10.1152/jn.00417.2001.

Thomann, P. A., Wüstenberg, T., Pantel, J., Essig, M., & Schröder, J. (2006a). Structural changes of the corpus callosum in mild cognitive impairment and Alzheimer's disease. *Dementia and Geriatric Cognitive Disorders*, *21*(4), 215–220. http://doi.org/10.1159/000090971

Thomann, P. A., Wüstenberg, T., Pantel, J., Essig, M., & Schröder, J. (2006b). Structural changes of the corpus callosum in mild cognitive impairment and Alzheimer's disease. *Dementia and Geriatric Cognitive Disorders*, *21*(4), 215–220. http://doi.org/10.1159/000090971

Tomaiuolo, F., Nocentini, C. A. U., Grammaldo, L., & Caltagirone, C. (2001). Interhemispheric transfer time in a patient with a partial lesion of the corpus callosum. *NeuroReport*, *12*(7), 1469–1472. http://doi.org/10.1097/00001756-

200105250-00035

Treitz, F. H., Heyder, K., & Daum, I. (2007). Differential course of executive control changes during normal aging. *Aging, Neuropsychology, and Cognition*, *14*(4), 370–393. http://doi.org/10.1080/13825580600678442

Ukmar, M., Makuc, E., Onor, M. L., Garbin, G., Trevisiol, M., & Cova, M. A. (2008). Risonanza magnetica con tensori di diffusione nella valutazione delle alterazioni della sostanza bianca nei pazienti con malattia di Alzheimer e nei pazienti con mild cognitive impairment. *Radiologia Medica*, *113*(6), 915–922. http://doi.org/10.1007/s11547-008-0286-1

Valenzuela, M. J., & Sachdev, P. (2006). Brain reserve and dementia: A systematic review. *Psychological Medicine*, *36*(4), 441-454. http://doi.org/10.1017/S0033291705006264

van Bruggen, T., Stieltjes, B., Thomann, P. A., Parzer, P., Meinzer, H. P., & Fritzsche, K. H. (2012). Do Alzheimer-specific microstructural changes in mild cognitive impairment predict conversion? *Psychiatry Research - Neuroimaging*, *203*(2–3), 184–193. http://doi.org/10.1016/j.pscychresns.2011.12.003

Van Camp, N., Blockx, I., Camón, L., De Vera, N., Verhoye, M., Veraart, J., … Van der Linden, A. (2012). A complementary diffusion tensor imaging (DTI)-histological study in a model of Huntington's disease. *Neurobiology of Aging*, *33*(5), 945–959. http://doi.org/10.1016/j.neurobiolaging.2010.07.001

van der Knaap, L. J., & van der Ham, I. J. M. (2011). How does the corpus callosum mediate interhemispheric transfer? A review. *Behavioural Brain Research*, *223*(1),

211–221. http://doi.org/10.1016/j.bbr.2011.04.018

Vecchio, F., Miraglia, F., Bramanti, P., & Rossini, P. M. (2014). Human brain networks in physiological aging: A graph theoretical analysis of cortical connectivity from EEG data. *Journal of Alzheimer's Disease*, *41*(4), 1239–1249. http://doi.org/10.3233/JAD-140090

Vecchio, F., Miraglia, F., Curcio, G., Altavilla, R., Scrascia, F., Giambattistelli, F., … Rossini, P. M. (2015). Cortical Brain Connectivity Evaluated by Graph Theory in Dementia: A Correlation Study between Functional and Structural Data. *Journal of Alzheimer's Disease*, *45*(3), 745–756. http://doi.org/10.3233/JAD-142484

Venegas-Barrera, C. S., & Manjarrez, J. (2011). *Patrones espaciales de la riqueza espec??fica de las culebras Thamnophis en M??xico*. *Revista Mexicana de Biodiversidad* (Vol. 82). http://doi.org/10.1234/12345678

Vernooij, M. W., de Groot, M., van der Lugt, A., Ikram, M. A., Krestin, G. P., Hofman, A., … Breteler, M. M. B. (2008). White matter atrophy and lesion formation explain the loss of structural integrity of white matter in aging. *NeuroImage*, *43*(3), 470–477. http://doi.org/10.1016/j.neuroimage.2008.07.052

Vinck, M., Oostenveld, R., Van Wingerden, M., Battaglia, F., & Pennartz, C. M. A. (2011). An improved index of phase-synchronization for electrophysiological data in the presence of volume-conduction, noise and sample-size bias. *NeuroImage*, *55*(4), 1548–1565. http://doi.org/10.1016/j.neuroimage.2011.01.055

Voineskos, A. N., Rajji, T. K., Lobaugh, N. J., Miranda, D., Shenton, M. E., Kennedy, J. L., … Mulsant, B. H. (2012). Age-related decline in white matter tract integrity and

cognitive performance: A DTI tractography and structural equation modeling study. *Neurobiology of Aging*, *33*(1), 21–34. http://doi.org/10.1016/j.neurobiolaging.2010.02.009

Vos, S. B., Jones, D. K., Viergever, M. A., & Leemans, A. (2011). Partial volume effect as a hidden covariate in DTI analyses. *NeuroImage*, *55*(4), 1566–1576. http://doi.org/10.1016/j.neuroimage.2011.01.048

Vysata, O., Kukal, J., Prochazka, A., Pazdera, L., Simko, J., & Valis, M. (2014). Age-related changes in EEG coherence. *Neurologia i Neurochirurgia Polska*, *48*(1), 35–38. http://doi.org/10.1016/j.pjnns.2013.09.001

Wada, Y., Nanbu, Y., Koshino, Y., Yamaguchi, N., & Hashimoto, T. (1998). Reduced interhemispheric EEG coherence in Alzheimer disease: Analysis during rest and photic stimulation. *Alzheimer Disease and Associated Disorders*, *12*(3), 175–181. http://doi.org/10.1097/00002093-199809000-00009

Wakana, S., Jiang, H., Nagae-Poetscher, L. M., Zijl, P. C. M. van, & Mori, S. (2004). Fiber Tract–based Atlas of Human White Matter Anatomy. *Radiology*, *230*(1), 77–87. http://doi.org/10.1148/radiol.2301021640

Wang, L., Wang, W., Yan, T., Song, J., Yang, W., Wang, B., … Wu, J. (2017). Beta-band functional connectivity influences audiovisual integration in older age: An EEG study. *Frontiers in Aging Neuroscience*, *9*, 239. http://doi.org/10.3389/fnagi.2017.00239

Wang, P. J., Saykin, A. J., Flashman, L. A., Wishart, H. A., Rabin, L. A., Santulli, R. B., … Mamourian, A. C. (2006). Regionally specific atrophy of the corpus callosum in AD,

MCI and cognitive complaints. *Neurobiology of Aging*, *27*(11), 1613–1617. http://doi.org/10.1016/j.neurobiolaging.2005.09.035

Ward, A., Tardiff, S., Dye, C., & Arrighi, H. M. (2013). Rate of Conversion from Prodromal Alzheimer's Disease to Alzheimer's Dementia: A Systematic Review of the Literature. *Dementia and Geriatric Cognitive Disorders Extra*, *3*(1), 320–332. http://doi.org/10.1159/000354370

Wasylyshyn, C., Verhaeghen, P., & Sliwinski, M. J. (2011). Aging and Task Switching: A Meta-Analysis. *Psychology and Aging*, *26*(1), 15–20. http://doi.org/10.1037/a0020912

Weber, B., Treyer, V., Oberholzer, N., Jaermann, T., Boesiger, P., Brugger, P., … Marzi, C. A. (2005). Attention and interhemispheric transfer: A behavioral and fMRI study. *Journal of Cognitive Neuroscience*, *17*(1), 113–123. http://doi.org/10.1162/0898929052880002

Wei, P. T., Leong, D., Calabrese, E., White, L., Pierce, T., Platt, S., & Provenzale, J. (2013). Diffusion tensor imaging of neural tissue organization: Correlations between radiologic and histologic parameters. *Neuroradiology Journal*, *26*(5), 501–510. http://doi.org/10.1177/197140091302600502

Weis, S., Kimbacher, M., Wenger, E., & Neuhold, A. (1993). Morphometric analysis of the corpus callosum using MR: Correlation of measurements with aging in healthy individuals. *American Journal of Neuroradiology*, *14*(3), 637–645. https://doi.org/10.18410/jebmh/2017/639

Wen, W., & Sachdev, P. (2004). The topography of white matter hyperintensities on

brain MRI in healthy 60- to 64-year-old individuals. *NeuroImage*, *22*(1), 144–154. http://doi.org/10.1016/j.neuroimage.2003.12.027

Wernicke, C. (1974). *Der aphasische Symptomenkomplex*. *Breslau. Max Cohn & Weigert*. http://doi.org/10.1007/978-3-642-65950-8

Westerhausen, R., Grüner, R., Specht, K., & Hugdahl, K. (2009). Functional relevance of interindividual differences in temporal lobe callosal pathways: A DTI tractography study. *Cerebral Cortex*, *19*(6), 1322–1329. http://doi.org/10.1093/cercor/bhn173

Westerhausen, R., Kreuder, F., Woerner, W., Huster, R. J., Smit, C. M., Schweiger, E., & Wittling, W. (2006). Interhemispheric transfer time and structural properties of the corpus callosum. *Neuroscience Letters*, *409*(2), 140–145. http://doi.org/10.1016/j.neulet.2006.09.028

Westlye, L. T., Walhovd, K. B., Dale, A. M., Bjørnerud, A., Due-Tønnessen, P., Engvig, A., … Fjell, A. M. (2010). Life-span changes of the human brain white matter: Diffusion tensor imaging (DTI) and volumetry. *Cerebral Cortex*, *20*(9), 2055–2068. http://doi.org/10.1093/cercor/bhp280

Wiggins, R. C., Gorman, A., Rolsten, C., Samorajski, T., Bailinger, W. E., & Freund, G. (1988). Effects of aging and alcohol on the biochemical composition of histologically normal human brain. *Metabolic Brain Disease*, *3*(1), 67–80. http://doi.org/10.1007/BF01001354

Wong, N. M. L., Ma, E. P.-W., & Lee, T. M. C. (2017). The Integrity of the Corpus Callosum Mitigates the Impact of Blood Pressure on the Ventral Attention Network and Information Processing Speed in Healthy Adults. *Frontiers in Aging Neuroscience*, *9*,

108. http://doi.org/10.3389/fnagi.2017.00108

Xie, M., Budde, M., Chen, C., Trinkaus, K., Armstrong, R., Cross, A., & Song, S. (2009). Pathological Correlates of the Decreased Axial Diffusivity in White Matter Injury. *Proceedings 17th Scientific Meeting, International Society for Magnetic Resonance in Medicine*, *Honolulu*, 841.

Yamamoto, N., & DeGirolamo, G. J. (2012). Differential effects of aging on spatial learning through exploratory navigation and map reading. *Frontiers in Aging Neuroscience*, *4*(JUN), 1–7. http://doi.org/10.3389/fnagi.2012.00014

Yeatman, J. D., Wandell, B. A., & Mezer, A. A. (2014). Lifespan maturation and degeneration of human brain white matter. *Nature Communications*, *5*, 4932. http://doi.org/10.1038/ncomms5932

Yin, X., Zhao, L., Xu, J., Evans, A. C., Fan, L., Ge, H., … Liu, S. (2012). Anatomical Substrates of the Alerting, Orienting and Executive Control Components of Attention: Focus on the Posterior Parietal Lobe. *PLoS ONE*, *7*(11), e50590. http://doi.org/10.1371/journal.pone.0050590

Zahr, N. M., Rohlfing, T., Pfefferbaum, A., & Sullivan, E. V. (2009). Problem solving, working memory, and motor correlates of association and commissural fiber bundles in normal aging: A quantitative fiber tracking study. *NeuroImage*, *44*(3), 1050–1062. http://doi.org/10.1016/j.neuroimage.2008.09.046

Zaidel, E., & Iacoboni, M. (2003). *The parallel brain: The cognitive neuroscience of the corpus callosum.* MIT Press. https://doi.org/10.1001/jama.291.8.1006

Zhang, Y., Schuff, N., Camacho, M., Chao, L. L., Fletcher, T. P., Yaffe, K., … Weiner, M. W.

(2013). MRI Markers for Mild Cognitive Impairment: Comparisons between White Matter Integrity and Gray Matter Volume Measurements. *PLoS ONE*, *8*(6). http://doi.org/10.1371/journal.pone.0066367

Zhuang, L., Sachdev, P. S., Trollor, J. N., Kochan, N. A., Reppermund, S., Brodaty, H., & Wen, W. (2012). Microstructural white matter changes in cognitively normal individuals at risk of amnestic MCI. *Neurology*, *79*(8), 748–754. http://doi.org/10.1212/WNL.0b013e3182661f4d

Zigmond, A. S., & Snaith, R. P. (1983). The Hospital Anxiety and Depression Scale. *Acta Psychiatrica Scandinavica*, *67*(6), 361–370. http://doi.org/10.1111/j.1600-0447.1983.tb09716.x